

**3D seismic attributes analysis and inversions for prospect evaluation
and characterization of Cherokee sandstone reservoir
in the Wierman field, Ness County, Kansas**

by

BOUHARKET BOUMAAZA

B.S., Badji Mokhtar University, 2003

A THESIS

Submitted in partial fulfillment of the requirements for the degree

MASTER OF SCIENCE

Department of Geology
College of Arts and Sciences

KANSAS STATE UNIVERSITY
Manhattan, Kansas

2017

Approved by:

Co-Major Professor
Dr. Matthew W. Totten

Approved by:

Co-Major Professor
Dr. Abdelmoneam Raef

Copyright

© BOUHARKET BOUMAAZA 2017.

Abstract

This work focuses on the use of advanced seismically driven technologies to estimate the distribution of key reservoir properties which mainly includes porosity and hydrocarbon reservoir pay. These reservoir properties were estimated by using a multitude of seismic attributes derived from post-stack high resolution inversions, spectral imaging and volumetric curvature.

A pay model of the reservoir in the Wierman field in Ness County, Kansas is proposed. The proposed geological model is validated based on comparison with findings of one blind well. The model will be useful in determining future drilling prospects, which should improve the drilling success over previous efforts, which resulted in only few of the 14 wells in the area being productive. The rock properties that were modeled were porosity and Gamma ray. Water saturation and permeability were considered, but the data needed were not available.

Sequential geological modeling approach uses multiple seismic attributes as a building block to estimate in a sequential manner dependent petrophysical properties such as gamma ray, and porosity. The sequential modelling first determines the reservoir property that has the ability to be the primary property controlling most of the other subsequent reservoir properties. In this study, the gamma ray was chosen as the primary reservoir property. Hence, the first geologic model built using neural networks was a volume of gamma ray constrained by all the available seismic attributes.

The geological modeling included post-stack seismic data and the five wells with available well logs. The post-stack seismic data was enhanced by spectral whitening to gain as much resolution as possible. Volumetric curvature was then calculated to determine where major faults were located. Several inversions for acoustic impedance were then applied to the post-stack seismic data to gain as much information as possible about the acoustic impedance. Spectral attributes were also extracted from the post-stack seismic data.

After the most appropriate gamma ray and porosity models were chosen, pay zone maps were constructed, which were based on the overlap of a certain range of gamma ray values with a certain range of porosity values. These pay zone maps coupled with the porosity and gamma ray models explain the performance of previously drilled wells.

* The workflows discussed in this project are centered on **SIGMA³**'s proprietary software, **CRYSTAL**

Table of Contents

List of Figures	vii
List of Tables	xi
Acknowledgements	xii
Dedication	xiii
Chapter 1 - Introduction	1
1.1 Study Area	1
1.2 The Wierman Field Puzzle	2
Chapter 2 - Geological Setting and stratigraphic framework	9
2.1 Stratigraphy of Cherokee group	9
2.2 Upper Mississippian	13
2.3 Cherokee Group	13
Chapter 3 - Methodology	16
3.1 Data Loading	16
3.1.1 Field data	16
3.2 Geophysical Modelling	19
3.2.1 Summary	19
3.2.2 Spectral whitening and resolution enhancement	19
3.2.3 Acquisition Footprint Suppression	22
3.2.4 Well Ties	24
3.2.5 Fault Imaging	27
3.2.6 Spectral Attributes	30
3.2.7 Structural framework	32
3.2.8 Post-Stack Inversions	33
3.2.9 Inversions theories:	34
3.2.10 Inversions results:	42
3.3 Geological Modeling	48
3.3.1 Summary	48
3.3.2 3D Geocellular Grid	49

3.3.3 Facies Model Possibility	51
3.3.4 Porosity Model	52
3.3.5 Gamma Ray Model	54
3.3.6 Pay Model	56
Chapter 4 - Discussion	57
4.1 Discussion	57
4.2 Future Well Locations	65
Chapter 5 - Conclusions and recommendations.....	71
References	73
Appendix.....	75

List of Figures

Figure 1.1 Kansas County map. Blue star indicates study area in Ness County (Adjusted from Kansas Geological Survey, 2011).....	1
Figure 1.2 Map of oil and gas fields, Ness County, KS. Includes blue square indicating study area. Map obtained and modified from distribution of oil and gas fields of Ness County, Kansas (Kansas Geological Survey, 2011).	2
Figure 1.3 Approximate study area Wierman field (green box) relative to the York field (red box)	3
Figure 1.4 Seismic doublet found at the top of the Mississippian formation (from Abbas, 2009). 4	4
Figure 1.5 Location of Ness County within Kansas, and the location of the Wierman Field within Section 18 of Township 16 south, Range 22 west showing the well Keith#1 (from Abbas, 2009). Modified from (Kansas Geological Survey, 2009)	5
Figure 1.6 Seismic attributes; (a) time structural map of Mississippian-top seismic time horizon with interpreted paleovalley (arrows), (b) Cherokee-top time horizon with structural closures around the producer well Squier 1-18 and a lack of such closure around Keith 1, interpreted tidal channel branching off towards shoreline (c) isochron (time thickness) color map of Cherokee group and contours of the time structural map of Cherokee top seismic horizon, and (d) stratal amplitude time slice at 25 ms above the Mississippian horizon (flattened), an interpreted paleoshoreline at the time of Cherokee sand deposition is marked by a dashed line (from Raef et al., 2016).	7
Figure 2.1 Cross section through Ness County highlight our area of interest (Adjusted from Marriam, 1963).	10
Figure 2.2 Exhibits the relationship between SP/Neutron log and a stratigraphic section in the study area; the yellow box marks a channel sandstone facies (Adjusted from Stoneburner, 1982).	11
Figure 2.3 Updated tops from gamma ray and DT logs for the Mississippian System.	12
Figure 2.4 Map of Wierman Field wells and surrounding areas (Kansas Geological Survey, 2011).	14

Figure 2.5 Kansas Stratigraphic Column showing the Cherokee Group (Adjusted from Kansas Geological Survey, 2011).	15
Figure 3.1 Wierman Field seismic data and the corresponding wells. The wells with well logs used in our survey are displayed in green.	18
Figure 3.2 Amplitude spectrum for original data (left) and enhanced data using trapezoidal spectral whitening 20-25-110-115Hz (right).	20
Figure 3.3 The original seismic (left) versus the spectrally whitened seismic (right).....	21
Figure 3.4 Acquisition Footprint in around area of interest Trace 9 Time 700-1000 ms, Original (left) and Enhanced (right).	22
Figure 3.5 Most Positive Curvature, Exp 0.5, Time 710 ms, Original (left) and Enhanced (right).	23
Figure 3.6 Most Positive Curvature, Exp 0.5, Time 850 ms, original (left) and enhanced (right).	23
Figure 3.7 The amplitude (red) and phase (blue) spectra of the generated wavelet for the synthetic seismograms.	25
Figure 3.8 Seismic well ties for Keith 1 (left), Keith 2 (center), Squier 1_18 (right).	26
Figure 3.9 Seismic well ties for Squier A 1_18 (left) and Wierman 1_19 (right). Displays from left to right: seismic section at well location, synthetic seismogram at well, seismic at well, P-wave velocity (from sonic) and density logs.	26
Figure 3.10 Most Positive Curvature at time slice 850ms of the original seismic (left) versus the spectrally whitened seismic (right) (Pawnee Limestone formation). Structural features (Faults and fractured zones) and delineation of a feature in the North part of the section that may be the result of processing or signal-to-noise artifact	28
Figure 3.11 A seismic line going from East to West showing a feature that may be the result of processing or signal-to-noise artifact.	29
Figure 3.12 Total energy map (left) and maximum amplitude above average map (right) in the Cherokee group of the spectrally whitened seismic. The yellow box points out a feature that may be the result of processing or signal-to-noise artifact, and the red box points out a broken up channel.	31
Figure 3.13 Framework Model	32

Figure 3.14 Operating parameters low pass cut off and high pass cut off.....	35
Figure 3.15 Colored Inversion Operator Parameters: Length: 150ms , NRC: 1.0.....	37
Figure 3.16 Absolute Colored Inversion Parameters @ Time 850ms	38
Figure 3.17 Colored Inversion Result @ Time 850ms	39
Figure 3.18 Picked Absolute Colored Inversion Low Pass 22Hz, High Pass 113 Hz, Model High Frequency 123Hz @ Line 76 700-1000ms / Length 150ms, NRC 1.0.....	40
Figure 3.19 Stochastic Inversion Parameters @ Time 850ms using Absolute colored inversion as Soft Data	41
Figure 3.20 Post-stack inversion of acoustic impedance via sparse spike inversion at Squier 1-18 well.....	42
Figure 3.21 Post-stack inversion of acoustic impedance via deterministic inversion at Squier 1-18 well.....	43
Figure 3.22 Post-stack inversion of acoustic impedance via colored inversion at Squier 1-18 well.	43
Figure 3.23 Post-stack inversion of acoustic impedance via GLI at Squier 1-18 well.....	44
Figure 3.24 Post-stack inversion of acoustic impedance via stochastic inversion at Squier 1- 18 well.....	44
Figure 3.25 Post-stack inversions of acoustic impedance at Squier 1-18 well using the various inversion methods. From left to right: acoustic impedance computed at well, stochastic inversion, GLI, deterministic inversion, colored inversion, and sparse spiking inversion ...	45
Figure 3.26 Post-stack inversion of acoustic impedance via stochastic inversion at Squier A 1-18	46
Figure 3.27 Post-stack inversion of acoustic impedance via stochastic inversion at Keith-1 and Keith-2 wells.	47
Figure 3.28 Post-stack inversion of acoustic impedance via stochastic inversion at Wierman 1-19	47
Figure 3.29 3D Geocellular Grid	49
Figure 3. 30 The geologic grid used for modeling. This grid is divided into three zones where the first zone has 28 layers, the second zone has 18 layers, and the third zone has 14 layers....	50

Figure 3. 31 Cross plot between the gamma ray, impedance, and porosity (color scale) logs of the Squier 1-18 well, red box is clean sand, blue line represents the linear regression line fit to the data. Different facies cluster on the plot.	51
Figure 3.32 Comparison between the blind well (Keith_1) and the model's porosity log extracted at Keith_1's location.....	53
Figure 3.33 Comparison between the blind well (Keith-1) and the model's gamma ray log extracted at Keith-1's location.....	55
Figure 3.34 Defined pay zone for the upper Cherokee group. A pay zone is defined by being less than a gamma ray of 50 API and more than a porosity of 20%.	56
Figure 4.1 Most Positive Curvature, EXP 0.5, Time 850 ms of the spectrally whitened seismic	58
Figure 4.2 Most Positive Curvature exp 0.5 Notch with Max Amp Above Avg. Overlay, Time 857ms	59
Figure 4.3 Most Positive Curvature exp 0.5 Notch with Max Amp Above Avg. Overlay, Time 872ms	60
Figure 4.4 Most Positive Curvature exp 0.5 Notch with Total Energy Overlay, Time 857ms	61
Figure 4.5 Most Positive Curvature exp 0.5 Notch with Total Energy Overlay, Time 872ms	62
Figure 4.6 Post-stack inversions of acoustic impedance at Squier 1-18 well using the various inversion methods. From left to right: acoustic impedance computed at well, stochastic inversion, GLI, deterministic inversion, colored inversion, and sparse spiking inversion ...	63
Figure 4.7 Defined pay zone for the upper Cherokee group. A pay zone is defined by being less than a gamma ray of 50 API and more than a porosity of 20%.	64
Figure 4.8 Proposed drilling locations based on pay zone.....	66
Figure 4.9 Wierman 1-19 shallow and deep resistivity logs that could indicate a cross over at 4410 feet, which points to the start of the oil water transition zone.	67
Figure 4.10 Blocky Nature of Wells Points to an Oil Reservoir in the Upper Part of the Cherokee	68
Figure 4.11 Gamma ray model extracted at proposed well locations inside the Cherokee group.	69
Figure 4.12 View of the proposed drill locations with the seismic polygon outlined in red.	70

List of Tables

Table 1-Seismic volume perimeter coordinates:.....	16
Table 2-Project's well coordinates:	17

Acknowledgements

To all the people who helped me throughout my journey, I'm writing in the honor of thanking you all for what you've done for me.

I also wish to express my sincere thanks to my great advisers Dr. Matthew W. Totten and my co-advisor Dr. Raef Abdelmoneam at Kansas State University, who they made my research much easier and valuable by providing me with all the necessary advice, help and support even when I was abroad. I also take this opportunity to express gratitude to all of the Department faculty members who taught me valuable classes, to Dr Michael W. Lambert and Dr George R. Clarck, to the K-State Alumni, Mr. Paul Strunk and his wife Deana and Steve Kirkuk for providing financial assistance to all graduate teaching and research assistants at the geology department, and to the rest of my thesis committee members for their encouragement, insightful comments, and questions.

During the summer of my first year at Kansas State university, I interned with SIGMA³ in Denver, a great company that allowed me to work on my thesis within and use their software, CRYSTAL, and that is where I got the most support, so I place on record my sincere thanks and appreciation to the company as a whole and to the manager Dr. Ahmed Ouenes and my fellow and co-worker Chris Graziano from Colorado School of Mines, who was also an intern at SIGMA³ and I am extremely thankful and indebted to them for sharing their expertise, and sincere and valuable guidance and encouragement extended to me. These two men assisted me a lot while I was doing my thesis work and made my experience as an intern very interesting.

I'm also extremely thankful for my great mentors Chelsea Newgord, Eric, Dave Bard, Mohamed and Bilal, the colleagues whom I worked with in SIGMA³, for all of their help, and their powerful encouragement that pushed me to continue in developing my career.

A year later, while on an exchange program at NTNU University in Norway, I met two great teachers Dr Alexey Stovas and Dr Kenneth Duffaut, who shared with me their knowledge, expertise, and useful guidance in doing more work on my thesis, and that made the most out of my experience there, and I would extremely thank them for their support. I place on record, my sincere thanks to Dr. Brahim Abbad from STATOIL for his great help and support during my time at NTNU- Trondheim, Norway.

Dedication

I want to dedicate this work to the ones who brought me to life, these two people who were helping me in every single step that I took since I was a very weak child, till now, when I'm older and much stronger, who supported me and encouraged me a lot to further my studies abroad and without them this work would have been impossible. Thank you my wonderful parents, my father Khaled and my mother Kherfia, my brothers and sisters, and all members of my big family.

In closing, I would express my gratitude to my special friends and classmates: Saad, Sultan, Michael, Abdelbasset, Obair and Heather at Kansas State University, to Naph, Miłosz, Mouloud, Ali, Soheib, Samir, Abdelkrim, Abdelkader, Ahmed and Mohamed at NTNU, to Tayeb, Takyoueddine, Nacer and Houari, Brahim, Abdelkhalek, Sahnoune and Ali Fedhal, to my brother Ismael, Youcef, Salim and Kamal and all my friends.

Chapter 1 - Introduction

1.1 Study Area

Ness County is located in the western half of Kansas, which places the eastern part of the county on the western flank of the central Kansas uplift, as shown in Figure 1-1. Hydrocarbon fields in Ness County are shown in Figure 1-2. Coral Coast Petroleum, LLC drilled the # 1 Keith in 2003, located in section 18, T16S, R22W as a wildcat well, based upon a 3D seismic survey. This well's target area of production was the Cherokee sandstone, which is included in the Cherokee Group. Walters et al. (1979) identified the Cherokee Group as a single entity that contains channel sandstones as an oil reservoir. Keith #1 produced only 162 barrels of oil before it was plugged as a dry well and abandoned. The operator concluded that not enough sand development was present for economic reserves, and that the well must be on the edge of a sandstone channel. Several subsequent wells were drilled in the Wierman field attempting to find the channel, and all failed to produce any oil.



Figure 1.1 Kansas County map. Blue star indicates study area in Ness County (Adjusted from Kansas Geological Survey, 2011)

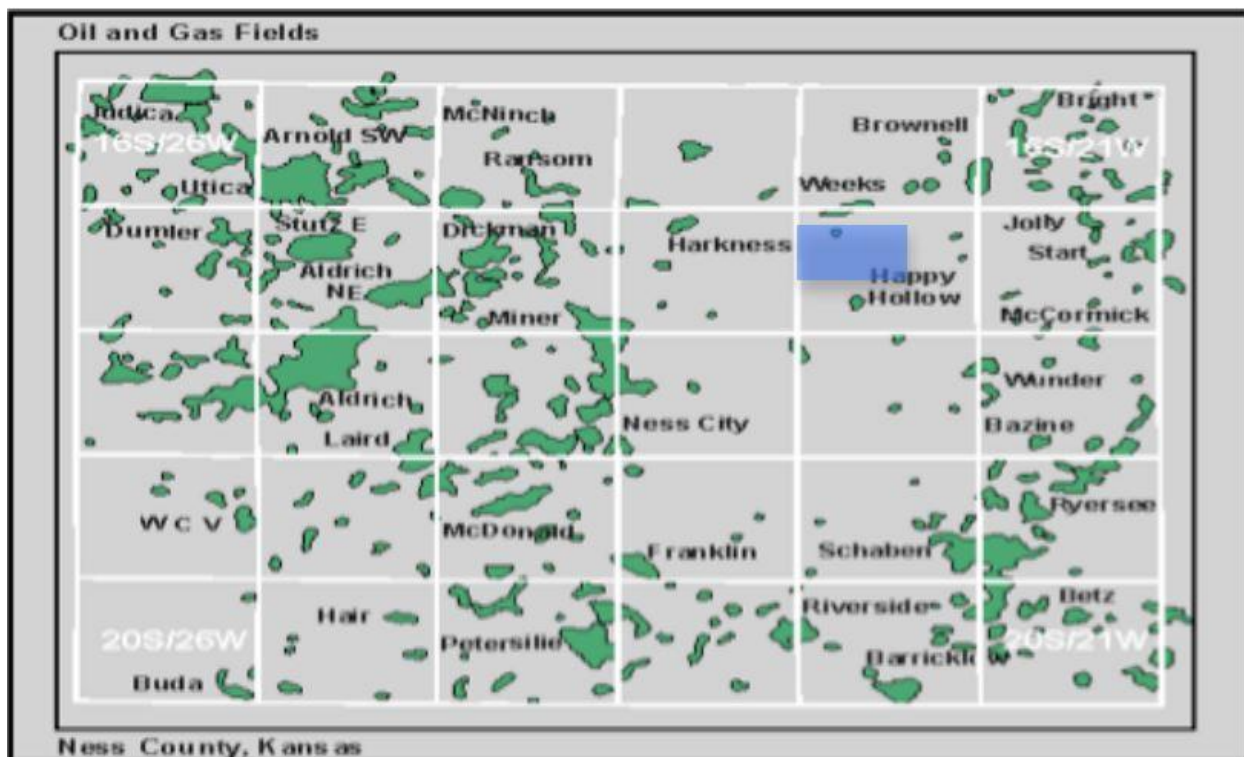


Figure 1.2 Map of oil and gas fields, Ness County, KS. Includes blue square indicating study area. Map obtained and modified from distribution of oil and gas fields of Ness County, Kansas (Kansas Geological Survey, 2011).

1.2 The Wierman Field Puzzle

The use of seismic attributes in stratigraphic characterization of hydrocarbon reservoirs has been reported by many authors, e.g. Chopra and Marfurt (2008); Lozano and Marfurt (2008); Chopra and Marfurt (2007); Russell et al. (2003). Seismic interpreters may have a difficult time in distinguishing shale-filled channels vs. sand-filled channels, without attribute-assisted interpretation (Suarez et al., 2008). In areas with high drilling risk as a result of the lack of spatial continuity and lithological variation of potential prospects, analysis of relevant seismic attributes is essential to successful placement of wells. According to Suarez et al. (2008), the use of different seismic attributes may assist in defining channel fill zones in more detail.

Coral Coast donated the seismic survey to Kansas State University for further research into why the original seismic interpretation was not successful in identifying productive well locations. This resulted in three previous thesis studies (Abbas, 2009; Philip, 2011; Meek, 2015)

that focused on establishing a suitable 3D seismic attribute analysis workflow for use in finding hydrocarbon production potential in areas of Ness County.

This study uses the same dataset as the previous works of Abbas and Philip in the Wierman field, the SW of Ness County, but develops a different workflow, while Meek used a nearby York Field dataset. Figure 1.3 illustrates the location of Wierman field, relative to the nearby York field, and all of them applied a similar workflow in the analysis of additional 3D seismic and well log data acquired from a nearby area in Ness County, to test the hypothesis that seismic attribute analysis is an essential component in the delineation of heterogeneous reservoir stratigraphy in Kansas lithologies,

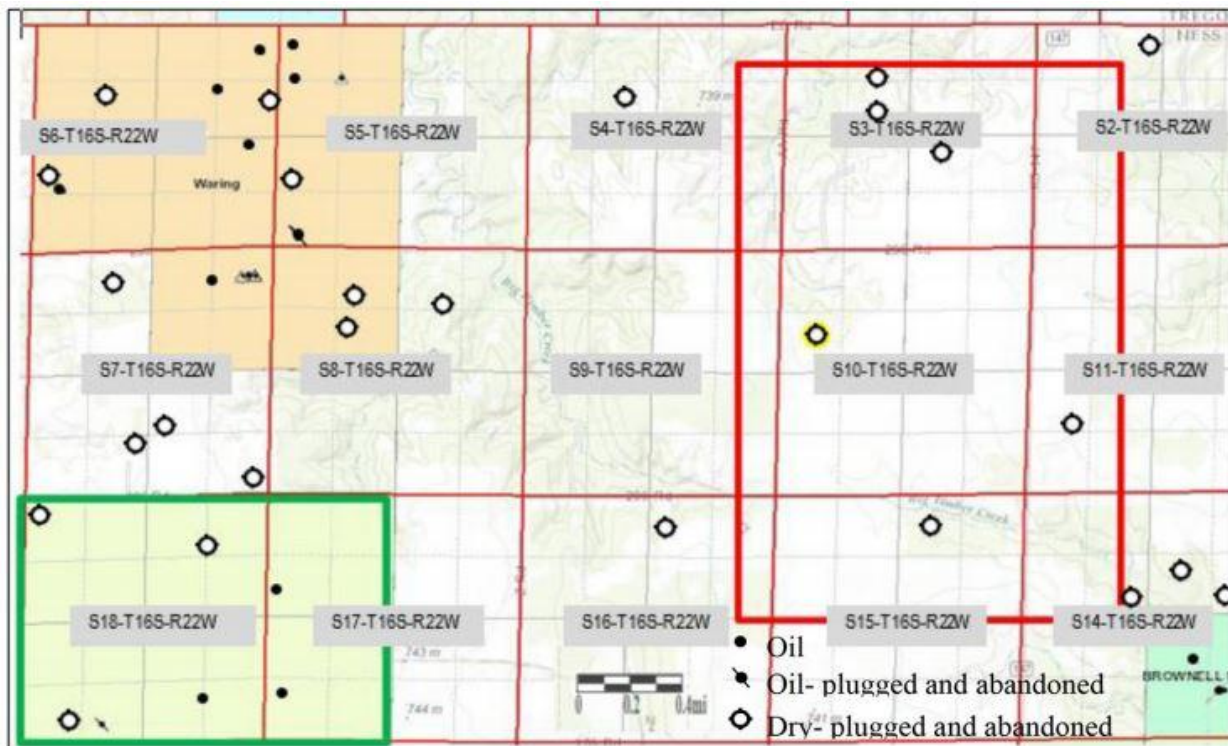


Figure 1.3 Approximate study area Wierman field (green box) relative to the York field (red box)

Abbas (2009) main focus was to answer the question of “what went wrong” with this prospect. In his thesis, he stated that the well operator revealed that on the seismic cross section, a potential sandstone target was identified through tracking of doublet reflections seen at the base of the Cherokee formation, on top of the Mississippian (Figure 1.4). Based on this interpretation Keith #1 was positioned with the aim of targeting these doublets, under the impression that they

may reflect a greater contrast between the underlying Mississippian surface and the lower Cherokee zone (Figure 1.5)

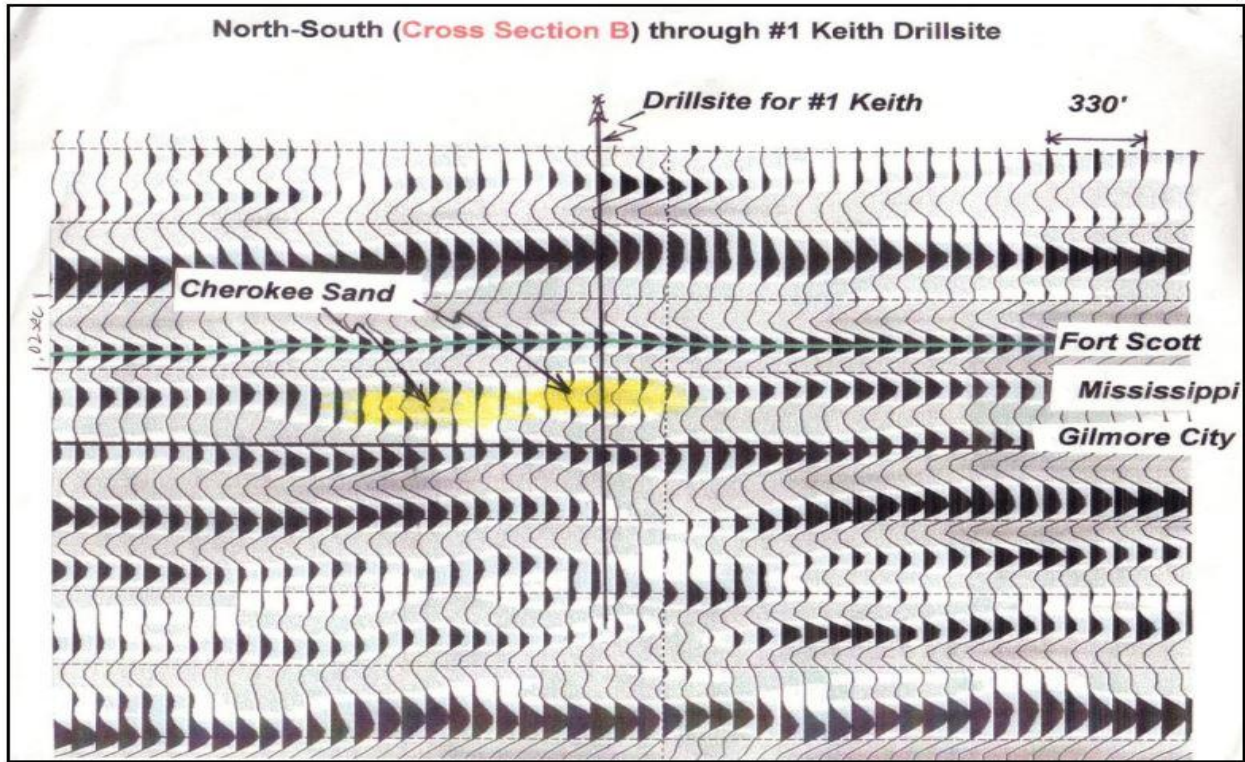


Figure 1.4 Seismic doublet found at the top of the Mississippian formation (from Abbas, 2009).



Figure 1.5 Location of Ness County within Kansas, and the location of the Wierman Field within Section 18 of Township 16 south, Range 22 west showing the well Keith#1 (from Abbas, 2009). Modified from (Kansas Geological Survey, 2009)

In an attempt to understand the Keith #1 results, Abbas used the same 3D seismic reflection data, well logs, and drilling reports related to the Wierman field, and created a workflow integrating 3D seismic attributes to explain better the poor results of the Keith#1 well. Finally, even though this doublet event appeared on the seismic data, seismic attributes analysis of relative acoustic impedance, RMS amplitudes, average energy, and amplitude attenuation illustrated that Keith #1 and several surrounding dry holes all fell outside of favorable areas.

Philip (2011) tried to develop the use of post-stack 3D seismic attributes in the Wierman field and apply them as part of a workflow integrating well logs, modern depositional analogs, core data and production data. The attributes used for the Wierman field were: acoustic impedance, amplitude attenuation, RMS amplitude, spectral decomposition, curvature and coherence, she successfully outlined a fluvial sandstone channel, extracting acoustic impedance, amplitude attenuation and root-mean-square, guided by a time window focused on the top of the Mississippian formation, correlating the calculated set of seismic attributes maps with each other

and compared them with available well information to map and understand reservoir facies heterogeneities. Her study resulted in an understanding of the key seismic channel-facies framework and further explained some of the disappointing drilling results at Wierman Field.

Many of the attributes used by Philip have been similarly used by Raef et al. (2015) in a recent work in the area of Ness county, with emphasis on Cherokee sands. The York field in the NE of Ness County (Fig. 1), Kansas, has a poor success rate, five wells were dry holes that targeted the Cherokee sands. These sand lenses are very narrow, thin and highly spatially discontinuous, making proper well placement critical. Raef et al. (2015) presents a confirmatory finding, showing a meandering fluvial channel system incised on the Mississippian stratigraphic unconformity north east of the Wierman field, reporting the position of a palaeoshoreline and associated submarine channels. Figure 1.6 illustrates interpreted paleo-valleys, structural closure, and the interpreted paleoshoreline.

Raef et al.'s work presented a synergistic approach integrating post-stack seismic attributes (TWTT-Two Way Travel Time, amplitude, coherency, parallel-bedding indicator, and curvature) and well-log facies analysis to understand the depositional setting of the Cherokee sands of Wierman Field. The conclusion of their study is that the dimensions and spatial relationships of the interpreted geobodies are in line with the modern shoreline analogs of a barrier beach or strand-plain adjoining an estuary.

Raef et al. (2015), proposes that “higher rates of drilling success in the basal Cherokee sands are achievable by:

- a) Focusing on the proximity of thicker sands, as evidenced by amplitude brightening of seismic reflections close to the Cherokee basal reflections.
- b) [Considering] the proximity of identified amplitude anomalies to the interpreted paleo shoreline.
- c) Favoring locations of paleo-topographic highs on the Mississippian unconformity, when associated with brightening of seismic amplitudes in the basal Cherokee reflections and dimming amplitudes below the Cherokee bottom reflection,
- d) [Locating] structural closures, [which] in association with the above factors, are of

significant weight in reducing drilling risk.”

Therefore, the focus of their study is three-fold: [1] apply methodologies guided by three previously mentioned studies to a seismic attribute analysis being conducted in a nearby area of Ness County and [2] validate results of interpreted palaeo-fluvial channel system based on sinuosity and aspects of post-confluence hydraulic geometry signatures, and [3] outline most prospective area(s)

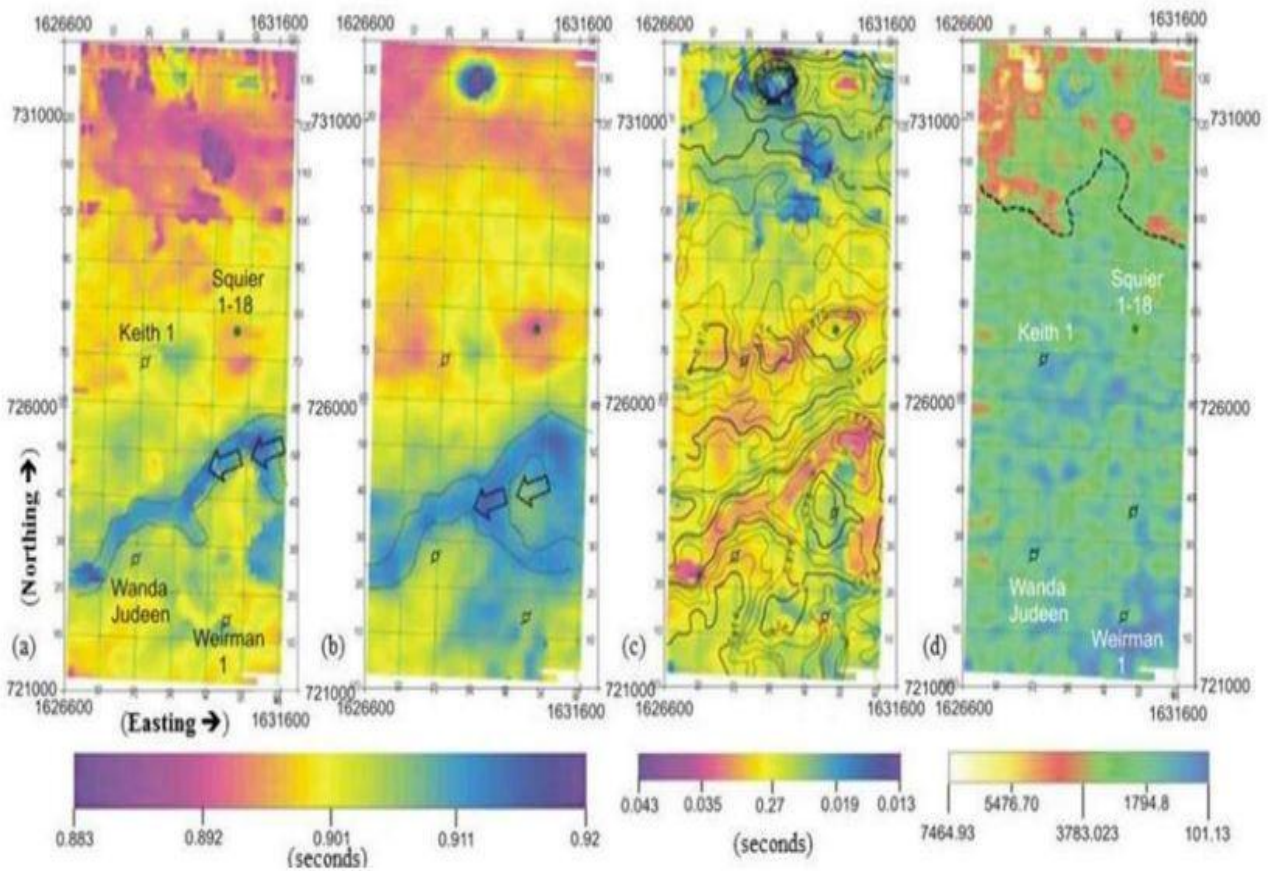


Figure 1.6 Seismic attributes; (a) time structural map of Mississippian-top seismic time horizon with interpreted paleovalley (arrows), (b) Cherokee-top time horizon with structural closures around the producer well Squier 1-18 and a lack of such closure around Keith 1, interpreted tidal channel branching off towards shoreline (c) isochron (time thickness) color map of Cherokee group and contours of the time structural map of Cherokee top seismic horizon, and (d) stratal amplitude time slice at 25 ms above the Mississippian horizon (flattened), an interpreted paleoshoreline at the time of Cherokee sand deposition is marked by a dashed line (from Raef et al., 2016).

Many of these attributes have been similarly used in Meek's 2015 work, amplitude attenuation, RMS amplitude, and acoustic impedance were selected primarily to emphasize lithology. Event continuity and similarity variance were picked to portray the emergence of structural patterns. Time-structure maps, along with time slices of several 3D seismic attributes including amplitude attenuation, acoustic impedance, and event continuity all seem to pinpoint that within the study area, previous drilling of five dry wells were off the boundary of a meandering fluvial channel, Cherokee sandstone body of potential reservoir quality.

Also, comparing Meek's results to previous studies conducted in Ness County have potentially contributed to paleodepositional interpretations made using a similar workflow (Raef et al., 2016), supporting a broadly NE-SW trend meandering channel system, which is in accord with the interpretations made by Raef et al., and that of Ramaker (2009).

This thesis describes a workflow using seismically driven technologies for basal sand analysis of the Cherokee group of the Wierman field, Ness County, Kansas. Using this workflow an estimation of porosity, gamma ray, and various pay zones were constructed. These estimations were based on several different seismic attributes from high resolution post-stack inversions, spectral imaging, and volumetric curvature.

Chapter 2 - Geological Setting and stratigraphic framework

2.1 Stratigraphy of Cherokee group

The area of interest is the Cherokee Group, which was deposited during the Desmoinesian Stage of the Pennsylvanian System that occurred after the Mississippian unconformity. This group is composed mostly of shales and sandstones, with small amounts of limestone. Stoneburner, (1982) noted that the Cherokee group in Ness County has a thickness that ranges from 5-200 feet.

The Cherokee Group was deposited in an environment that was transitioning from a continental to marginal marine environment. The Cherokee group was deposited during the Desmoinesian stage as the sea transgressed over the Mississippian unconformity out of the Hugoton Embayment and onto the central Kansas Uplift (Cuzella, 1991). The stratigraphic relationships of the Cherokee group can be seen in Figure 2-1. The study area is highlighted by the red box drawn on the cross section. The Cherokee group appears to become thinner as it approaches the Central Kansas uplift. The Cherokee sandstones are mostly deposited along the Mississippian unconformity, which controls trend and distribution of the sandstones, and ultimately produces a series of escarpments and valleys. The less resistant strata are then cut by streams and redeposited to form channel sands (Stoneburner, 1982).

Analysis of gamma ray logs shows areas of low gamma ray values in the clean sands. Figure 2-2 shows a relationship between SP/Neutron, where our zone of interest is highlighted in yellow on top of the Mississippian formation, and based on both DT and gamma ray logs the top of the Mississippian formation has been updated, because some of the tops were originally reported in the wrong place (Figure 2-3).

The sandstone shows an upward increase in radioactivity which points to the lower portion of the sand having a cleaner and coarser sand at the base, which fines upward. Based on Walter's Law, this fining up sequence corresponds to the lateral sequence across a channel, from shales and siltstones of the flood plain facies, to fine grained sandstones in the point-bar facies, to coarser grained sandstones and conglomerates in the channel facies (Stoneburner, 1982).

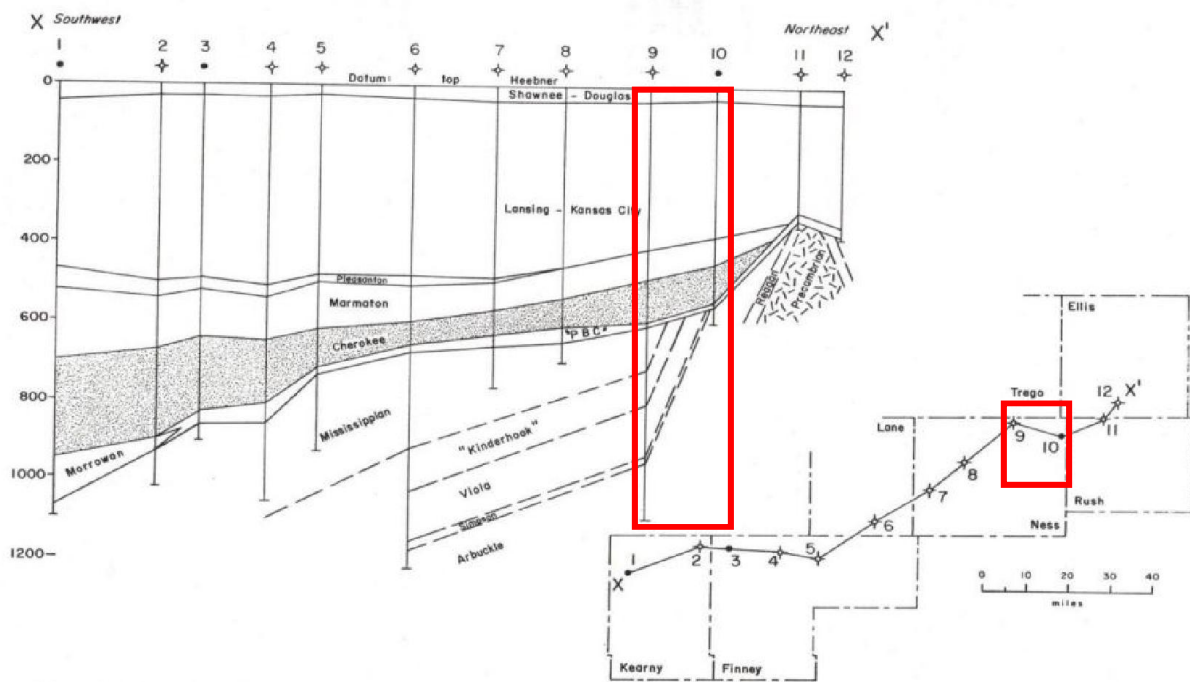


Figure 2.1 Cross section through Ness County highlight our area of interest (Adjusted from Marriam, 1963).

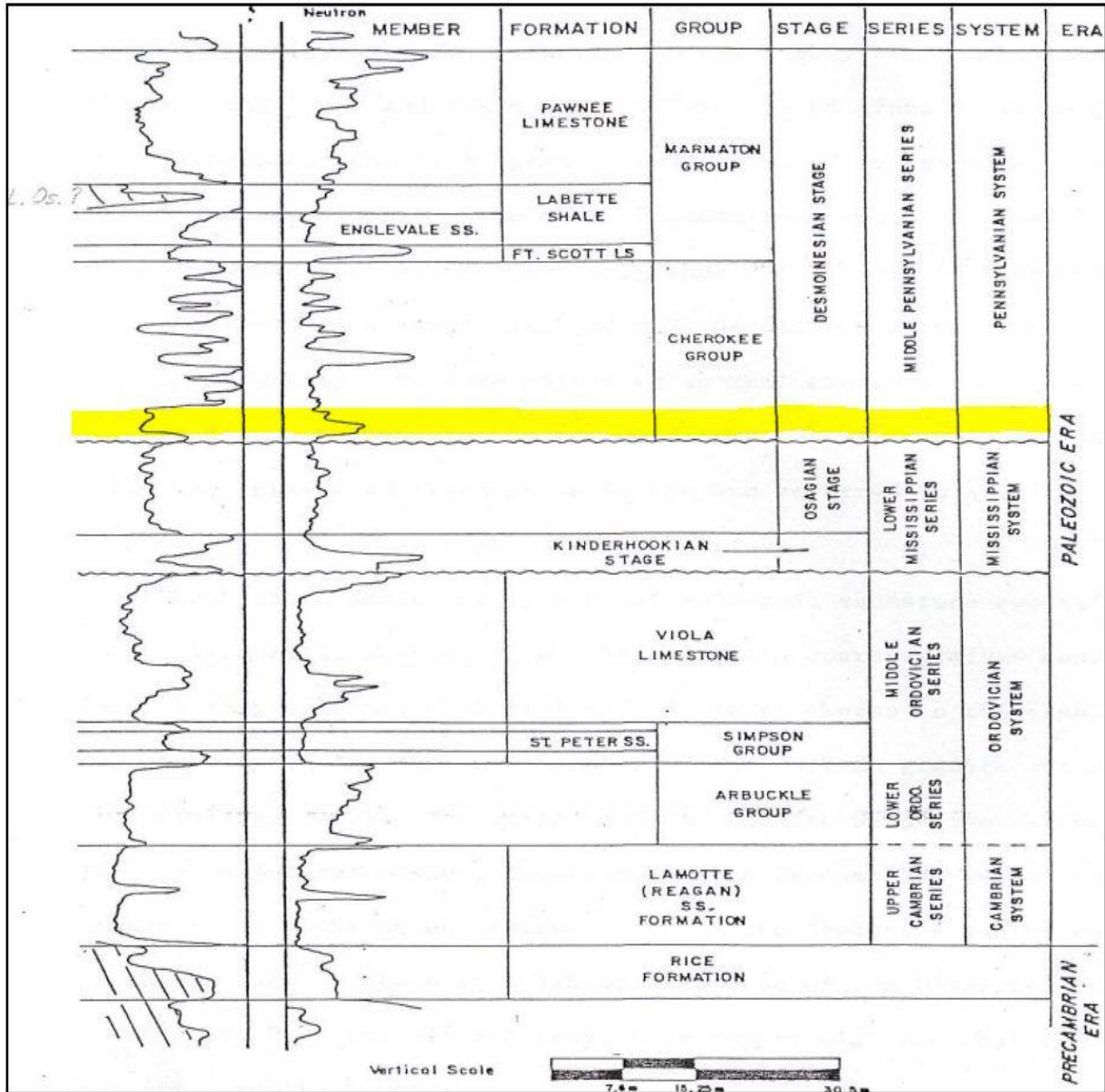


Figure 2.2 Exhibits the relationship between SP/Neutron log and a stratigraphic section in the study area; the yellow box marks a channel sandstone facies (Adjusted from Stoneburner, 1982).

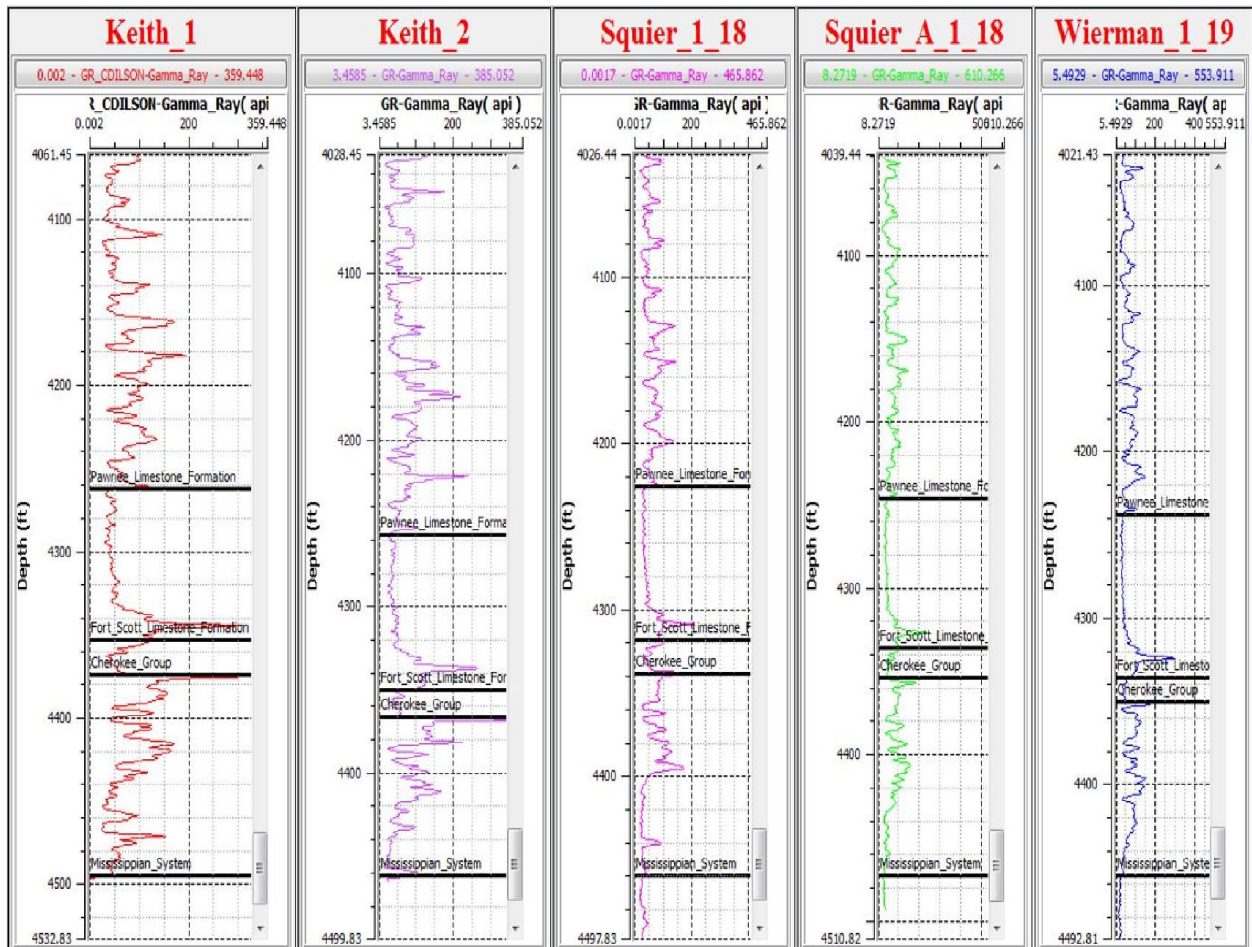


Figure 2.3 Updated tops from gamma ray and DT logs for the Mississippian System.

2.2 Upper Mississippian

Part of a stratigraphic column published by the Kansas Geological survey, Figure 2-5, shows rock classification in Kansas. The Mississippian System exists and wholly covers the subsurface of the state of Kansas, except for the crests of the Central Kansas uplift, Cambridge arch and Nemaha anticline. The Upper Mississippian series is a group that represents a major formation in this study. The Upper Mississippian series in Kansas is mostly represented by limestone and dolomite, and scattered beds of shales and sandstones, along with fewer quantities of chert (Goebel, 1968).

2.3 Cherokee Group

The Pennsylvanian System outcrops in the eastern part of Kansas; in the state's western area the Pennsylvanian rocks, which includes the Cherokee Group, lie underneath the surface. The Cherokee Group rocks had been deposited during the Desmoinesian Stage of the Middle Pennsylvanian series (Figure 2-5). These particular rocks are important stratigraphic indicators of widespread unconformities. The Cherokee Group consists of both marine and non-marine rocks and is mainly sandstone and sandy shales. The sandstone portion of the Cherokee is an elongated "shoestring" intercalated with Cherokee shales (Van Dyke, 1976). Stratigraphically, fluvial origin sandstone coupled with channel and overbank facies. Van Dyke (1976) classifies the Cherokee sandstones as litharenites, with 70% quartz, 20% metamorphic rock fragments, and 10% of accessory minerals. The Desmoinesian (Middle Pennsylvanian) rocks were deposited in a cyclic manner, alternating between non-marine shales and sands with marine limestones. The Cherokee Group varies greatly from the overlying Marmaton Group and the underlying Mississippian rocks. The formations within the Cherokee Group include Krebs Formation, which consists mainly of shales, limestones, underclay and coal, and its members Warner Sandstone Member, Bluejacket Sandstone Member, and Seville Limestone Member. The other formation included in this group is the Cabaniss Formation, which consists mostly of shales, some sandstone, limestone and coal; and

its members are the following: Chelsea Sandstone Member, Verdigris Limestone Member, and the Breezy Hill Limestone Member.

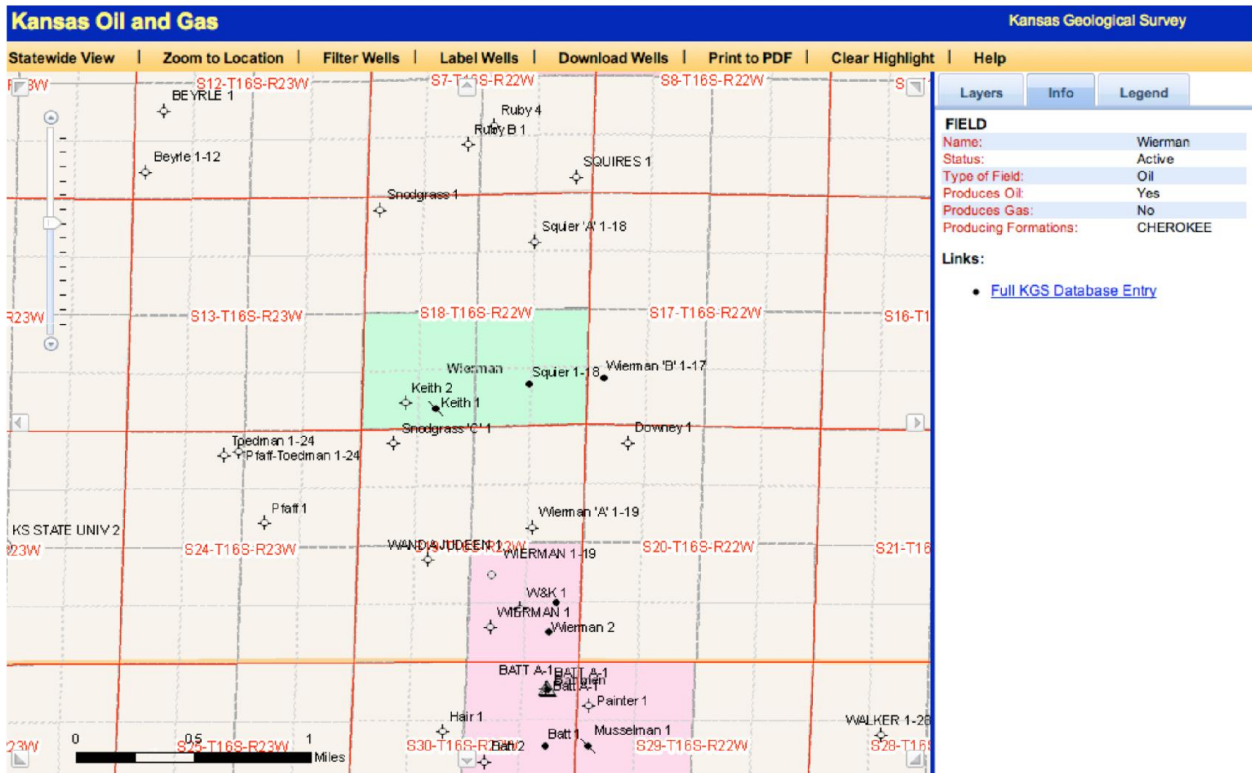


Figure 2.4 Map of Wierman Field wells and surrounding areas (Kansas Geological Survey, 2011).

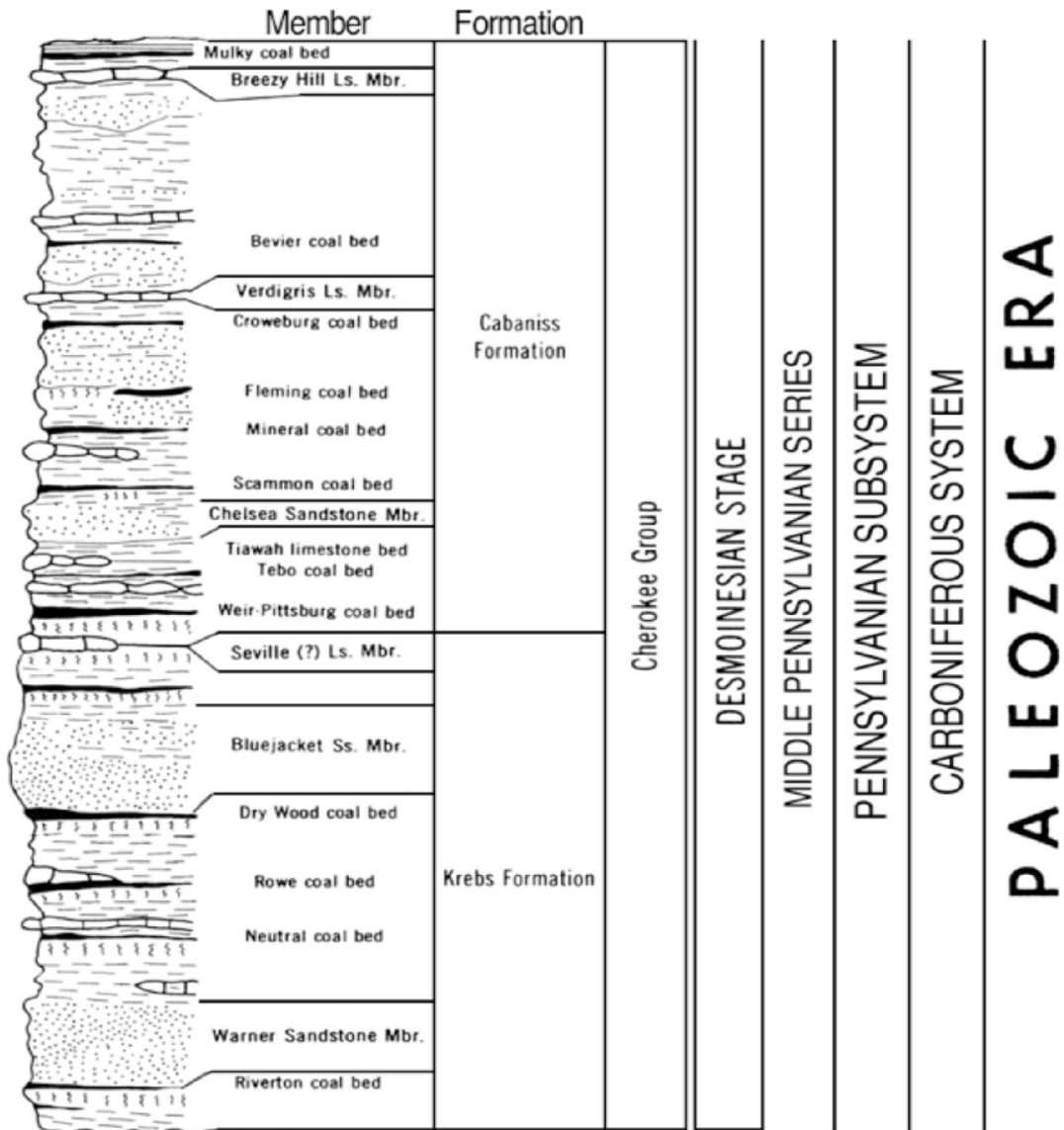


Figure 2.5 Kansas Stratigraphic Column showing the Cherokee Group (Adjusted from Kansas Geological Survey, 2011).

Chapter 3 - Methodology

3.1 Data Loading

3.1.1 Field data

Seismic data and well logs:

Coral Coast Petroleum conducted the seismic acquisition survey in 2002, in the Wierman Field, Ness County, Kansas. The seismic data has a bin size of 82 feet in the x and y direction and has an inline count of 136 (west to east) and a crossline count of 61 (south to north) with a sampling rate of 2.0 milliseconds. The survey boundaries (Figure 3-1) are located 0.9 miles from the west side of section 18-T16S-R22W, and about 2.1 miles from the northern edge of 18-T16S-R22W. Seismic data was uploaded (SEGY-file Post-Stack Migrated Volume) into CRYSTAL software using a Seismic Reference Datum of 2700 feet and a replacement velocity of 9000 feet per second. The survey was projected to a specific location using parameters for the projection system of NAD 27, Southern Zone, US Feet.

Seismic data was enhanced using SMT Kingdom's Spectral Whitening, as every software has its own algorithm to increase the resolution of the seismic data and attempt to correct for frequency attenuation, and equalize the amplitude spectrum without overly boosting noise. The resulting spectrally whitened seismic data was re-sampled to 0.5ms to use in all following processes.

Table 1-Seismic volume perimeter coordinates:

X	Y
1626652.02	721250.009
1631599.02	721090.009
1631959.02	732222.009

Most of the 14 wells in the area covered by seismic data had well logs, although several lacked LAS format. For the remaining wells with logs in TIF format, SMT Kingdom software

was used to digitize the well logs. For example, Keith#2 needed a digital format to extract DT and Gamma ray curves from the original TIF file. Only 5 wells had been used to develop porosity data, these wells are displayed in green color in Figure 3-1.

Well logs listed below were used within the limits of the survey boundaries.

Table 2-Project's well coordinates:

Well	X	Y	KB	TD	Operator
Keith_1	1628475.943	726761.145	2455	4520	Coral Coast Petroleum LC
Keith_2	1627806.495	726887.051	2456	4510	Coral Coast Petroleum LC
Squier_1_18	1630602.596	727305.409	2446	4578	Mull Drilling Co., Inc.
Squier_A_1_18	1630747.299	730526.645	2455	4520	Mull Drilling Co., Inc.
Wierman_1_19	1631185.249	722341.727	2429	4550	Mull Drilling Co., Inc.

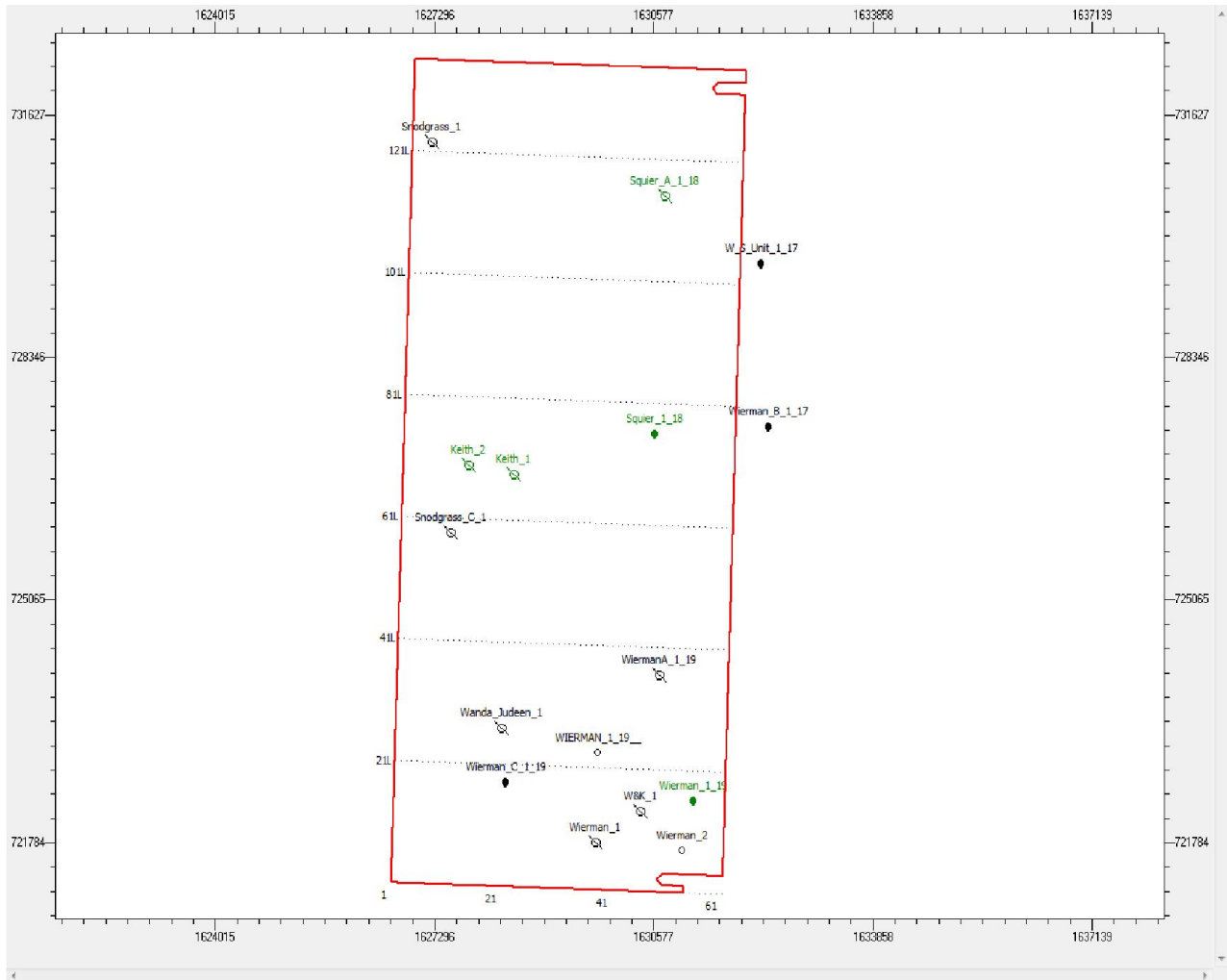


Figure 3.1 Wierman Field seismic data and the corresponding wells. The wells with well logs used in our survey are displayed in green.

3.2 Geophysical Modelling

3.2.1 Summary

Spectral whitening was applied to the post-stack data to improve seismic resolution by expanding the amplitude spectrum. A number of horizons were picked on the post-stack seismic sections using available well markers (tops). This includes the Mississippian and the Cherokee group with two other horizons, thus dividing the Cherokee group into three different interpreted seismic horizons to describe the structural framework of the reservoir.

Volumetric curvature and spectral attributes (Spectral decomposition) were then performed on the spectrally whitened data set to generate useful attributes, including most positive curvature, total energy, and max amplitude above average attributes. Several types of inversions were applied to the spectrally whitened data set to estimate acoustic impedance. The post-stack inversion process derives acoustic impedance values from seismic amplitude values. Acoustic impedance is computed by multiplying compressional velocity by density, which gives a rock property. In sandstones reservoirs, acoustic impedance is usually related to lithology and porosity, and may provide very useful information about the reservoir.

These include the stochastic inversion, Generalized Linear Inversion (GLI), sparse spike, deterministic, and colored inversion. Increasing the resolution of our seismic data is a crucial step in this process.

3.2.2 Spectral whitening and resolution enhancement

It is important to note that the seismic data provided to us already enhanced. The lowest frequency we were able to enhance was 20 Hz. The criteria for acceptable enhancement are the ability to whiten (flatten) the original amplitude spectrum, and to resolve thin bedding while avoiding ringing artifacts in the section.

The type of resolution enhancement (Yilmaz, O., 2001) chosen was the trapezoidal spectral whitening feature used in Kingdom SMT software (aka. Spectral Balancing). The trapezoid was defined using four frequencies: 20, 25, 110, and 115Hz. The input sampling rate of

the stack section was 1 msec. The amplitude spectra for the original seismic data and the spectrally whitened data are depicted in Figure 3.2. The application of the trapezoidal spectral whitening operator helped in flattening the amplitude spectrum of the data and boosting attenuated frequencies due to absorption effects during wave propagation and processing effects. This is especially visible for frequencies above 50 Hz where the original data suffer a clear reduction of the amplitude spectrum above this limit.

The comparison between the original and enhanced seismic data can be seen in Figure 3.3 where the seismic is plotted for the time interval 700-1000 msec. The enhanced section shows better event continuity, higher resolution and signal strength than in input section. To improve the results of the trapezoidal spectral whitening, the high-frequency filter parameters have been tested using several values to avoid creation of artificial events and boosting noise at the high frequency end.

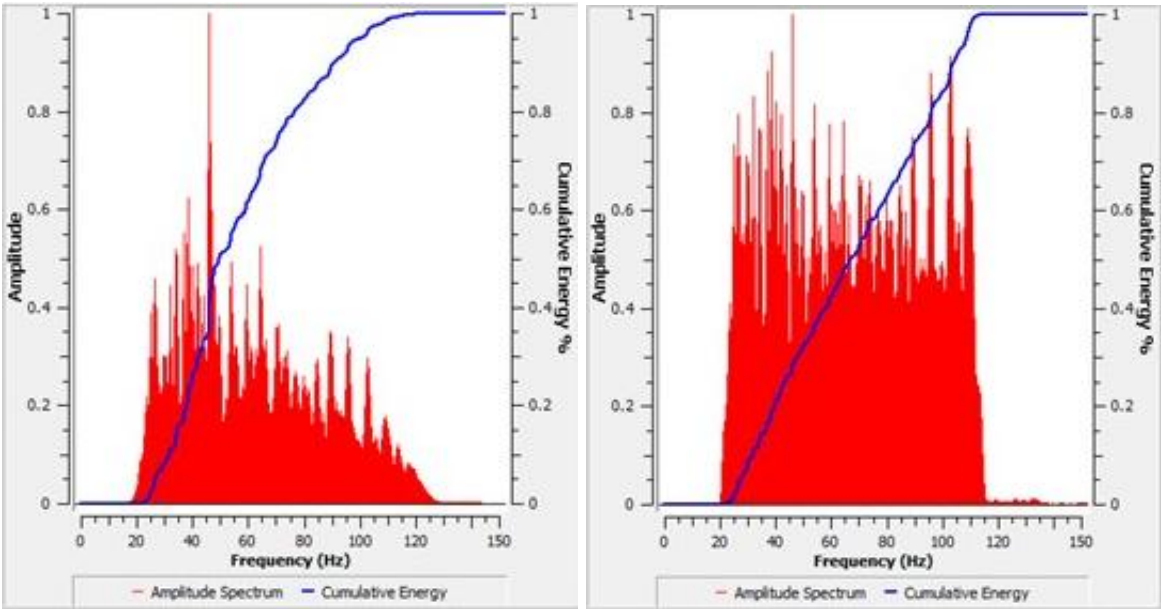
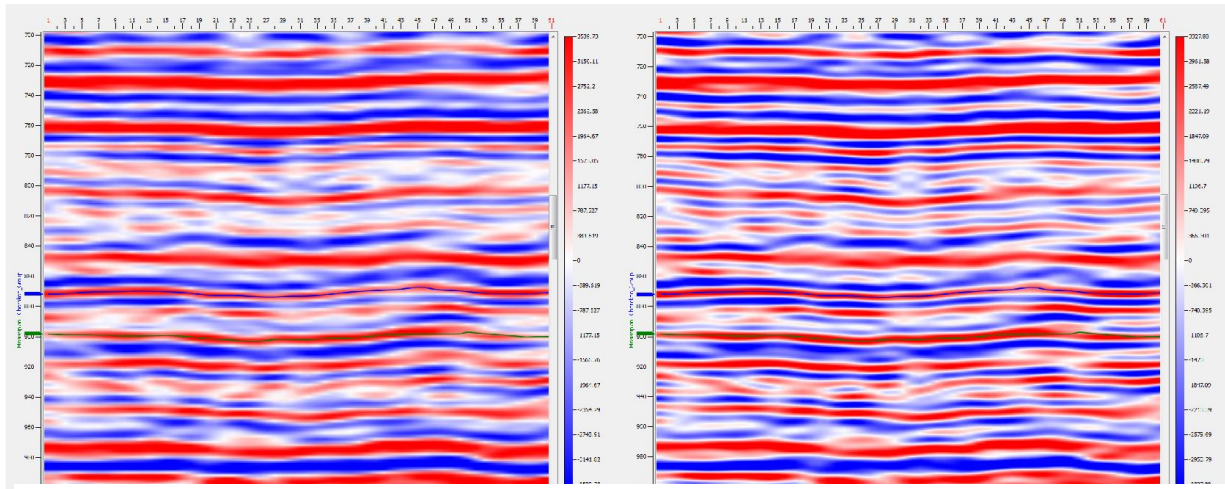


Figure 3.2 Amplitude spectrum for original data (left) and enhanced data using trapezoidal spectral whitening 20-25-110-115Hz (right).



Line 76, Original Data

Line 76, Spectrally Whited Data

Figure 3.3 The original seismic (left) versus the spectrally whited seismic (right)

3.2.3 Acquisition Footprint Suppression

Any amplitude or phase anomaly seen on our seismic data that doesn't correlate with the subsurface geology, but correlates to surface data-acquisition geometry, is defined as acquisition footprint. This results in spatial periodicity in enhanced seismic signal, and in noise rejection caused by spatial periodic changes in stacking fold, source-receiver azimuths and source-receiver offsets, creating artifacts that imitate the source-receiver geometry, where most seismic attributes react to these periodic changes in seismic data. To suppress these data-acquisition footprints we applied a filter on seismic amplitude time slices. The figures below show an example of noise suppression around our area of interest on Figure 3.4 , on original seismic data and enhanced data, where most of the vertical striping seen on the amplitude data shown on the left picture is removed on the right one, followed by most positive curvature attribute calculated from seismic data at different time slices 710 and 850 ms, (Figures 3.5 and 3.6) where attributes that are not affected by acquisition footprints do not show acquisition geometry artifacts and provide us with more accurate interpretation.

Original

Enhanced

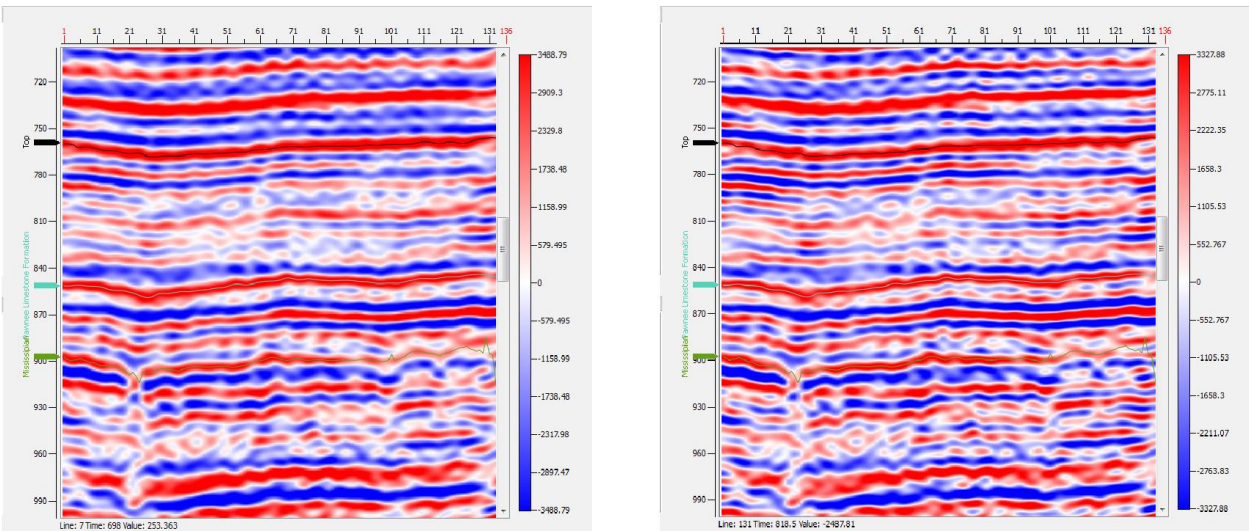
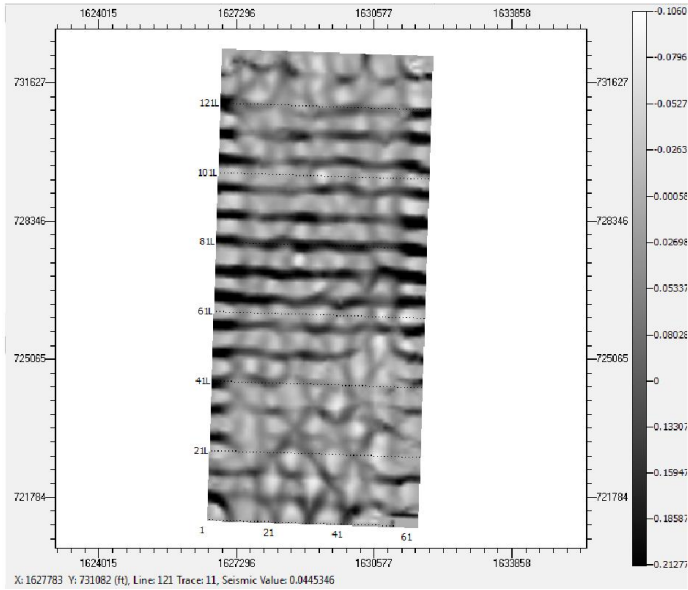


Figure 3.4 Acquisition Footprint in around area of interest Trace 9 Time 700-1000 ms, Original (left) and Enhanced (right).

Original



Enhanced

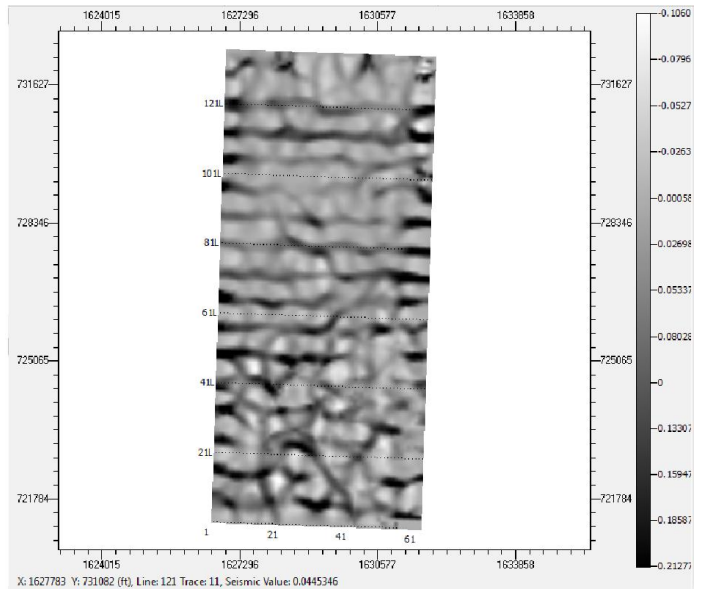
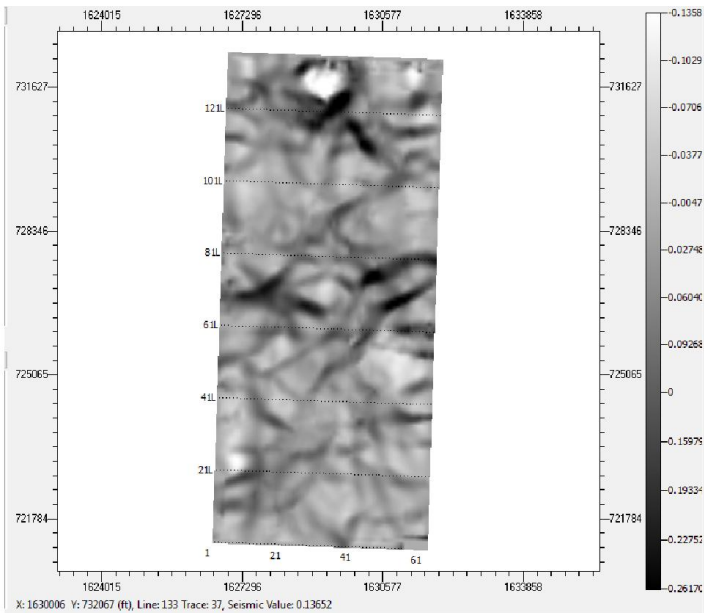


Figure 3.5 Most Positive Curvature, Exp 0.5, Time 710 ms, Original (left) and Enhanced (right).

Original



Enhanced

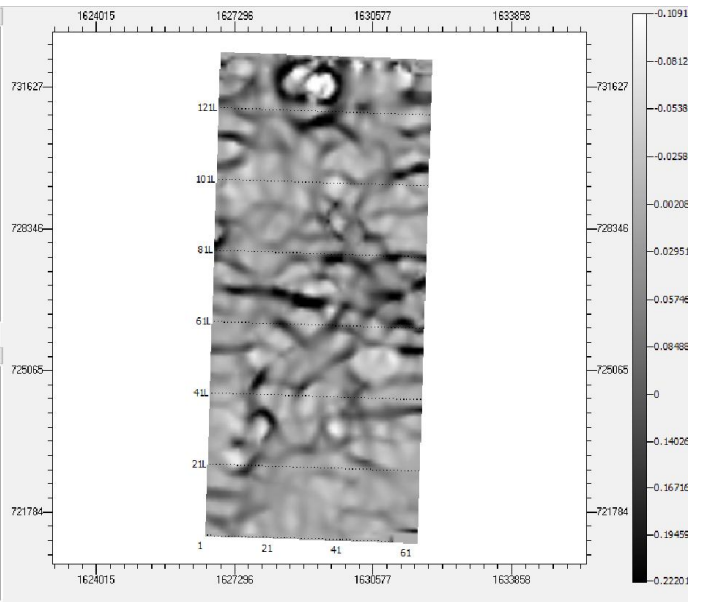


Figure 3.6 Most Positive Curvature, Exp 0.5, Time 850 ms, original (left) and enhanced (right).

3.2.4 Well Ties

The aim of the well ties is to correlate the seismic data at well locations with synthetic seismograms generated at wells to estimate time differences due to processing. Prior to creating the synthetic seismograms, the density and compressional wave sonic log were edited to remove spiky and bad peaks from the logs. A wavelet was derived to better approximate the seismic wavelet in the data. Several types of wavelets were tested including Ricker, band-pass wavelet, and Klauder wavelet. The band-pass wavelet with corner frequencies 20-30-100-120 Hz was used to simulate the seismic wavelet in the data. To account for the right polarity in the seismic data, a phase rotation of 180° (polarity reversal) was applied to the designed wavelet to match the seismic. The amplitude and phase spectra of the wavelet used for the generation of the synthetic seismograms are shown in Figure 3.7. The synthetic seismograms were created only for zero-offset as no shear wave logs were available to use in the modeling. The resulting synthetic seismograms are displayed side by side with seismic data at well locations and velocity and density curves. These are depicted in Figure 3.8 and 3.9 for the five wells: Keith-1, Keith-2, Squier 1-18, Squier A 1-18, and Wierman 1-19.

The obtained results show overall good match between the modeled synthetic traces and the reflection seismic at various well location. This is the case in particular for the Mississippian top.

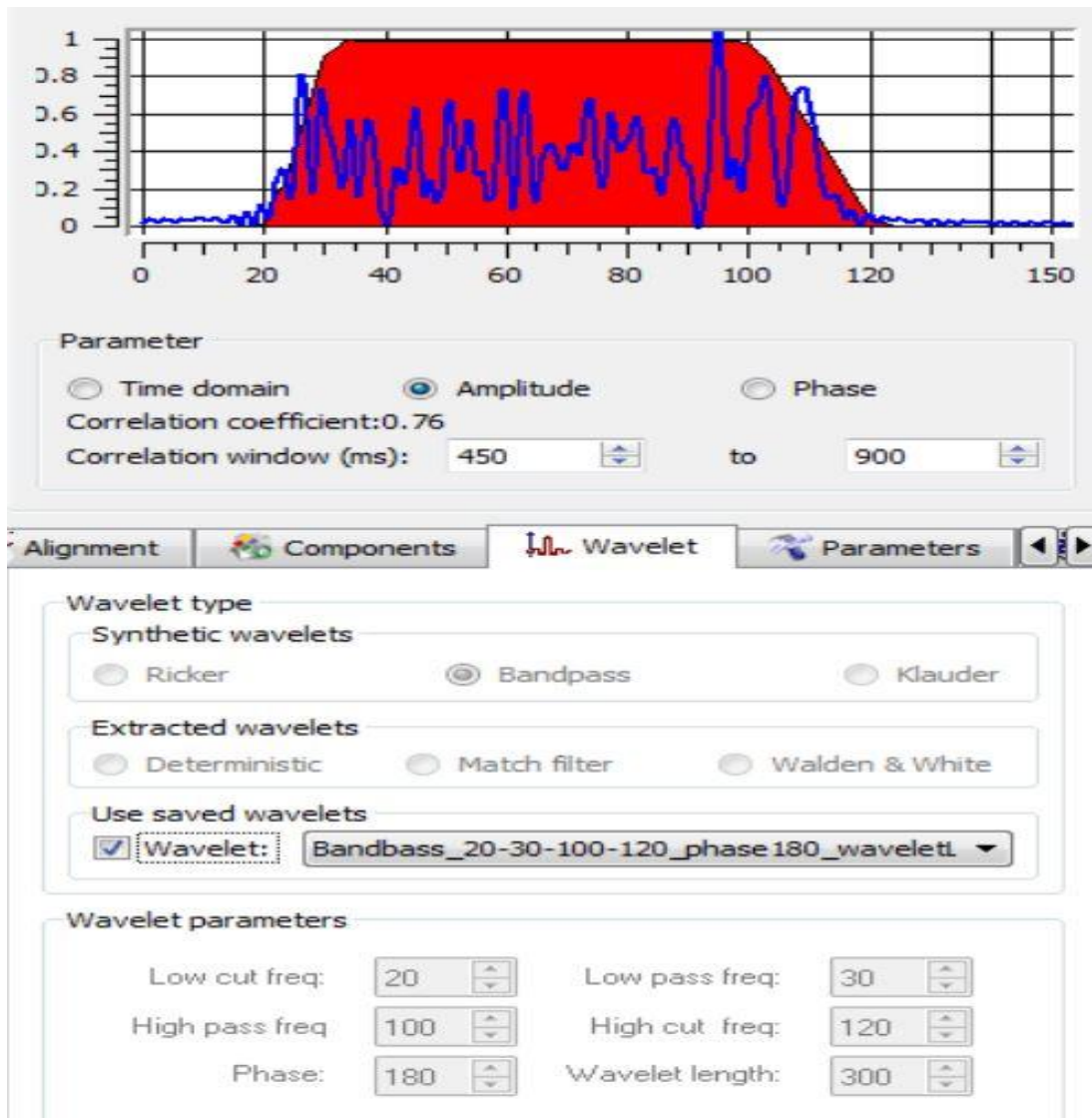


Figure 3.7 The amplitude (red) and phase (blue) spectra of the generated wavelet for the synthetic seismograms.

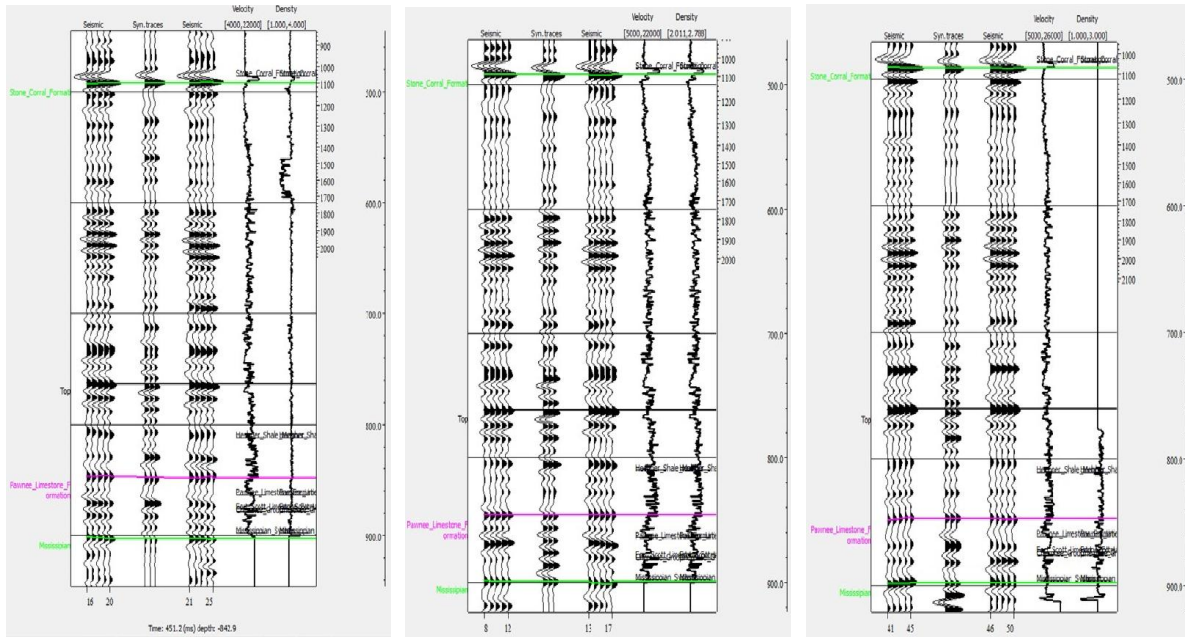


Figure 3.8 Seismic well ties for Keith 1 (left), Keith 2 (center), Squier 1_18 (right).

Displays from left to right: seismic section at well location, synthetic seismogram at well, seismic at well, P-wave velocity (from sonic) and density logs.

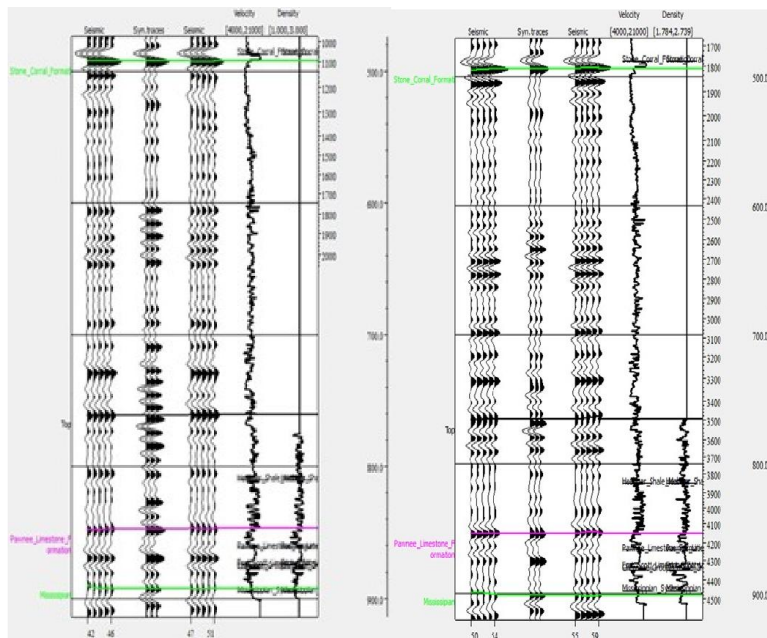


Figure 3.9 Seismic well ties for Squier A 1_18 (left) and Wierman 1_19 (right). Displays from left to right: seismic section at well location, synthetic seismogram at well, seismic at well, P-wave velocity (from sonic) and density logs.

3.2.5 Fault Imaging

Volumetric curvature (Al-Dossary and Marfurt, 2006) is easy to run and an efficient process that helps in mapping small fault networks in detail not easily seen by interpreters. This is achieved by transforming seismic data into dip vectors that enables the identification of small faults associated with changes in the computed dip vectors, to run volumetric curvature we only need the seismic data (no horizons, no well ties).

There are a number of volumetric curvature attributes provided by **CYRSTAL** for imaging faults and fractures that can be identified from seismic data. The most positive curvature was run on both original seismic and spectrally whitened dataset. The results are illustrated in Figure 3.10 for a time slice at 850 msec (Pawnee Limestone formation) and show a dramatic improvement in highlighting channels when the spectrally enhanced seismic was used as input. A total of 8 faults were identified on the seismic volume in addition to the delineation of a feature in the North part of the section that may be the result of processing or signal-to-noise artifact (Figure 3.11). These results prove again the benefit of the conditioning applied to the input dataset where the enhancement of the high frequencies through the whitening process helped in better defining faults in the area of study.

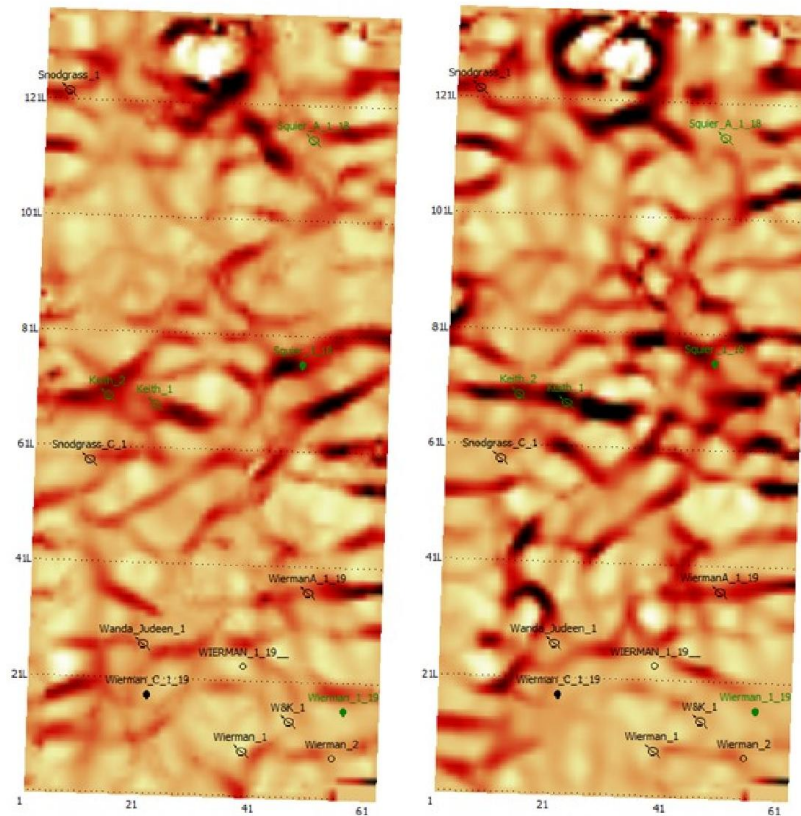


Figure 3.10 Most Positive Curvature at time slice 850ms of the original seismic (left) versus the spectrally whitened seismic (right) (Pawnee Limestone formation). Structural features (Faults and fractured zones) and delineation of a feature in the North part of the section that may be the result of processing or signal-to-noise artifact

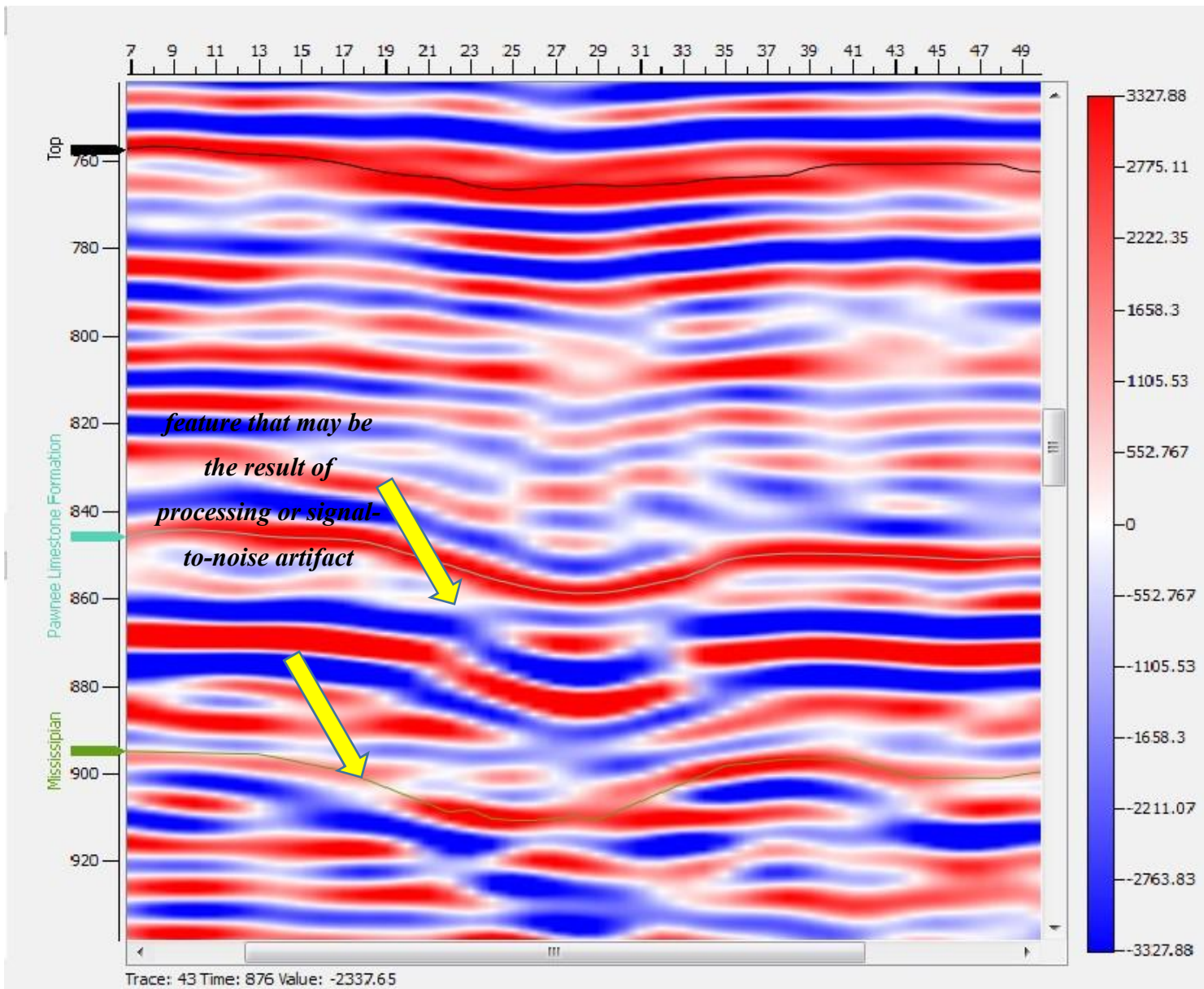


Figure 3.11 A seismic line going from East to West showing a feature that may be the result of processing or signal-to-noise artifact.

3.2.6 Spectral Attributes

Spectral attributes generate a great number of attributes. The two most important are total energy and max amplitude above average. These attributes best reflect the geologic features in the seismic data.

Spectral decomposition is a technique that decomposes seismic data into the time-frequency domain, which contains useful information for layer thickness estimation (Partyka et al., 1999; Puryear and Castagna, 2008), stratigraphic interpretation (Marfurt and Kirlin, 2001; F2005). We can generate many spectral decomposition algorithms and frequency attributes from spectral decomposition volumes. Spectral decomposition uses the wavelet transform to decompose the broad-band seismic signal into discrete sub-bands. CRYSTAL uses two types of spectral attributes one of them is narrow frequency sub-band attributes derived from Spectral Decomposition. The spectral attributes represent information derived from the analysis of the power spectrum at individual samples. For example, Total Energy is the sum of the energy (amplitude squared) in all of the sub-bands, performed on a sample-by-sample basis.

In Figure 3.12, the max amplitude above average and total energy maps in the Cherokee group point out a feature that may be the result of processing or signal-to-noise artifact, highlighted by the yellow box, that was also seen with the curvature attribute discussed previously. Similarly, a broken up channel highlighted by the red box can be seen.

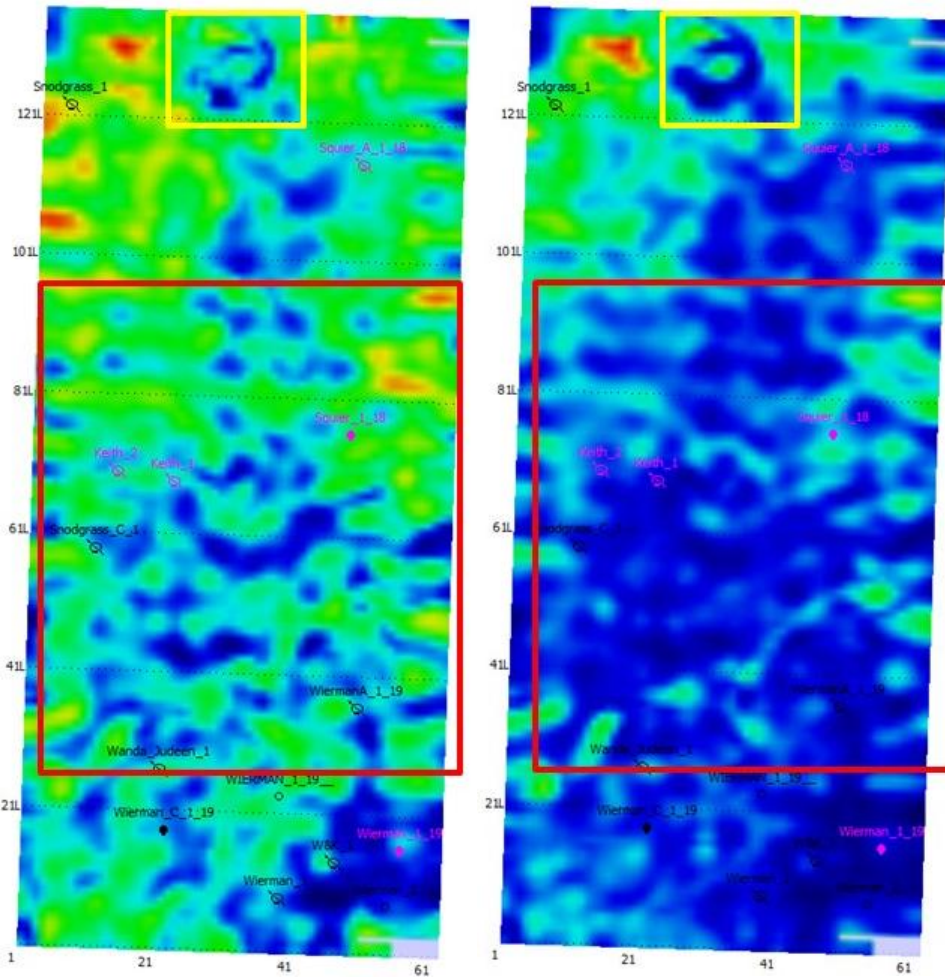


Figure 3.12 Total energy map (left) and maximum amplitude above average map (right) in the Cherokee group of the spectrally whitened seismic. The yellow box points out a feature that may be the result of processing or signal-to-noise artifact, and the red box points out a broken up channel.

3.2.7 Structural framework

Using the horizons and the 8 interpreted faults a structural framework (Figure 3.13) was built for the inversion and geologic modeling.

Structural Framework Model is a Polygon defined by horizons and faults in the time or depth domain. This polygon defines boundaries which are honored during inversions and in the creation of geologic grids, hence creating inversions and grids that are more geologically accurate than would otherwise be possible. 8 faults from the Geophysical model are included. Viewed from the West of the survey. This is in TIME! Times 10 exaggeration.

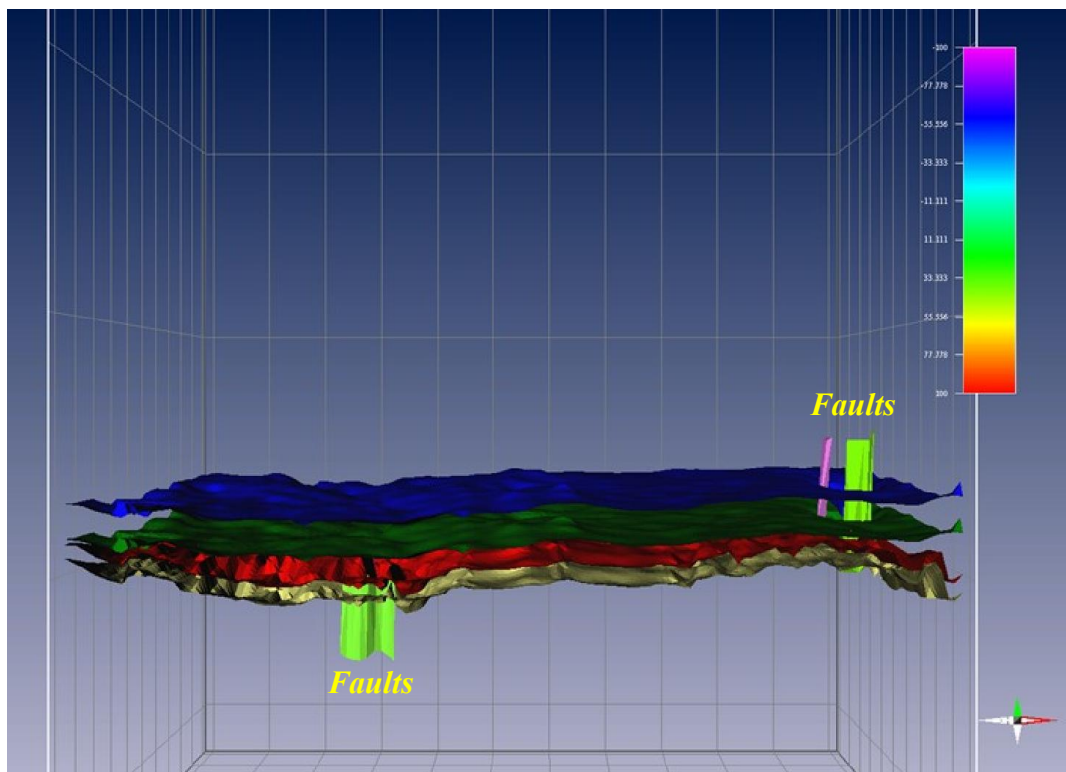


Figure 3.13 Framework Model

3.2.8 Post-Stack Inversions

Seismic inversion is done through inverting seismic data into elastic properties of the reservoir, which helps in the generation of more a precise rock property model, and to do inversion in CRYSTAL software a minimum amount of input data is needed.

The aim of post-stack acoustic inversion is to estimate a model for acoustic impedance from seismic data that will help in better understanding rock properties, and providing laterally continuous information that cannot be obtained from well locations, which is an important input for reservoir characterization. There are several inversion methods for acoustic impedance which vary in resolution and computing time. Five inversion methods were run to produce acoustic impedance volumes in the area, which were checked against an acoustic impedance log computed at the five well locations.

Before running any of the post-stack inversions, a background framework model was built using seismic data and information from well logs in the area, except for the colored inversion, which can be done without a background model, with the result of relative, not absolute, impedance.

Background Impedance Model:

- Seismic
 - Spectrally Whitened
- Wavelet used for well ties
 - Bandpass, 20-30-100-120 Hz,
 - 180 deg phase
 - 300 ms length
- Wells Used
 - Keith 1, Keith 2, Squier_1_18, Squier_A_1_18, Wierman_1_19
- Extend Mode: SSI
- Power For Inverse Distance Interpolation
 - 2

3.2.9 Inversions theories:

1. Sparse spike (SSI) & Deterministic inversion (DI)

The parameters for deterministic inversion (DI) are nearly identical to that of sparse spike inversion (SSI). In sparse spike and deterministic inversion, using an impedance model allows inversion to use frequencies above and below the seismic bandwidth. Lower frequencies that range from (0 - 10HZ) are needed to scale the inversion result to absolute impedance, higher frequencies are used to increase the frequency content of the resulting impedance. Without an impedance model, the inversion process is limited to the seismic bandwidth, resulting in relative impedance values.

2. Generalized linear inversion (GLI)

In the generalized linear inversion (GLI), (Cooke and Schneider, 1983), a background model is required in addition and the process is implemented iteratively until convergence is reached. GLI method is a model-based approach, which is sometimes known as model perturbation, it perturbs the background impedance model until a suitable match with the seismic is found. The background model is updated gradually and steadily. After a perturbation is made to the background model the reflectivity is convolved with the wavelet and compared to the seismic trace. If the resulting synthetic trace matches the seismic trace to within a user-determined threshold, the process stops and acoustic impedance is computed from the reflectivity series, operating parameters used are shown on Figure 3.14.

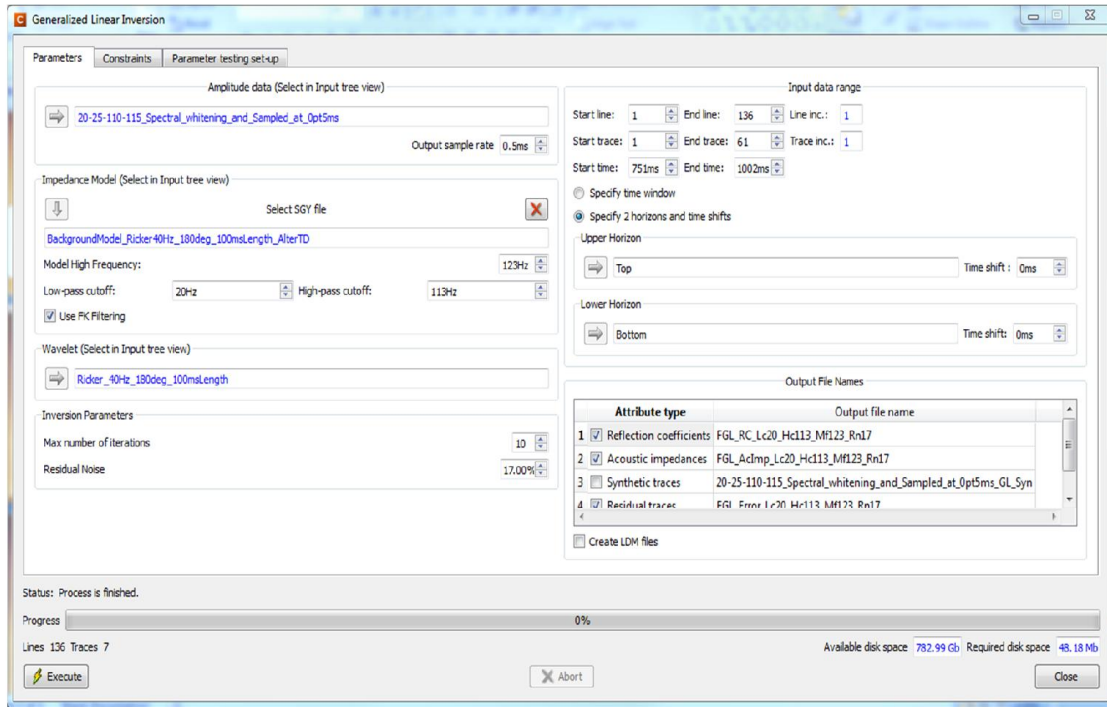


Figure 3.14 Operating parameters low pass cut off and high pass cut off

3. Colored inversion

Colored inversion (Lancaster and Whitcombe, 2000) converts seismic amplitude traces to seismic impedance traces (relative colored impedance traces if no frequency component (Background or impedance model) is added; absolute colored impedance traces if a frequency component is added), the latter colored inversion has been used. Absolute colored inversion is accomplished by convolving the input amplitude data with a filter that converts the amplitude data to impedance data. This inversion process does not require a wavelet (no wavelet extraction is needed). As the inversion is accomplished by convolving a filter with the data, the process is very quick. The inversion result provides the geophysicist with an impedance section with a minimum of effort, but before calculating a colored inversion, we must derive a “colored inversion operator”, which is a deconvolutional operator derived by comparing the seismic and log data that will transform the seismic amplitude to relative impedance values.

- **The colored inversion operator (convolution operator):**

After testing the Colored Inversion Operators, the 150ms length was chosen as a **convolution operator** because it creates the best match between the synthetic response and the

approximated log response within the seismic bandwidth. (See the figures below, the screen shots of the colored inversion operator, parameters and results, as seen on Figures 3.15, 3.16, 3.17, 3.18 respectively).

- Colored Inversion Operator Parameters:

- Operator Length: 150ms
 - Avoid low freq. noise below 7.5 Hz from being used in the inversion process.
- Polarity: 180 degrees
 - The phase used for well ties.
- Noise Related Coefficient: 1.0
 - To preserve the seismic bandwidth and not force an artificial frequency response.
- Wells Used: Keith 1, Keith 2, Squier 1-18, Squier A 1-18, Wierman 1-19
 - These wells have well ties.

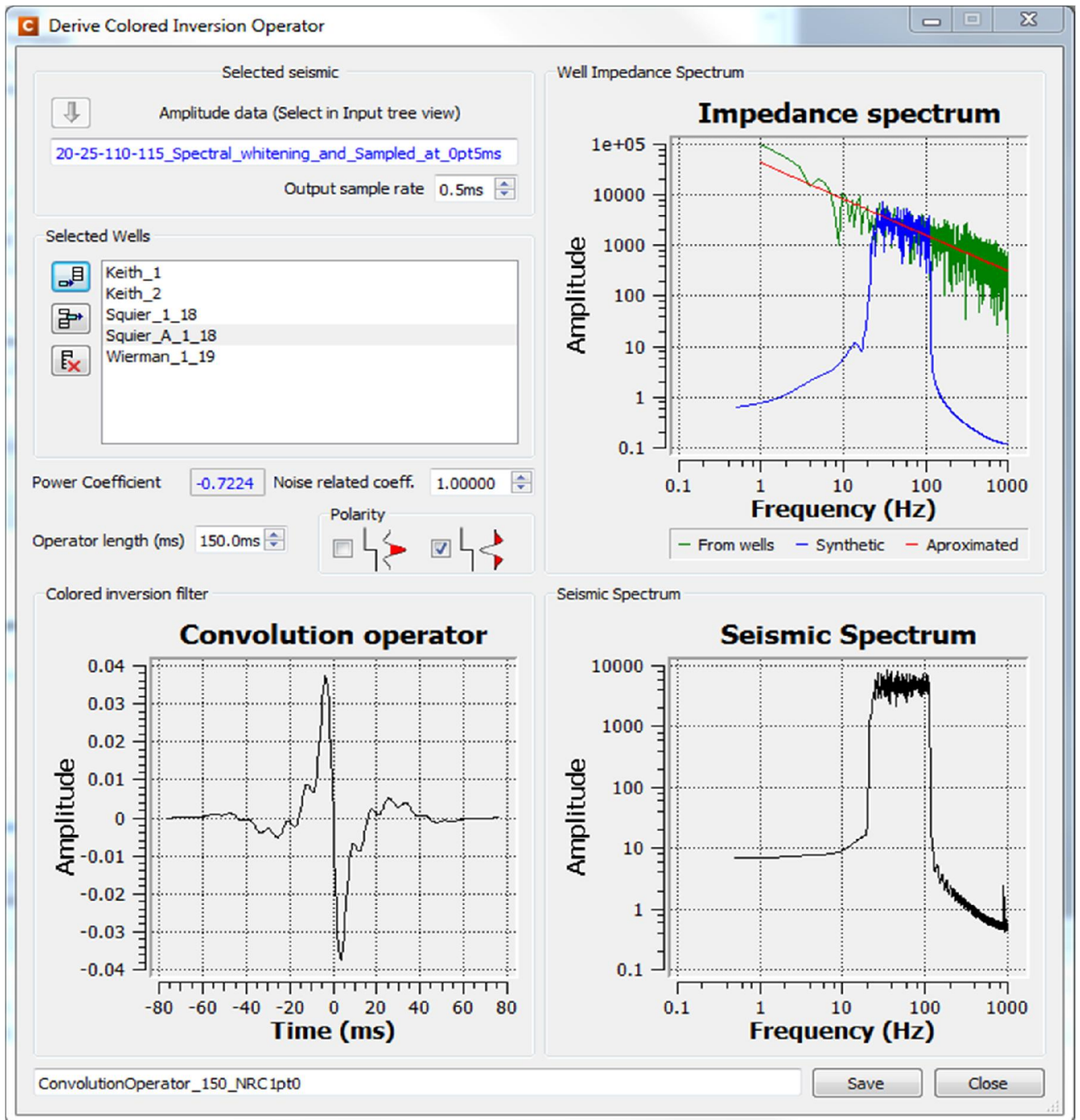


Figure 3.15 Colored Inversion Operator Parameters: Length: 150ms , NRC: 1.0

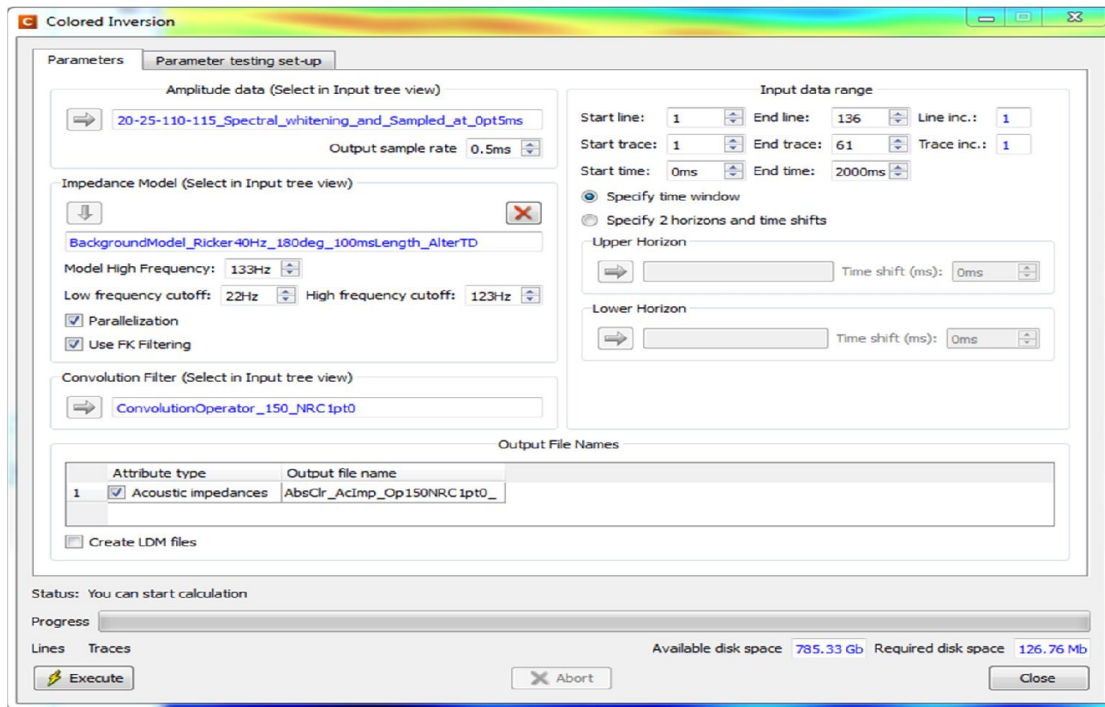


Figure 3.16 Absolute Colored Inversion Parameters @ Time 850ms

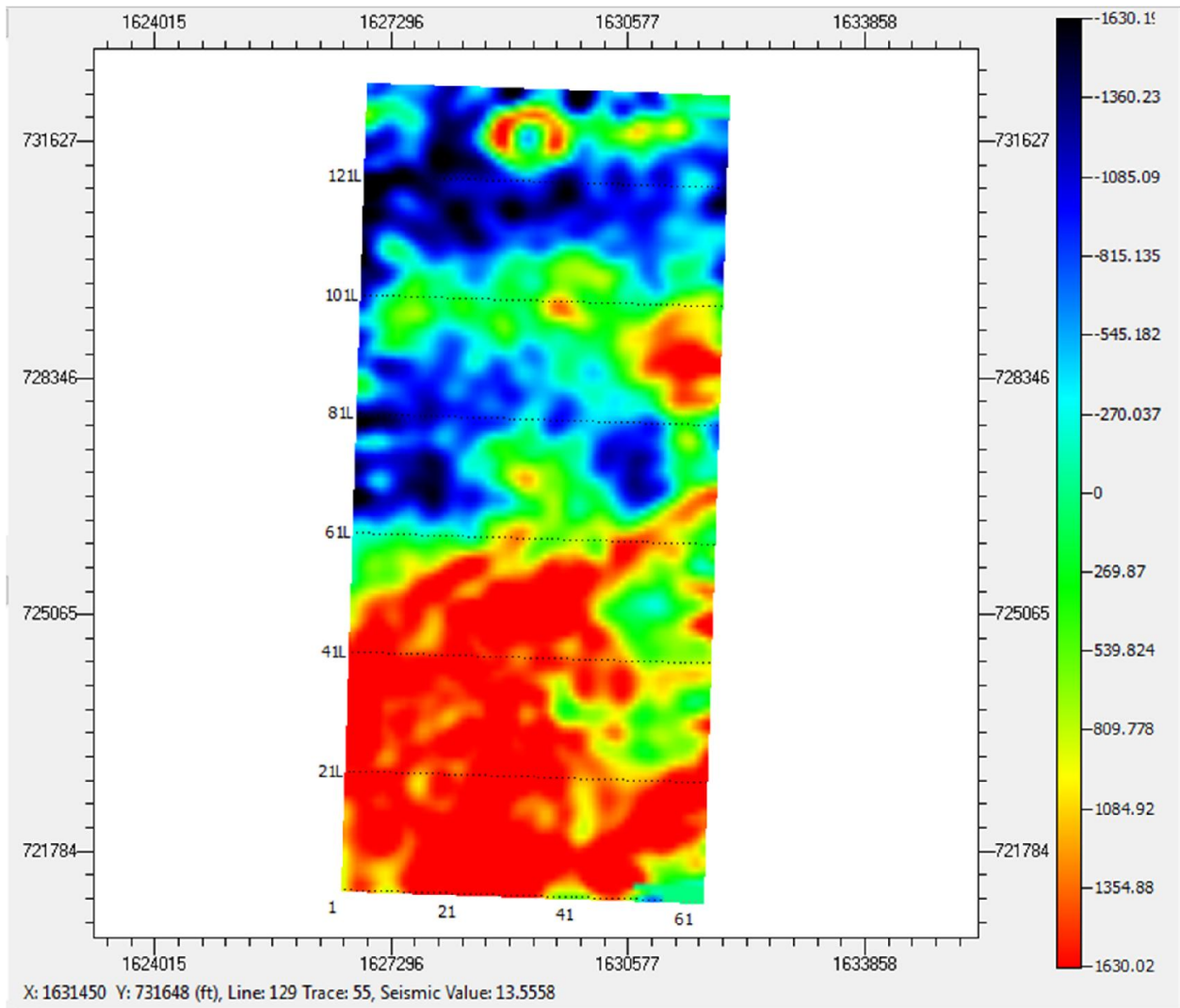


Figure 3.17 Colored Inversion Result @ Time 850ms

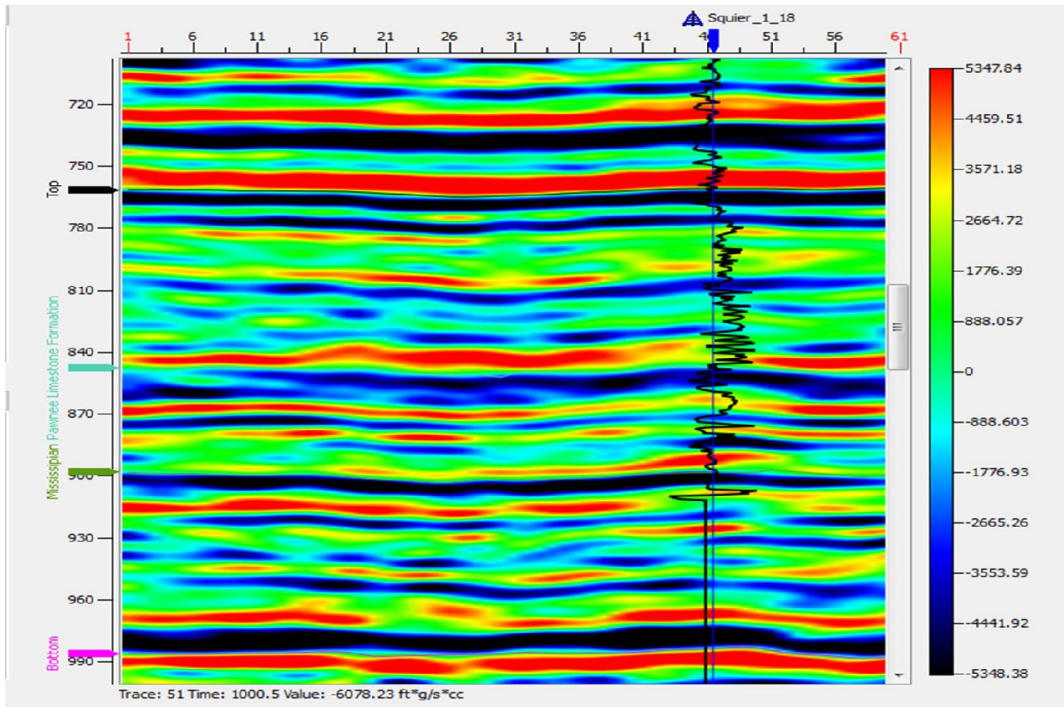


Figure 3.18 Picked Absolute Colored Inversion Low Pass 22Hz, High Pass 113 Hz, Model High Frequency 123Hz @ Line 76 700-1000ms / Length 150ms, NRC 1.0

4. Stochastic inversion

Stochastic inversion (SI) (Haas and Dubrule, 1994) does not require a background model since it uses geostatistics, and it takes into account both seismic and well logs (Sonic and density) , it generates a large number of possibilities (predictions) of impedance traces at each seismic trace location. The impedance trace which produces the best correlation between the synthetic trace (generated from the impedance trace and an input wavelet) and the actual seismic trace is retained. As these equally probable impedance traces are generated from the impedance log data, the resulting inversion has the resolution of the logs at the output time sample rate, and therefore produces a very high resolution inversion. I used Absolute Colored Inversion (CI) as soft data with 0.4 correlation coefficient to further constrain the possibilities of the output impedance, as seen on Figure 3.19.

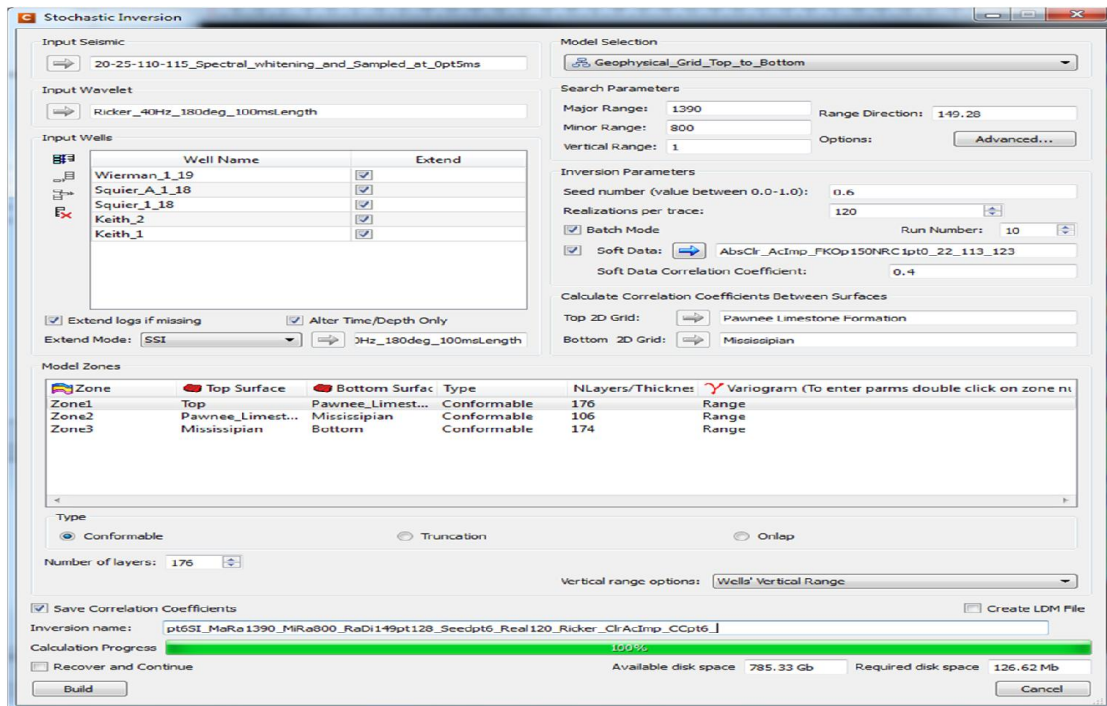


Figure 3.19 Stochastic Inversion Parameters @ Time 850ms using Absolute colored inversion as Soft Data

3.2.10 Inversions results:

Figures 3.20 through 3.24 depict inversion results at Squier 1-18 well using sparse spiking, deterministic inversion, colored inversion, GLI, and stochastic inversion, respectively. The latter method has produced the highest resolution power in retrieving detailed information on the acoustic log (shown in black color) at the well position. Local impedance peaks were successfully identified via stochastic inversion where the other methods fail to produce similar resolution. The inversion results have the advantage of producing acoustic impedance values down to the maximum recording time while the log values are limited by the maximum logging depth. This also applies to the Cherokee group, located in the time range between 870 and 900 msec, which is our area of interest.

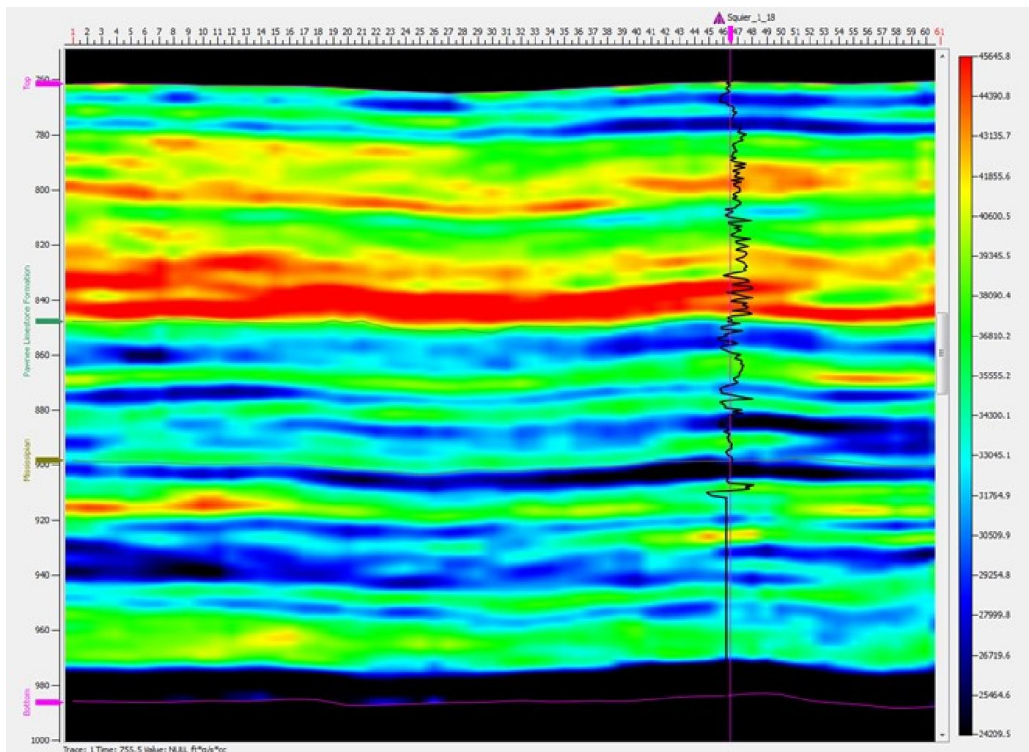


Figure 3.20 Post-stack inversion of acoustic impedance via sparse spike inversion at Squier 1-18 well.

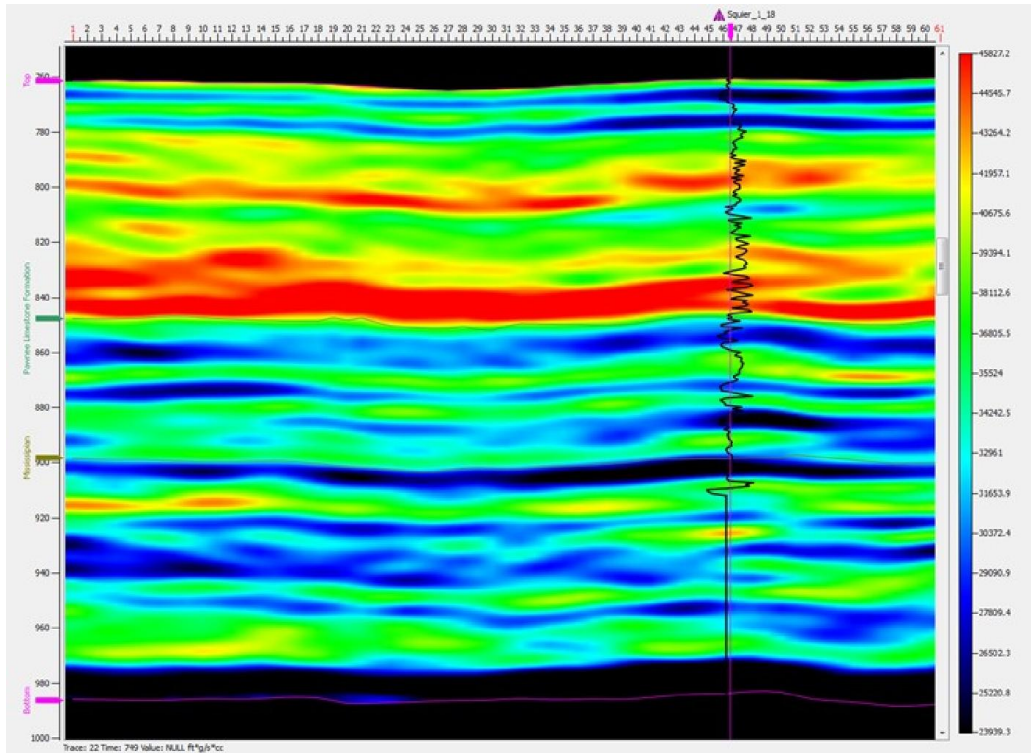


Figure 3.21 Post-stack inversion of acoustic impedance via deterministic inversion at Squier 1-18 well.

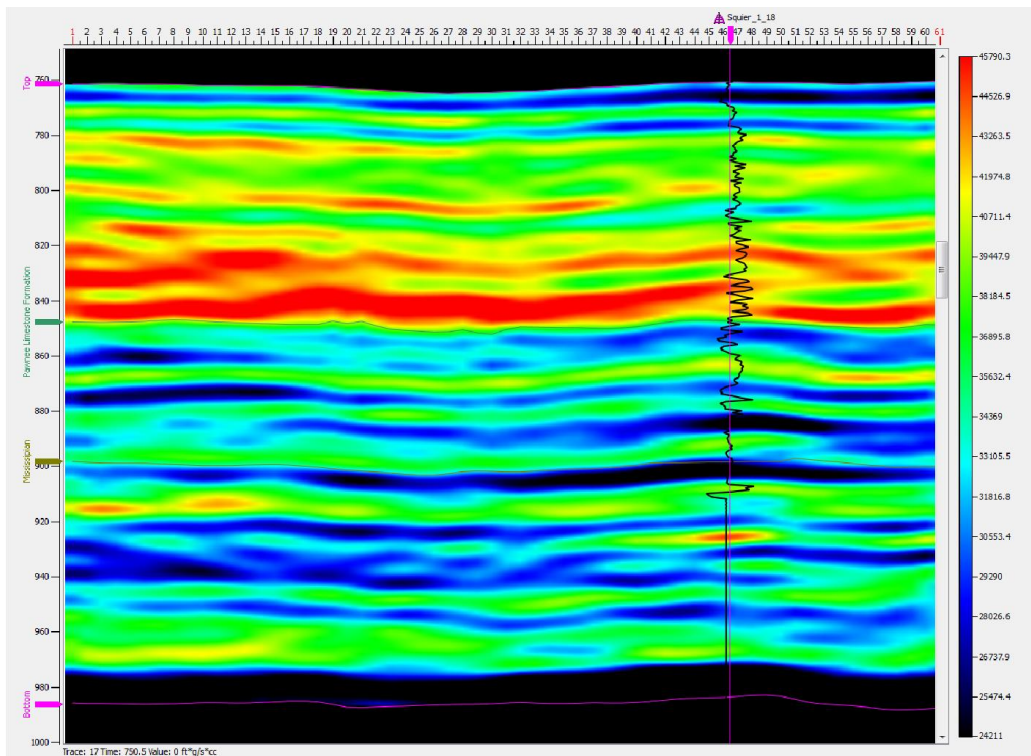


Figure 3.22 Post-stack inversion of acoustic impedance via colored inversion at Squier 1-18 well.

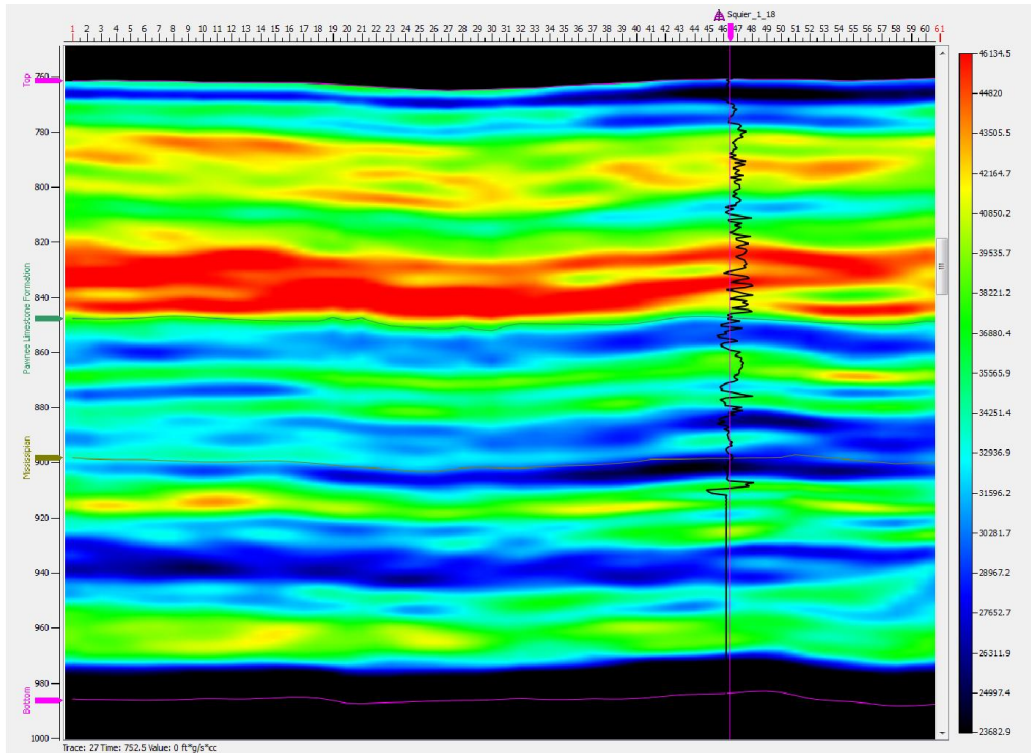


Figure 3.23 Post-stack inversion of acoustic impedance via GLI at Squier 1-18 well.

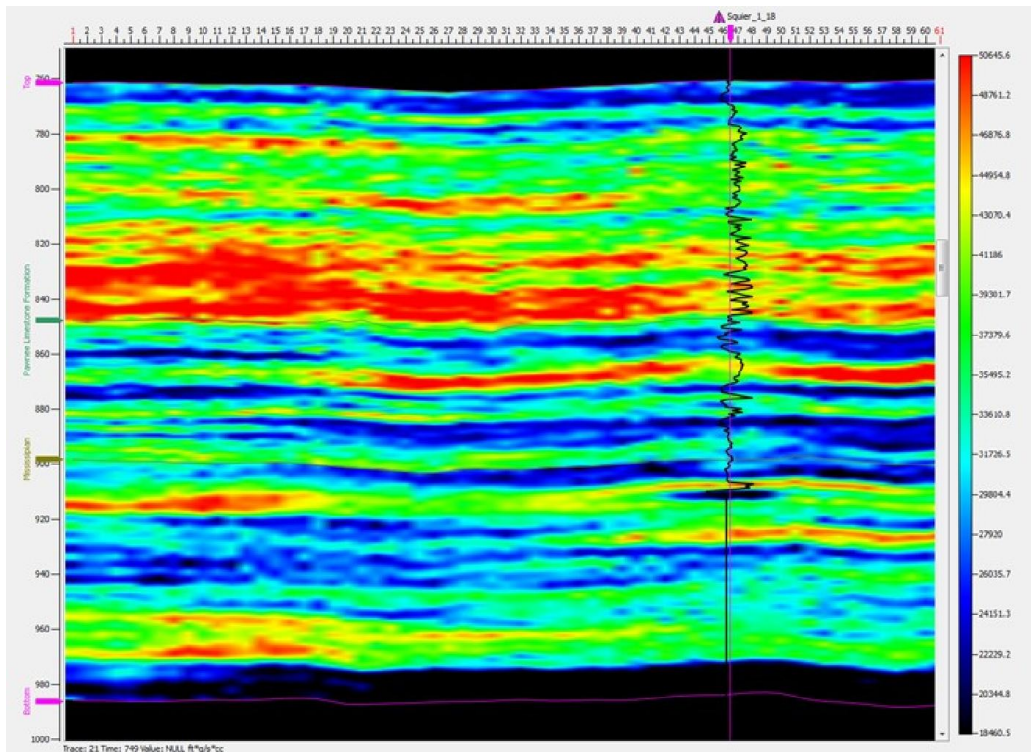


Figure 3.24 Post-stack inversion of acoustic impedance via stochastic inversion at Squier 1-18 well

Figure 3.25 illustrates extracted acoustic impedance traces at Squier 1-18 well location. The comparison of the various inversion techniques favor the stochastic inversion method which were able to reveal the impedance variations beyond the resolution limits of the other algorithms being tested.

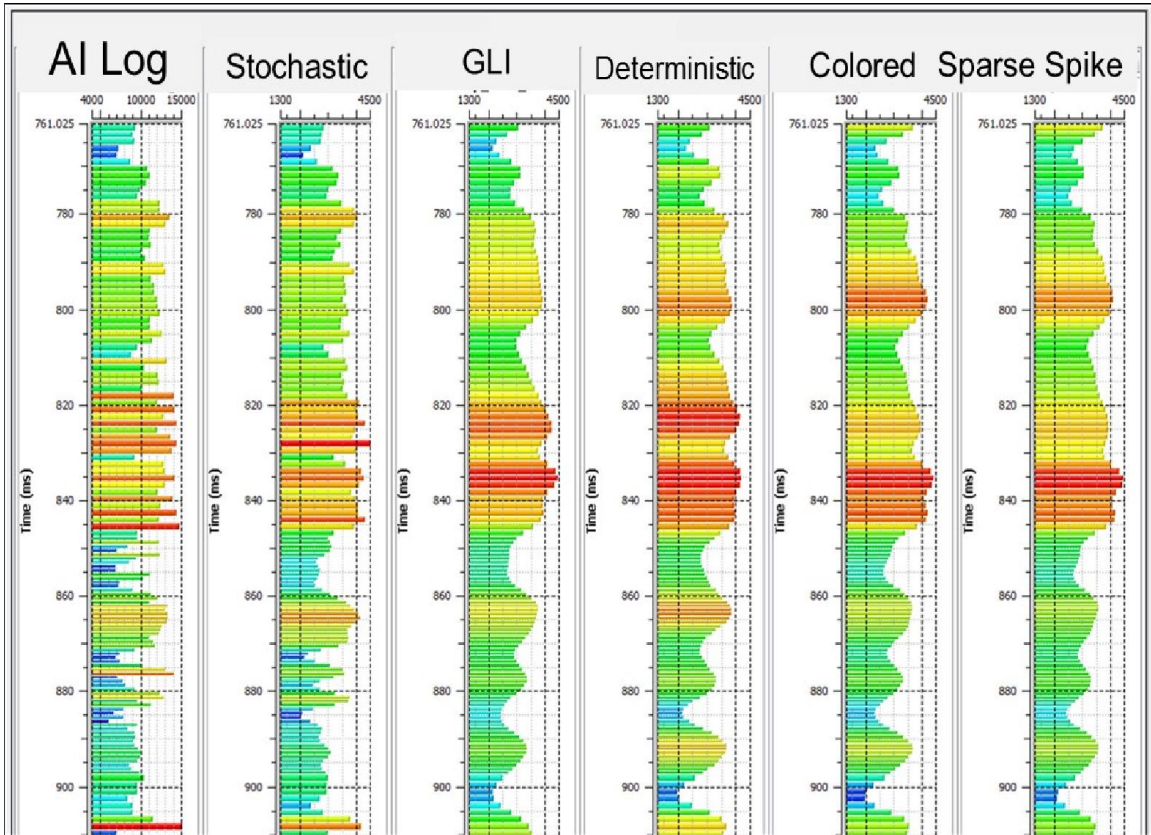


Figure 3.25 Post-stack inversions of acoustic impedance at Squier 1-18 well using the various inversion methods. From left to right: acoustic impedance computed at well, stochastic inversion, GLI, deterministic inversion, colored inversion, and sparse spiking inversion

The five inversion algorithms have been implemented on the full stack volume and produced acoustic impedance attribute volume which covers the full seismic volume. For brevity, only the inversion results using the stochastic inversion on the four remaining wells are shown due to its resolution power compared to the other inversion methods being tested on Squier 1-18.

Figures 3.26 through 3.28 show the inversion results using the stochastic inversion method for acoustic impedance around wells Squier A 1-18, Keith-1, Keith-2, and Wierman 1-19, respectively. The obtained results on these wells confirm the conclusions made on Squier 1-18 well, where the stochastic inversion shows a great resolving power of impedance variations details observed on the original computed logs. This gives the method more confidence away from well locations when it compares to other existing algorithms.

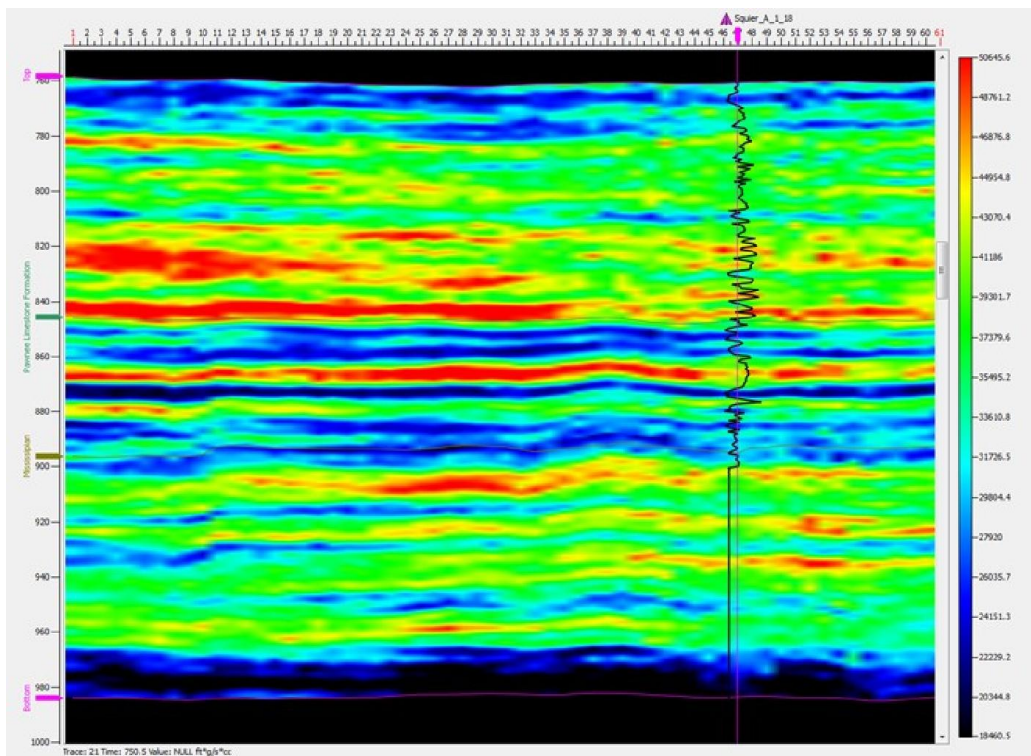


Figure 3.26 Post-stack inversion of acoustic impedance via stochastic inversion at Squier A 1-18

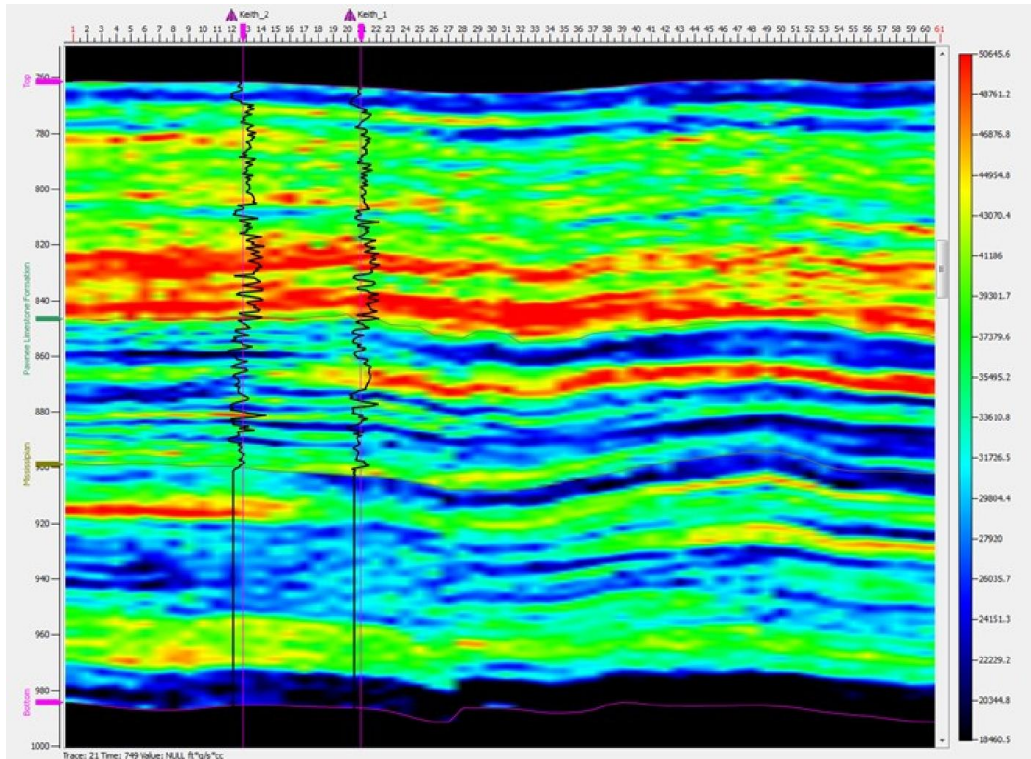


Figure 3.27 Post-stack inversion of acoustic impedance via stochastic inversion at Keith-1 and Keith-2 wells.

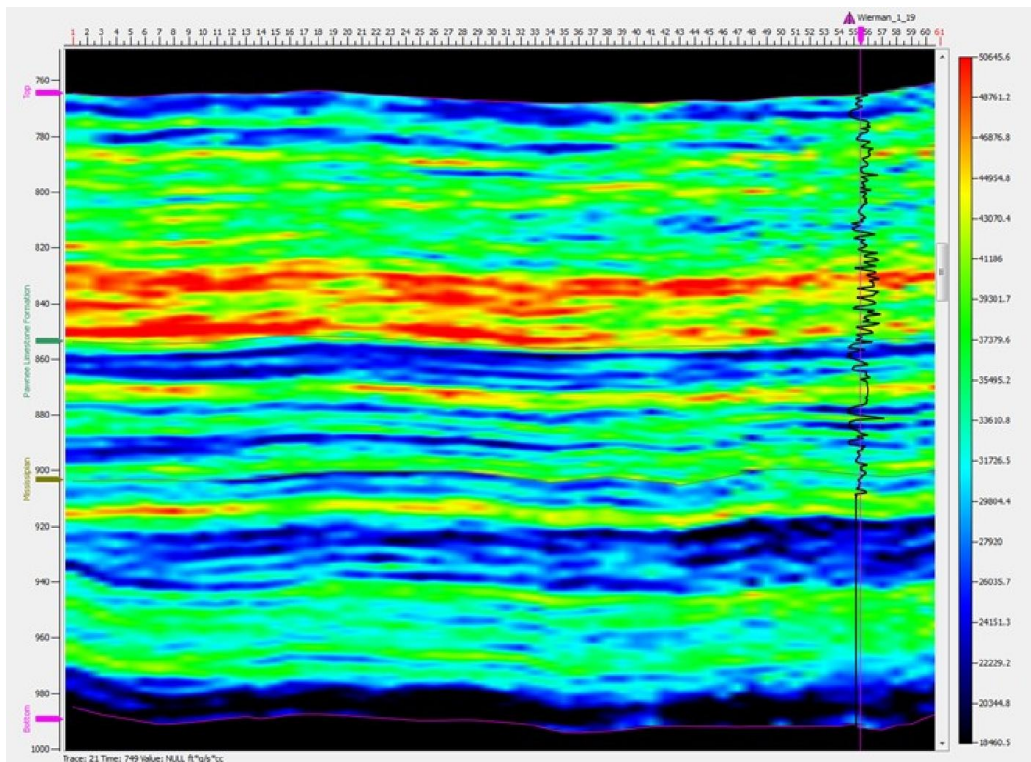


Figure 3.28 Post-stack inversion of acoustic impedance via stochastic inversion at Wierman 1-19

3.3 Geological Modeling

3.3.1 Summary

The geological modeling has been prepared using a plethora of seismic attributes, these attributes have been used quantitatively to model reservoir properties where each tells something different about the reservoir. The 3D geocellular grid in the time domain is converted to depth and all post stack attributes are snapped and used simultaneously for the geologic modeling. Sequential geologic modeling approach (Ouenes et al. 2007) is used to generate various geological 3D models and the models constructed were:

1. Gamma ray model
2. Porosity model
3. Pay model (Sweet Spot Model)

For each model, all the seismic attributes (Curvature, spectral attributes and inversions) and the previously derived geologic models are used simultaneously in a neural network process. These models were constructed by CRYSTAL's neural network, which attempts to find a relationship between rock property logs at all the wells, except for one blind well, and the multitude of seismic attributes, in other words, Neural Network looks for a relationship between the seismic attributes and well logs and once it finds an equation it propagates it in the whole grid (Upscaling). Several realizations were developed for each model and were tested against the blind well for model's accuracy.

3.3.2 3D Geocellular Grid

To create our rock property models, a structural framework is needed. This includes the faults and horizons that were picked in previous steps. This framework is then used to build a 3D grid. The 3D grid in this project is the volume represented by the Cherokee group. Originally this grid is in time, but it is later converted to depth before any modeling occurs. The final depth grid ended up having the following parameters:

Number of cells in the X direction $NX = 60$

Number of cells in the Y direction $NY = 135$

Number of layers in the Z direction $NZ = 60$

A Cells DX and $DY = 82\text{ft}$

A Cells Thickness $DZ = 2\text{ft}$

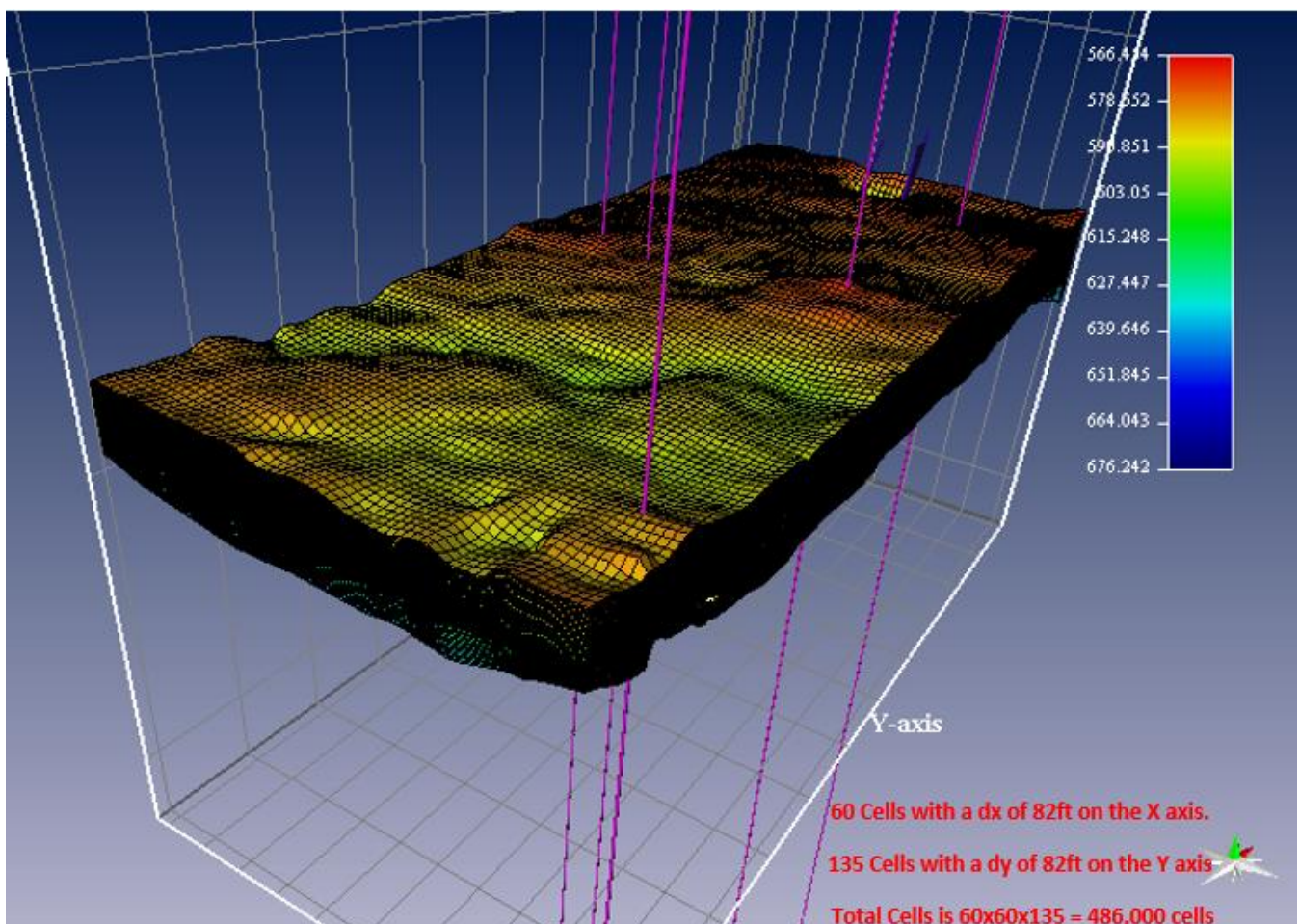


Figure 3.29 3D Geocellular Grid

The resulting number of cells is 486,000 cells. It is important to note that all the layers are conformable and that the total number of layers was divided into three zones based on analysis of the well logs.

Figure 3.30 displays the bounding horizons of the three zones and notes that the first zone has 28 layers, the second zone has 18 layers, and the third zone has 14 layers. The top horizon is the Cherokee group top in blue and the bottom horizon is the Mississippian horizon in yellow. It is important to note the grid displayed has a vertical exaggeration of 10 times.

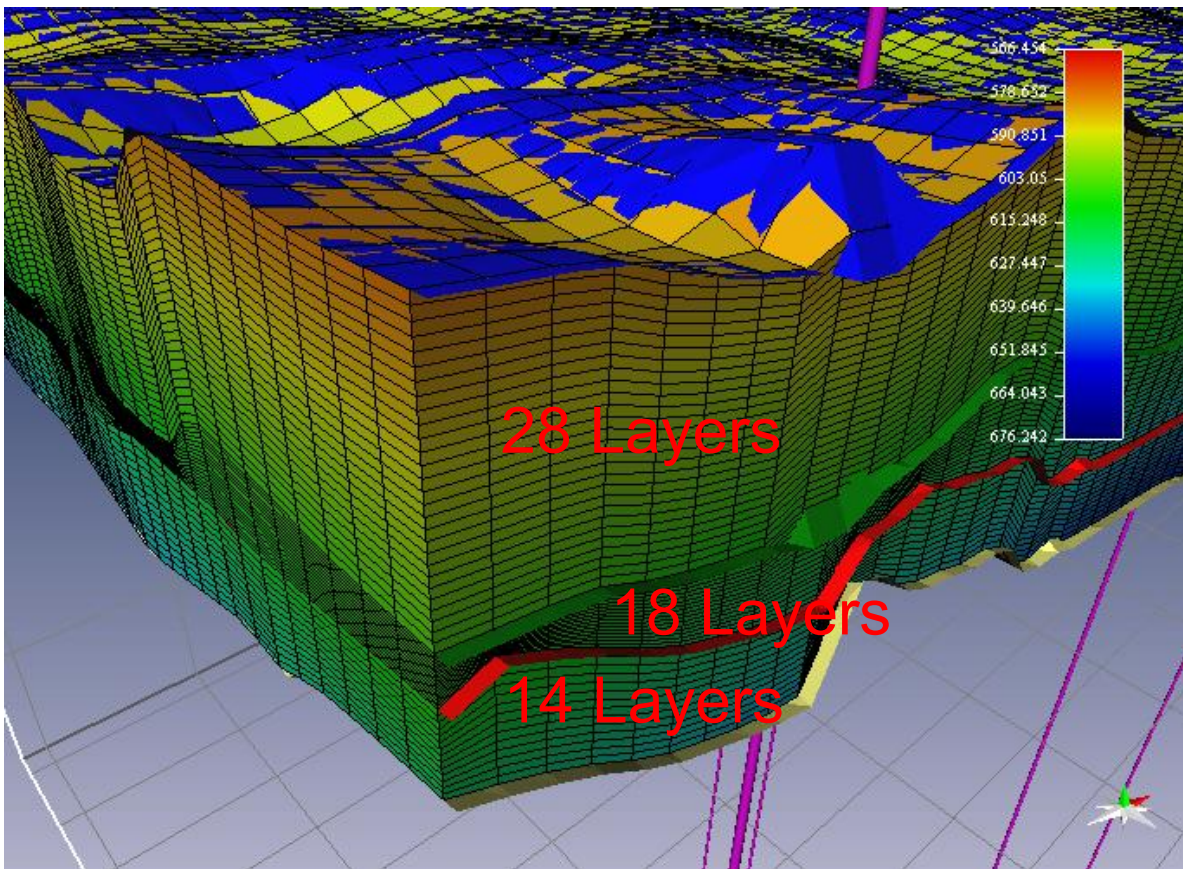


Figure 3. 30 The geologic grid used for modeling. This grid is divided into three zones where the first zone has 28 layers, the second zone has 18 layers, and the third zone has 14 layers.

Visualization of the grid with edges and horizons toggled on

3.3.3 Facies Model Possibility

From well log character of the Cherokee group, it can be seen that this group is not one clean sandstone. There is significant variability, which include shales, and a spectrum of clean and dirty sandstones. A cross plot between impedance and GR, signifies a cluster of clean sand that has a low gamma ray, the blue line signifies the linear regression. This was confirmed by the cross plot between gamma ray, impedance, and porosity logs of Squier 1-18. In this manner several different types of facies are recognizable, as seen in Figure 3.31.

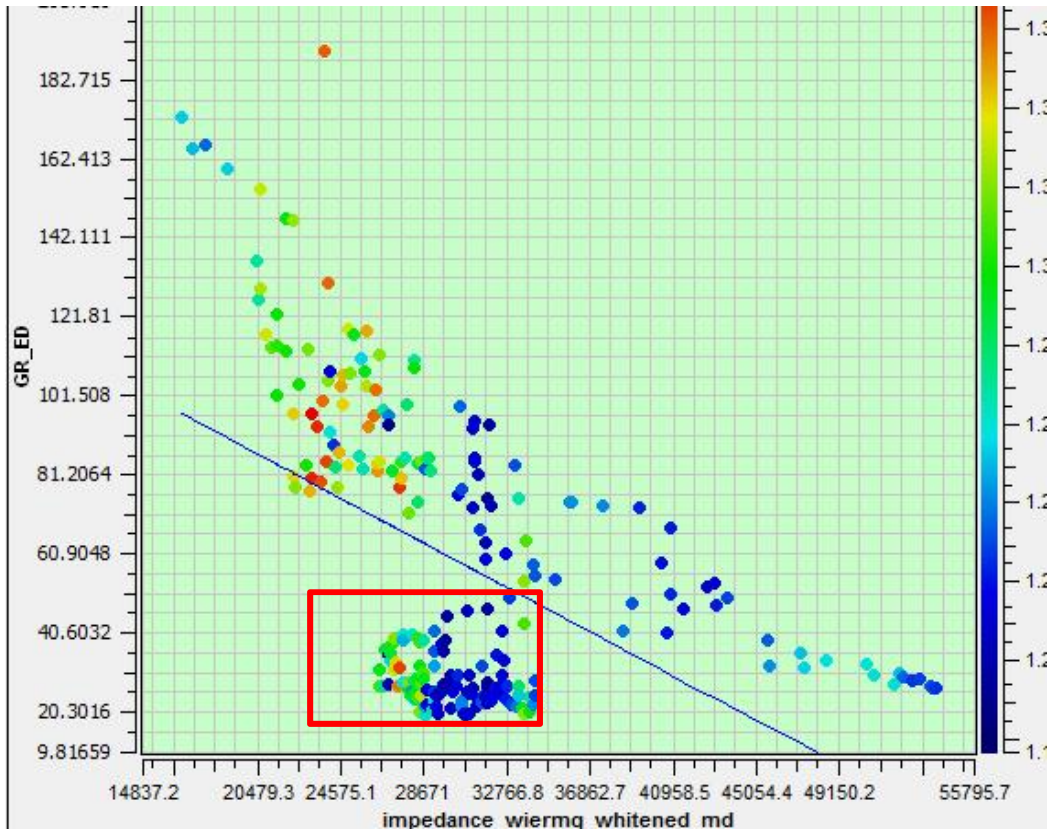


Figure 3. 31 Cross plot between the gamma ray, impedance, and porosity (color scale) logs of the Squier 1-18 well, red box is clean sand, blue line represents the linear regression line fit to the data. Different facies cluster on the plot.

It is important to note that it is difficult to tell between the different types of sand and shale. The isolated group, highlighted by a red box is clean sand. From this cross plot, we concluded that a facies model would not be possible and that pre-stack data would be needed, we saw multiple points within the cross plot that have the same impedance but different GR and

porosity values, we would need pre-stack data to be able to distinguish between the different facies by looking at V_p , V_s and density instead of just acoustic impedance) to distinguish between the different facies. (Hard to see a good separation between different facies, cross plots of impedance vs. gamma ray vs. porosity point to a very complicated geology).

3.3.4 Porosity Model

The input to this model are the porosity logs and the constraints are the multiple seismic attributes generated previously. With these parameters, the neural network will generate multiple realizations where each realization is judged on its ability to predict the blind well not used in the modeling. The blind well chosen for the porosity model is Keith-1. This particular model did extremely well at predicting the Keith-1 well, as seen in Figure 3.32.

- Attributes chosen in porosity modeling of Zone 1: are SubBand, Azimuth Curvature, Absolute Colored Inversion, Stochastic Inversion, Max Amplitude Above Average.
- Attributes chosen in porosity modeling of Zone 2 are: Euler Curvature, Instantaneous Frequency, Total Energy, Max Amplitude Above Average, Stochastic Inversion.
- Attributes chosen in porosity modeling of Zone 3 are: ILDip Curvature, Instantaneous Frequency, Deterministic inversion, Max Amplitude Curvature.

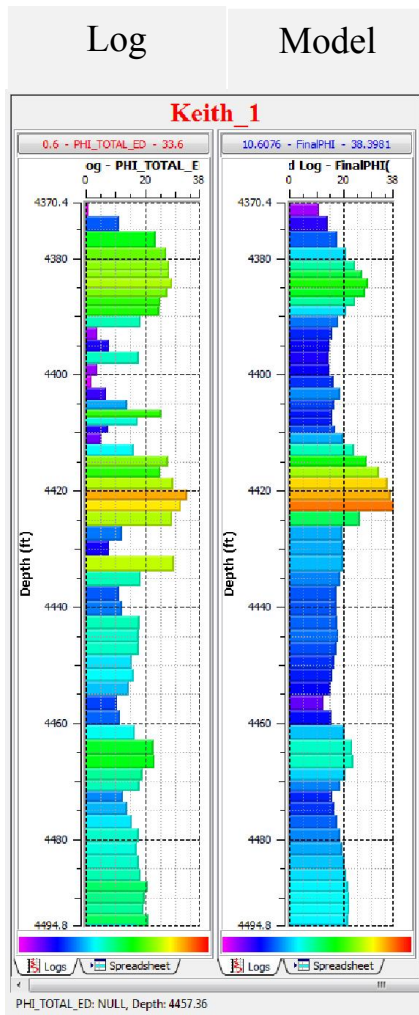


Figure 3.32 Comparison between the blind well (Keith_1) and the model's porosity log extracted at Keith_1's location.

3.3.5 Gamma Ray Model

The input to this model are the gamma ray logs and the constraints are the multiple seismic attributes generated previously along with the derived porosity. With these parameters, the neural network will generate multiple realizations were each realization will be judged on its ability to predict the blind well not used in the modeling. The blind well chosen for the gamma ray model is Keith-1. This particular model was able to capture the general trends of the Keith-1 well, as seen in Figure 3.33.

- Attributes chosen in gamma ray modeling of Zone 1 are: Sub Band, Stochastic Inversion, Euler Curvature, and Effective Porosity Model.
- Attributes chosen in gamma ray modeling of Zone 2 are: Instantaneous Frequency, Total Energy, Maximum Principal Curvature, Stochastic Inversion, and Absolute Colored Inversion.
- Attributes chosen in gamma ray modeling of Zone 3 are: Instantaneous Frequency, IL Dip Curvature, Stochastic inversion, Generalized Linear Inversion, and Effective Porosity Model.

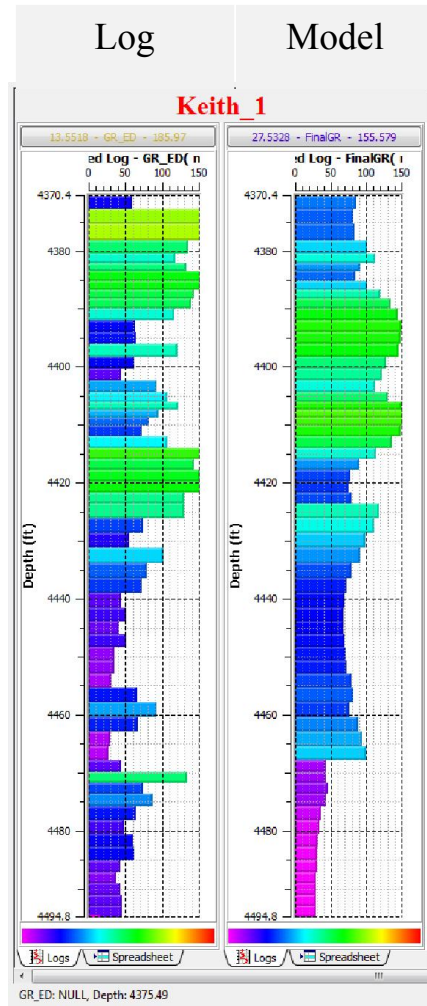


Figure 3.33 Comparison between the blind well (Keith-1) and the model's gamma ray log extracted at Keith-1's location

Chapter 4 - Discussion

4.1 Discussion

By integrating key seismic attributes such as: most positive curvature, total energy, and max amplitude above average attributes in sequential geologic modeling of reservoir properties which were successfully applied and validated on the gamma ray, and porosity, I was able to conclude that previously drilled dry wells within the study area were outside the boundary of a meandering, Cherokee sand channel system of potential reservoir quality. This compares favorably to previous studies, and to that of Raef et al., 2015, where a palaeoshoreline was interpreted, and further supports the existence of a broadly NE-SW trending meandering channel system with SE flow direction (with relatively low acoustic impedance). Spectral attributes have been used to delineate facies and depositional environments such as sand channels.

Most positive curvature seismic attribute was determined on spectrally whitened seismic dataset after foot print removal. Whitening process applied to the input dataset in the enhancement of high frequencies helped in better defining the fault network, 8 faults were identified (Figure 4.1 for a time slice at 850 msec). It shows intense faulting compartmentalization that is not continuous, and this could be a major reason as to why none of the other wells in the Wierman field were productive (Charlotte, 2009). A major advantage of the volumetric curvature over any other fault imaging technology is the ability to image the faults at different scales. Structural framework that can be built for any complex geology with as many faults as possible. When dealing with a fractured reservoir where the faults play a major role during deposition and after, a correct structural framework that accounts for all the faults and horizons is a key feature for a correct inversion

Total energy and max amplitude above average attributes best reflect the geologic features and point out a feature in the north part of the section that may be the result of processing or signal-to-noise artifact, (Figure 4.2). This is in agreement with evidence using the curvature attribute.

Wierman field is dominated by a discontinuous channel highlighted on the overlay of Most Positive Curvature with Max Amp Above Average, and an overlay of Most Positive Curvature with Total Energy at different time slices, 857ms and 872ms (Figure 4.2, 4.3, 4.4, 4.5) of thickness below seismic resolution that lies above the Mississippian limestone, this channel sandstone holds the highest oil reservoir potential, with its greater acoustic impedance contrast with underlying Mississippian limestone, and lower acoustic impedance.

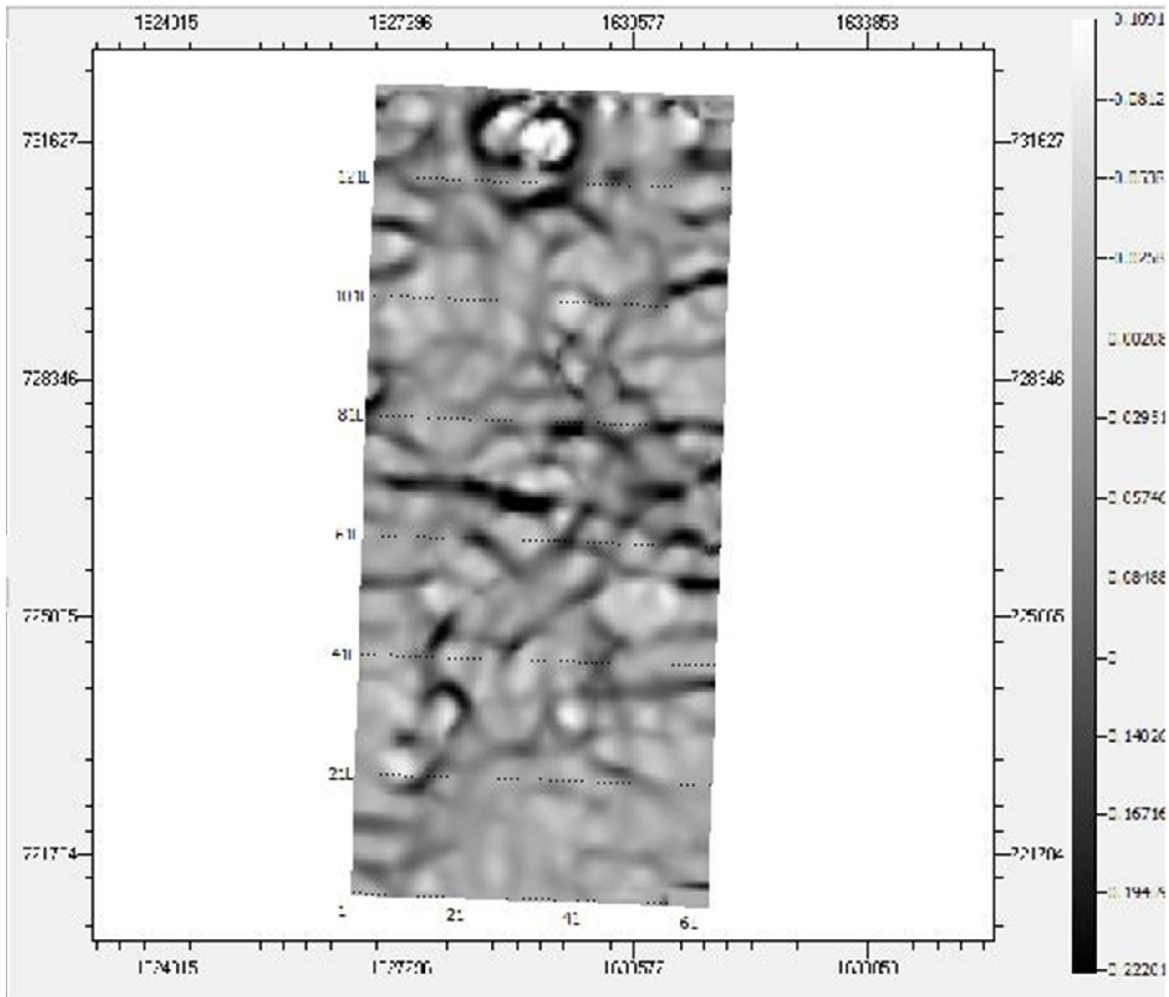


Figure 4.1 Most Positive Curvature, EXP 0.5, Time 850 ms of the spectrally whitened seismic

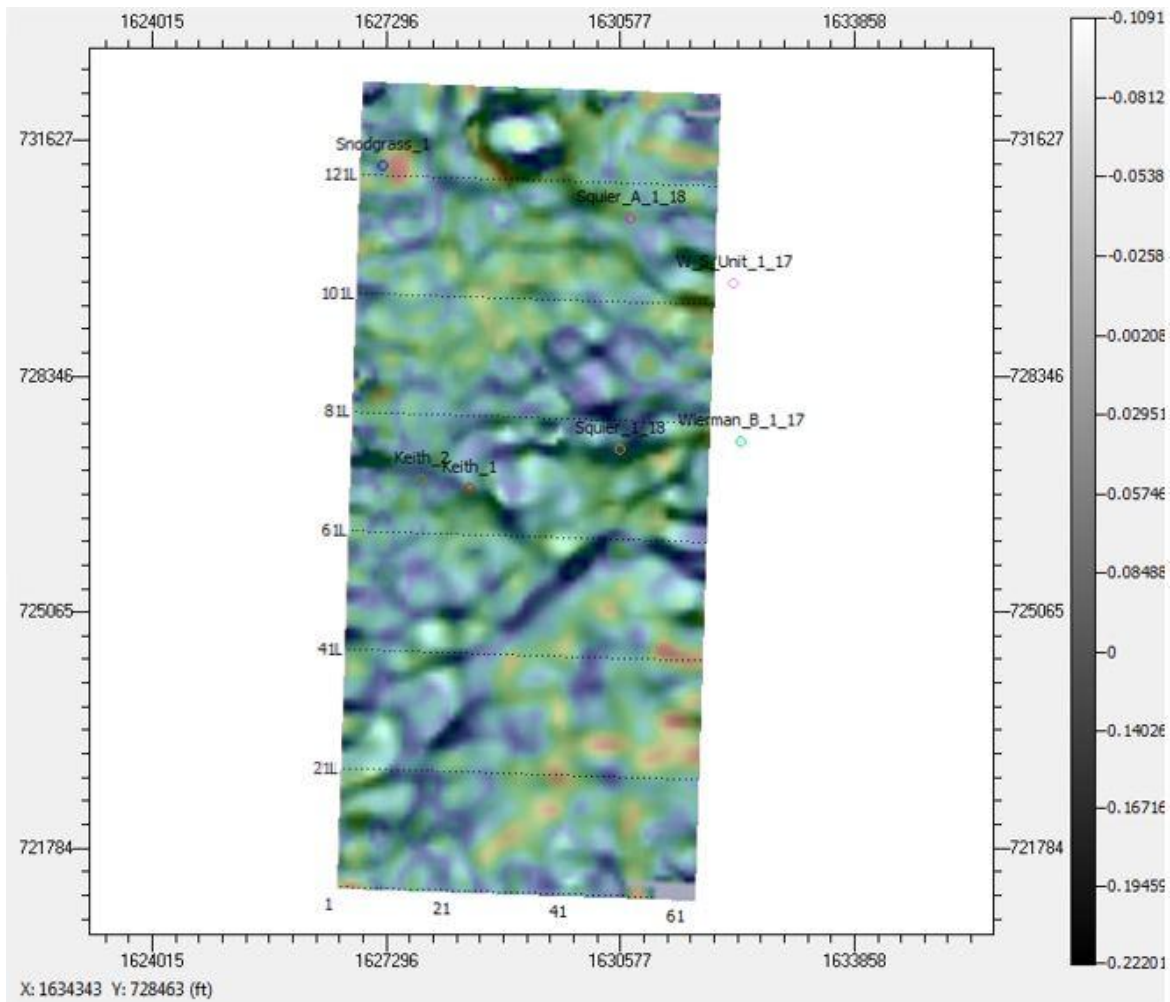


Figure 4.2 Most Positive Curvature exp 0.5 Notch with Max Amp Above Avg. Overlay, Time 857ms

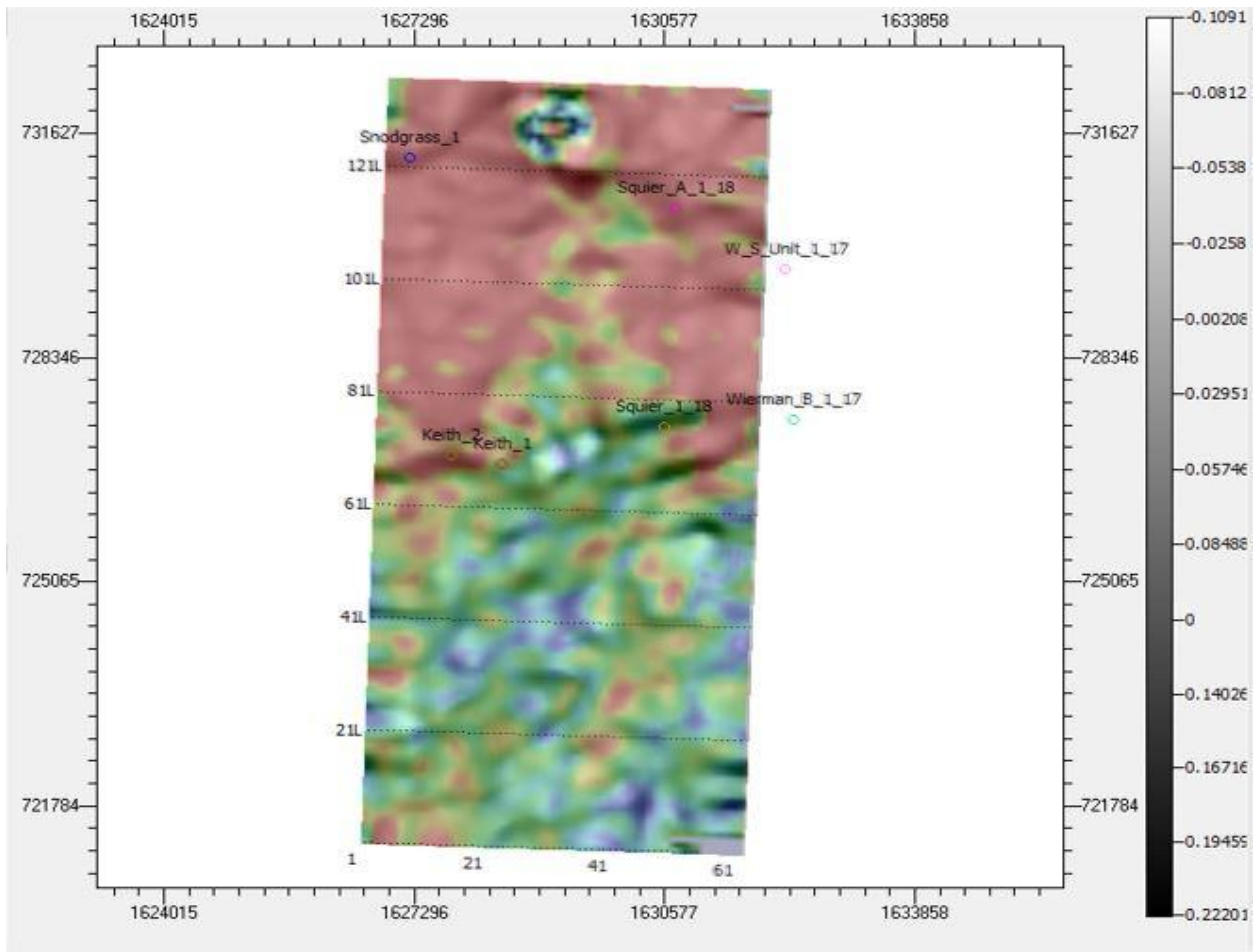


Figure 4.3 Most Positive Curvature exp 0.5 Notch with Max Amp Above Avg. Overlay, Time 872ms

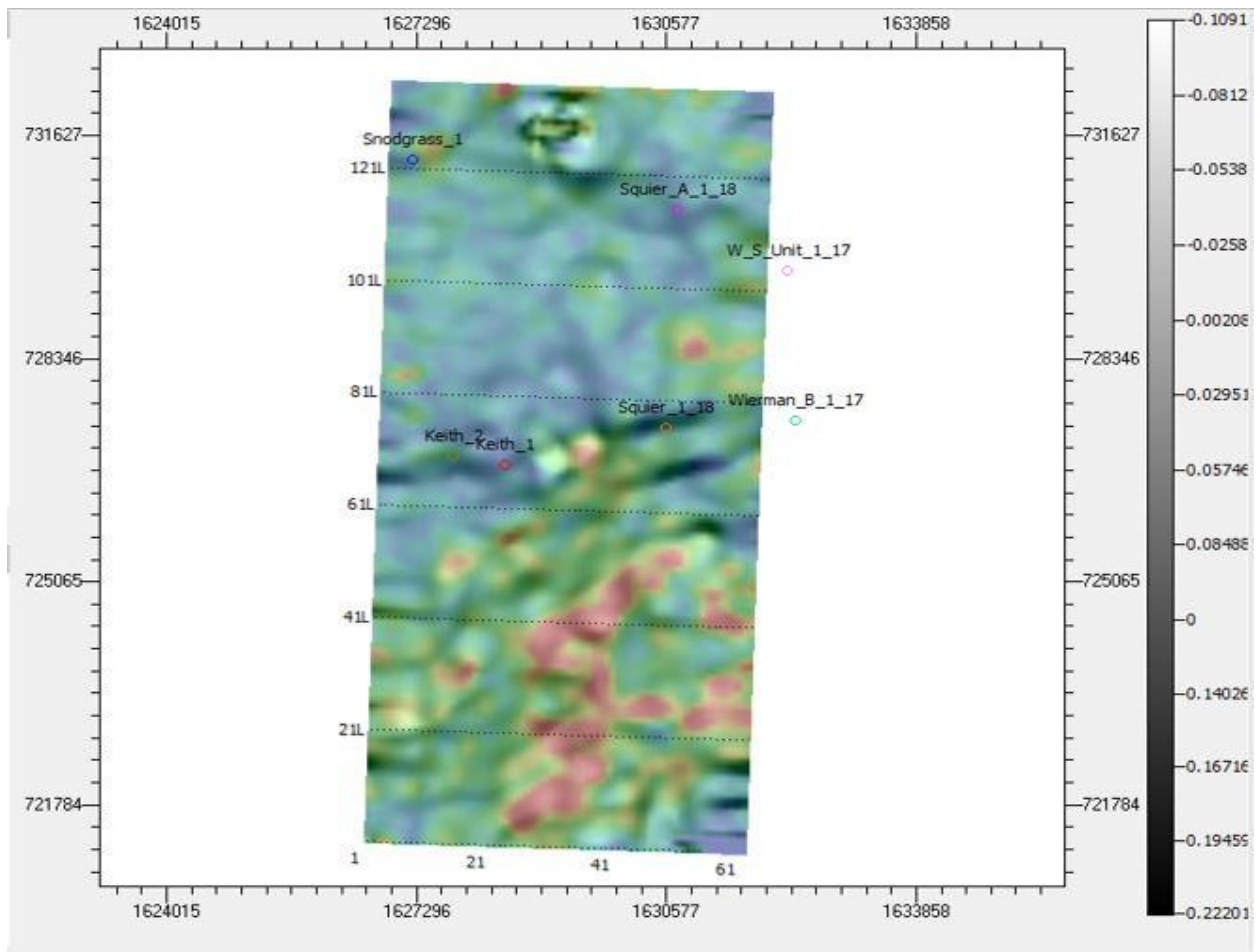


Figure 4.4 Most Positive Curvature exp 0.5 Notch with Total Energy Overlay, Time 857ms

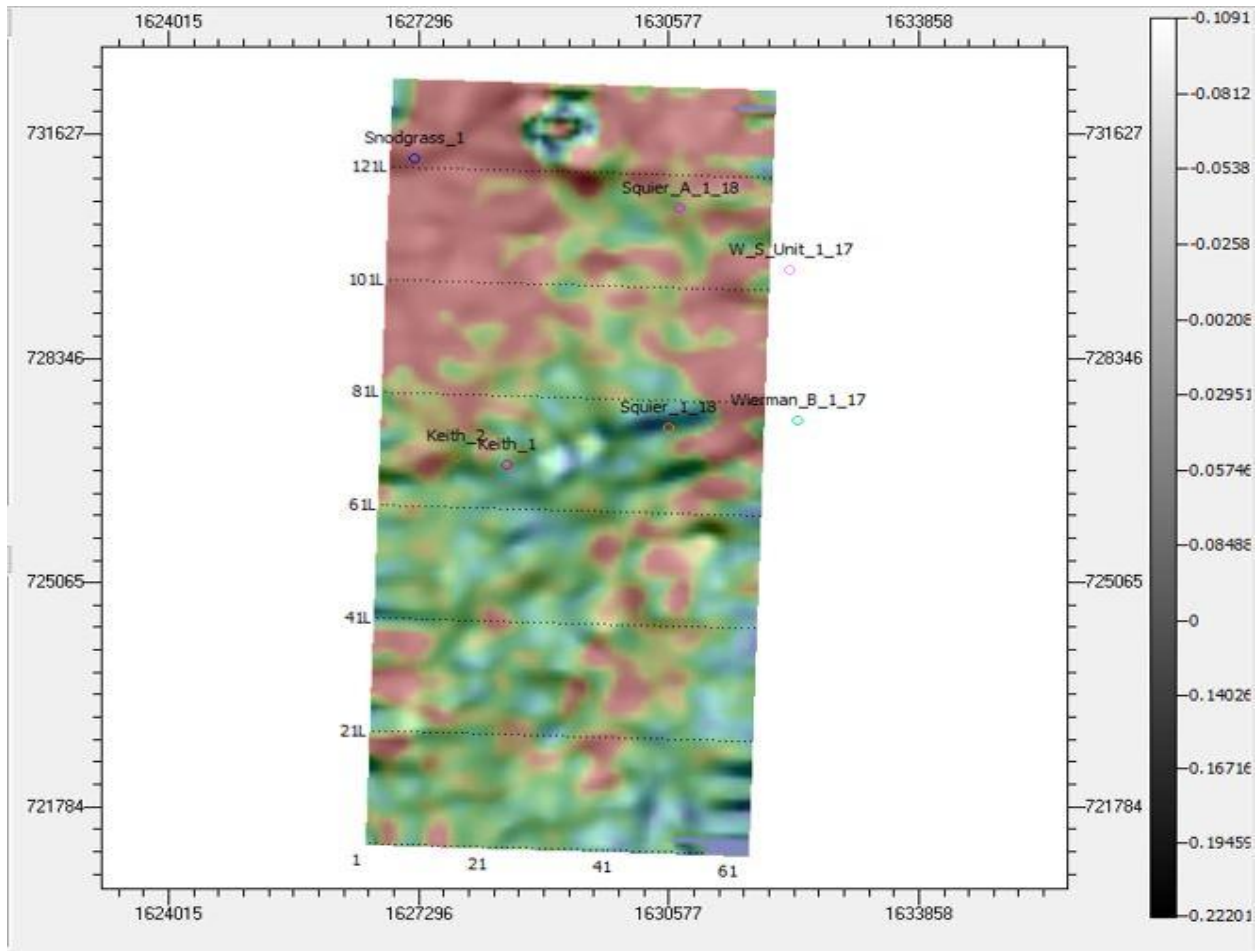


Figure 4.5 Most Positive Curvature exp 0.5 Notch with Total Energy Overlay, Time 872ms

Post-stack inversions derive the acoustic impedance from seismic data. This is important because acoustic impedance is a product of the velocity and density of the rock, which can in turn tell us more about the rock being modeled. The stochastic inversion is usually the most detailed inversion, after creating a blocked log for each well, and comparing its acoustic impedance log with the 5 inversions, it shows that stochastic inversion is the best and most similar one to the impedance log, as it is shown in the previous well Squier 1-18, (Figure 4.6).

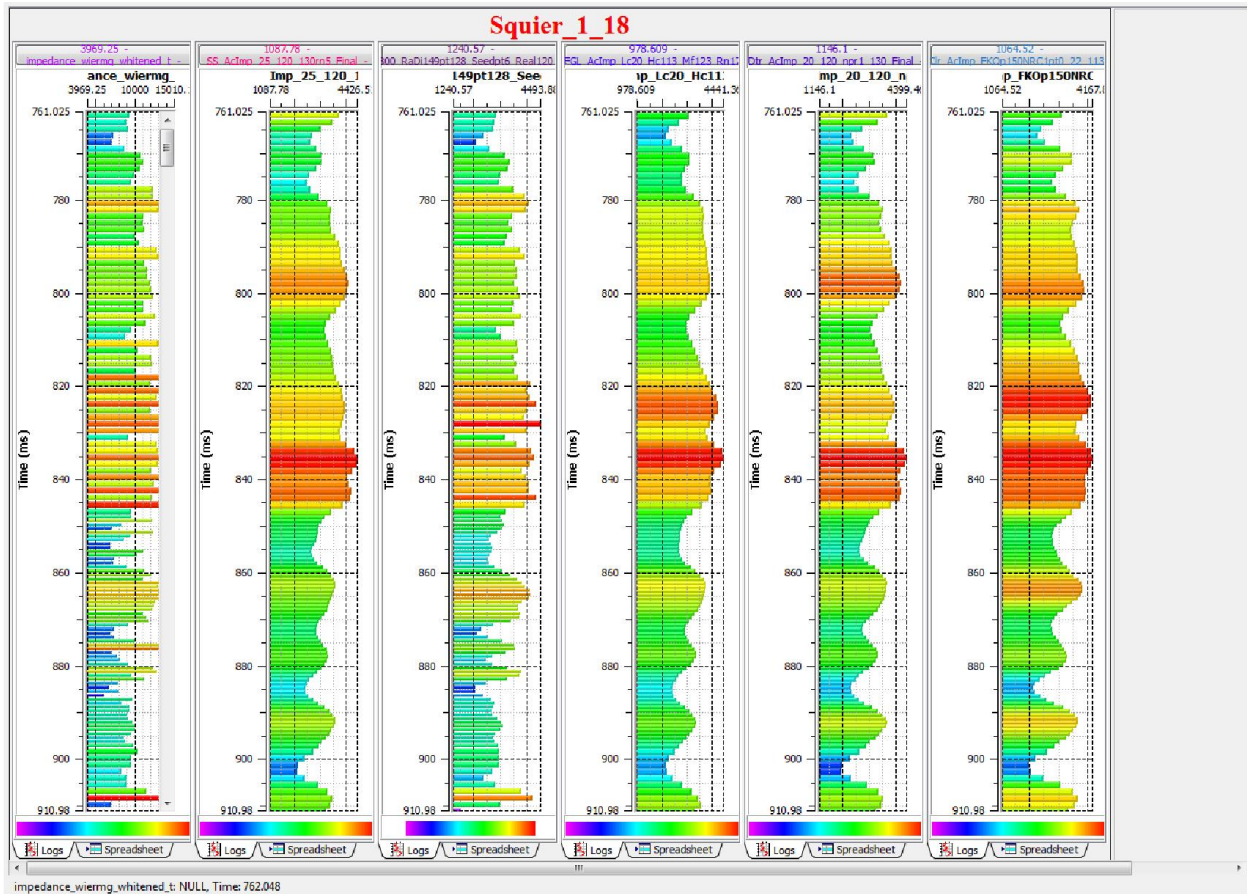


Figure 4.6 Post-stack inversions of acoustic impedance at Squier 1-18 well using the various inversion methods. From left to right: acoustic impedance computed at well, stochastic inversion, GLI, deterministic inversion, colored inversion, and sparse spiking inversion

The geological modeling prepared based on a set of seismic attributes, which were used quantitatively to model reservoir properties, using CRYSTAL software’s neural network to generate these models such as, Porosity model, and gamma Ray model, and a Pay model that combines the two geological reservoir properties, gamma Ray and Porosity. Spectral imaging,

volumetric curvatures and post stack inversions are useful seismic attributes but not sufficient for the full understanding of the Wierman field channel reservoirs

Pay zones in this reservoir were defined based on gamma ray less than 50 API and a porosity higher than 20%. These values were selected based on the values in the producing wells. The upper layer of the Cherokee group can be seen in Figure 4.7.

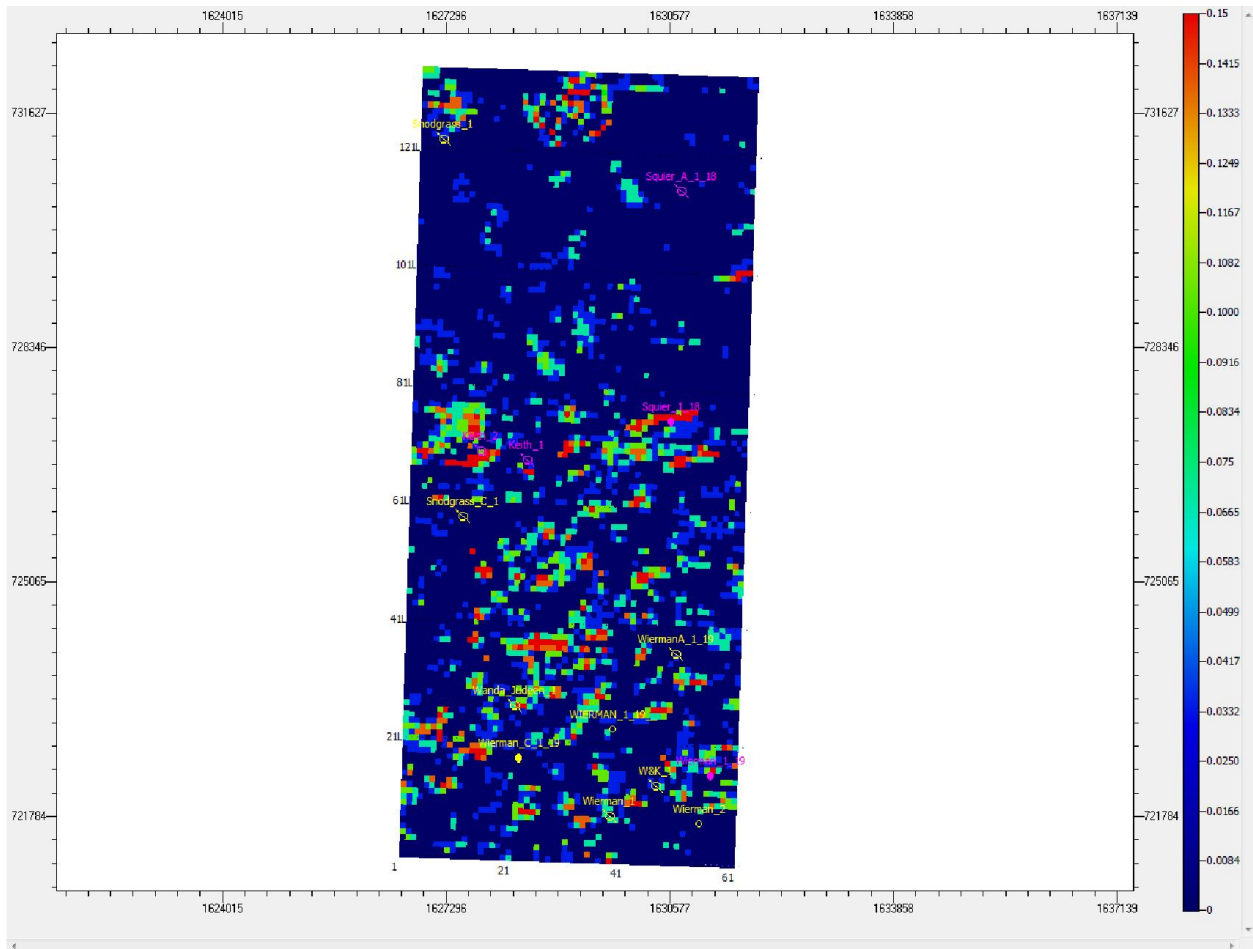


Figure 4.7 Defined pay zone for the upper Cherokee group. A pay zone is defined by being less than a gamma ray of 50 API and more than a porosity of 20%.

Given the depositional environment, and the knowledge acquired by other data in the study area, it appears clearly that the key in solving Wierman problems is to have high resolution seismic attributes. The previous attributes and stochastic inversion as used in this study, is revealing the true geology of the Wierman field. Although similar attributes were used

previously in other studies in the Wierman field, it was not combined with other processes such as stochastic inversion to reveal the actual thin sand bodies.

4.2 Future Well Locations

Possible drill locations needed a large pay zone with great connectivity. These locations are defined as Drill Prospect 1, 2, and 3. Each location is outlined by a large pink rectangle, which can be seen in Figure 4.8.

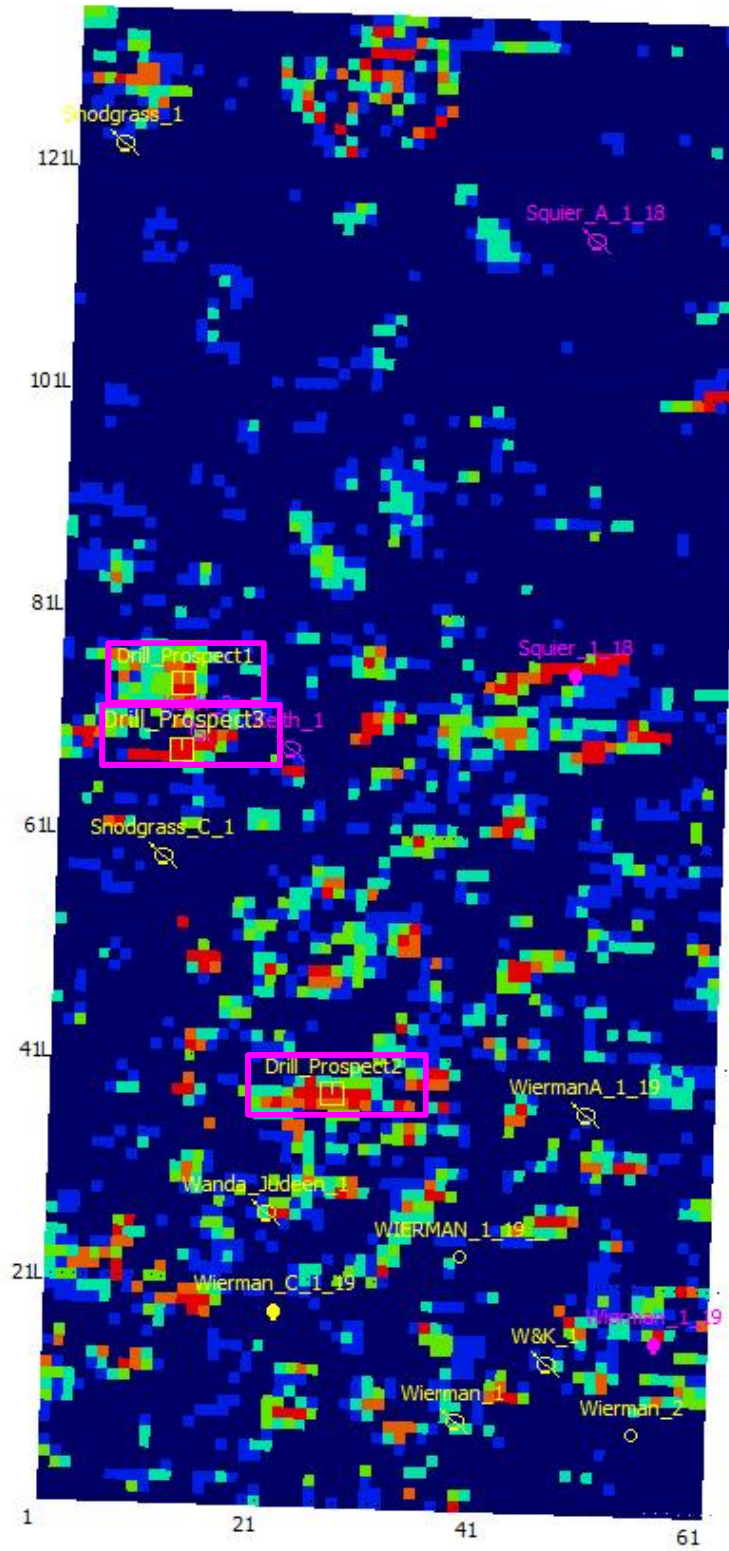


Figure 4.8 Proposed drilling locations based on pay zone.

One reason that only the upper portion of the Cherokee group is being examined with a pay zone map is the likely oil water transition zone discovered in the Wierman 1-19. The shallow and deep resistivity log cross over could indicate the start of the transition from oil to water is at 4400 feet, as seen in Figure 4.9.

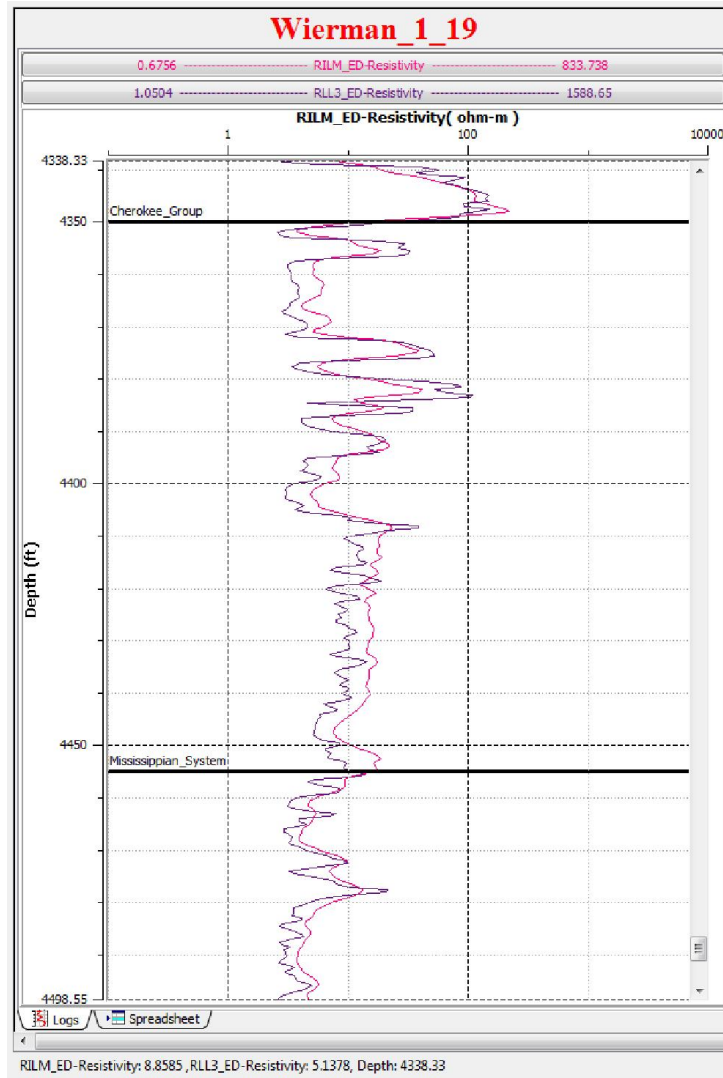


Figure 4.9 Wierman 1-19 shallow and deep resistivity logs that could indicate a cross over at 4410 feet, which points to the start of the oil water transition zone.

In the resistivity logs of the producing wells, we notice that there is a cross over between the deep and shallow resistivity logs, which indicates higher water saturation. This confirms that the lower part of the Cherokee is less likely to be a producing layer. This confirms the start of the water saturated transition zone at 4400 feet.

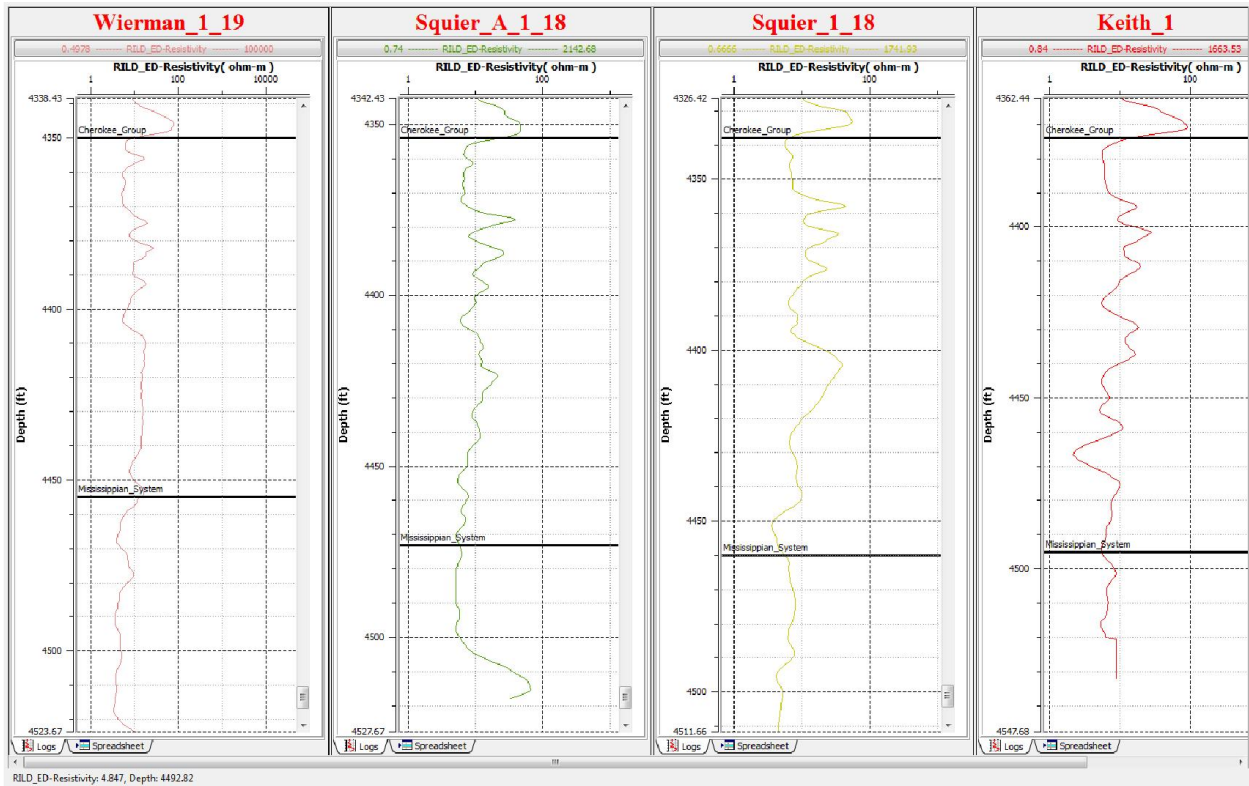


Figure 4.10 Blocky Nature of Wells Points to an Oil Reservoir in the Upper Part of the Cherokee

If we assume that the start of the oil-water transition is at 4400 feet, only Drill Prospects 1 and 2 are structurally high enough to avoid water. To ensure that the reservoir is not water producing, Drill Prospect 2 is highly recommended. This can be seen in the extracted gamma ray logs at the proposed well locations shown in Figure 4.11.

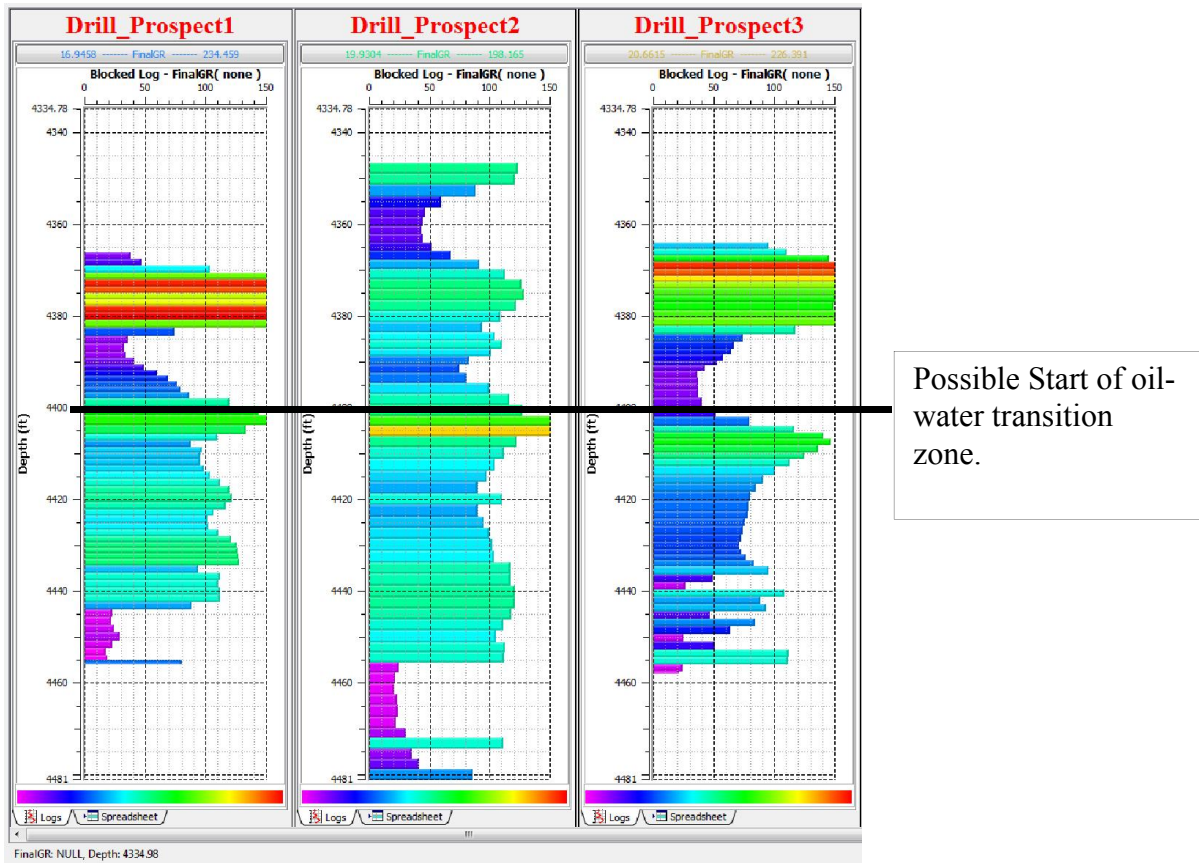


Figure 4.11 Gamma ray model extracted at proposed well locations inside the Cherokee group.

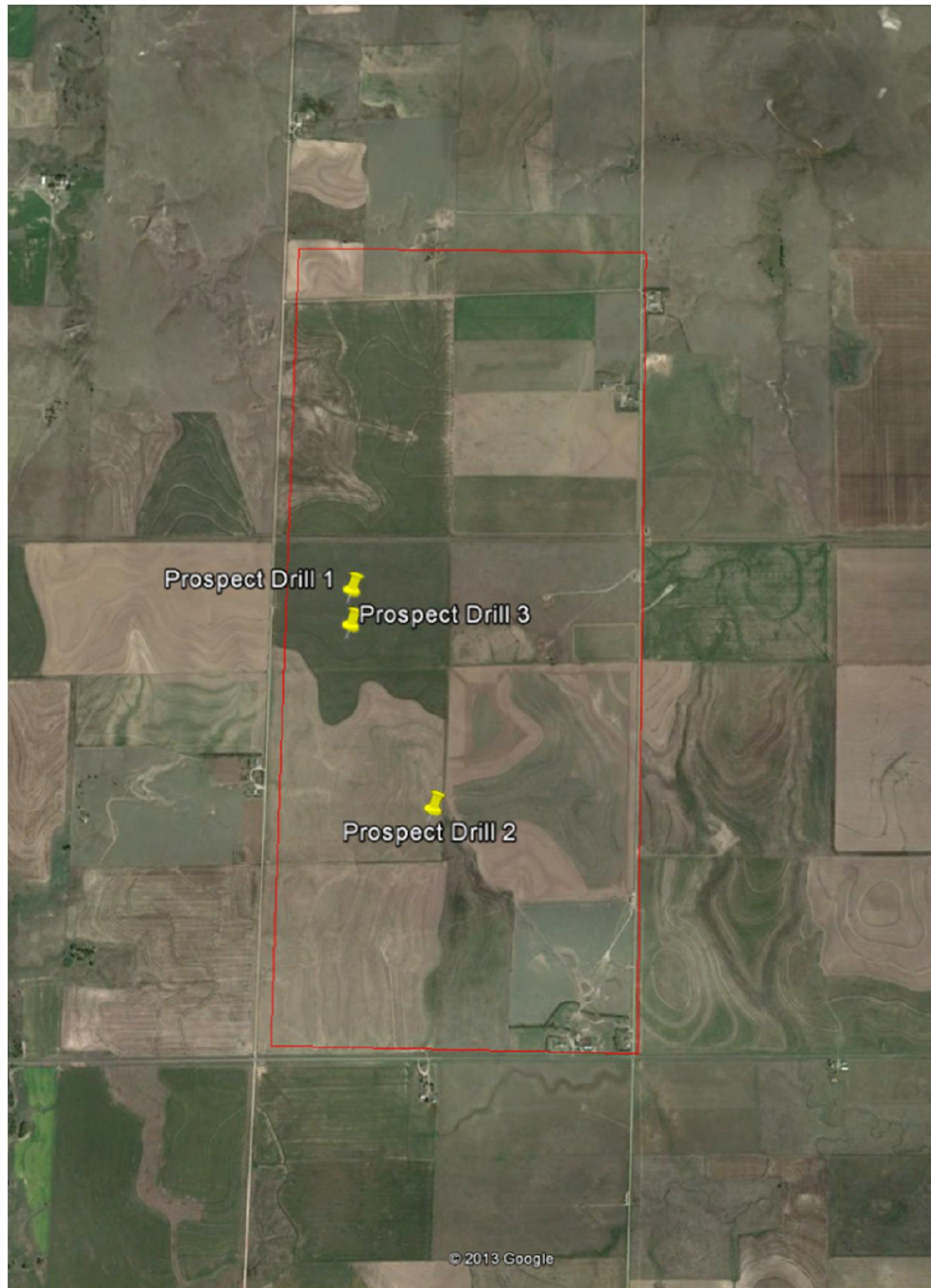


Figure 4.12 View of the proposed drill locations with the seismic polygon outlined in red.

Chapter 5 - Conclusions and recommendations

In this study, many geophysical methods have been applied on the Wierman Field; Ness County, Kansas, and a combination of seismic attributes with inversion technology was able to effectively improve the precision of our sand channel reservoir interpretation. Seismic attributes (most positive curvature, total energy and max amplitude above average attributes), helped identifying an intense faulting compartmentalization on the seismic volume that is discontinuous, which could be a major reason as to why none of the other wells in the Wierman field were productive, in addition to the delineation of a feature in the north part of the section that may be the result of processing or signal-to-noise artifact, this feature is very close to the edge of the survey and low signal-to-noise ratio is expected.

Seismic attributes are strongly affected by acquisition parameters where curvature attribute better highlighted sand channels when spectrally enhanced seismic data was used as input.

Different inversion methods, including sparse spike, deterministic, Generalized Linear Inversion (GLI), colored inversion, and stochastic inversion were run to produce acoustic impedance volumes that were compared against an acoustic impedance log computed at the five well locations to identify seismic lithofacies and to discriminate lithologies and relate them to the defined sand channel in the Cherokee group formation based on the channel sinuosity, and based on several different seismic attributes from high resolution post-stack inversions, spectral attributes, and volumetric curvature, sequential geological modelling through the application of neural network was applied where each model was used as a driver for the next model, and an estimation of porosity, gamma ray, and various pay zones were constructed with the aim of understanding the subsurface lithofacies heterogeneities, prospect generation and evaluation of the subject area, and based on combined qualitative and quantitative results, it showed the existence of a highly variable broken up meandering channel facies consisting mainly of sandstone which is home to a potential hydrocarbon recovery. Stochastic inversion has given the most detailed information about the reservoir, and by modelling of reservoir properties, pay zones in this reservoir were defined as having a gamma ray less than 50 API and a porosity higher than

20%. This suggests 3 different drilling prospects, however, due to the presence of the potential oil water transition zone at 4400 feet Drill Prospect2 is most highly recommended. Drill Prospect1 and 3 may be too close to the oil-water transition zone to produce a large amount of oil compared to water.

References

Abbas, M. Y., 2009. Incorporating Seismic Attribute Variation into the Pre-well Placement Workflow: A case study from Ness County, Kansas, USA. Master's Thesis. Kansas State University.

Cooke, D. A. and W. A. Schneider (1983). "Generalized linear inversion of reflection seismic data." *Geophysics* 48(6): 665-676.

Chopra, S. and Marfurt. K.J. 2007, "Seismic Attributes for Prospect Identification and Reservoir Characterization." Society for Exploration Geophysicists. Tulsa, OK, USA.

Chopra, S. and Marfurt, K.J. 2008, "Seismic attributes for stratigraphic feature characterization", 78th Annual International Meeting, SEG Technical Program Expanded Abstracts, vol. 27, no. 1, pp. 1590-1594

Cuzella, J. J., 1991, Depositional environments and facies analysis of the Cherokee Group in West-central Kansas. AAPG bulletin, 75, no. 3, p. 560

Dennis A. Cooke, William A. Schneider, June 01, 1983. Generalized linear inversion of reflection seismic data. Society of Exploration Geophysicists

Goebel, E. D. (1968). "Mississippian rocks of western Kansas." AAPG Bulletin 52(9): 1732-1778.

Haas, A. and O. Dubrule (1994). "Geostatistical inversion-a sequential method of stochastic reservoir modelling constrained by seismic data." *First Break* 12(11): 561-569.

Lancaster, S., & Whitcombe, D, January 1, 2000. Fast-track 'colored' Inversion. Society of Exploration Geophysicists.

Lozano, F. A. and K. J. Marfurt (2008). 3D seismic visualization of shelf-margin to slope channels using curvature attributes. SEG Technical Program Expanded Abstracts 2008, Society of Exploration Geophysicists: 914-918.

Meek, N. Tyler, 2015. Applications of 3D seismic attribute analysis workflows: a case study from Ness County, Kansas, USA, USA. Master's Thesis. Kansas State University.

Marfurt, K. and R. Kirlin (2001). "Narrow-band spectral analysis and thin-bed tuning." *Geophysics* 66(4): 1274-1283.

Ouenes, A., et al. (2007). Integrated Property and Fracture Modeling Using 2D Seismic Data: Application to a Cambrian Field in Algeria. SPE Annual Technical Conference and Exhibition, Society of Petroleum Engineers.

Philip, C. C., 2011, 3-D seismic attributes analysis to outline channel facies and reveal heterogeneous reservoir stratigraphy; Wierman field, Ness County, Kansas, USA, , Master's Thesis. Kansas State University.

Partyka, G., et al, 1999. Interpretational applications of spectral decomposition in reservoir characterization. *The Leading Edge* 18(3): 353-360.

Puryear, C. I. and J. P. Castagna (2008). "Layer-thickness determination and stratigraphic interpretation using spectral inversion: Theory and application." *Geophysics* 73(2): R37-R48.

Russell, B. H., et al. (2003). "Application of the radial basis function neural network to the prediction of log properties from seismic attributes." *Exploration Geophysics* 34(1/2): 15-23.

Raef, A., T. Meek, and M. Totten, 2016, Applications of 3D seismic attribute analysis in hydrocarbon prospect identification and evaluation: Verification and validation based on fluvial palaeochannel cross-sectional geometry and sinuosity, Ness County, Kansas, USA: *Marine and Petroleum Geology*, v. 73, p. 21–35

Ramaker, B.J. 2009. Influence of Mississippian Karst Topography on Deposition of the Cherokee Group: Ness County, Kansas. Master's thesis, University of Kansas, 183 p.

Suarez, Y., et al. (2008). Seismic attribute-assisted interpretation of channel geometries and infill lithology: A case study of Anadarko basin Red Fork channels. *SEG Technical Program Expanded Abstracts 2008*, Society of Exploration Geophysicists: 963-967.

Saleh Al-Dossary and Kurt J. Marfurt (2006). "3D volumetric multispectral estimates of reflector curvature and rotation." *GEOPHYSICS*, 71(5), P41-P51.

Sinha, S. et al., 2005. Spectral Decomposition of Seismic Data with Continuous Wavelet Transform. *Geophysics*, November-December 2005; 70: p19-p25.

Stoneburner, R. K., 1982, Subsurface study of the Cherokee Group on the western flank of the Central Kansas Uplift in portions of Trego, Ellis, Rush and Ness counties, Kansas.

Van Dyke, R, 1976, Depositional environments of Cherokee reservoir sands, Kincaid Oil Field, Southeast Kansas. *AAPG Bulletin* v. 60, iss. 2, 322-323.

Walters et al., 1979, Channel Sandstone Oil Reservoirs of Pennsylvanian Age, Northwestern Ness County, Kansas: *AAPG Meeting Abstract*, 63, 2120

Yilmaz, O., 2001, Seismic data analysis: *SEG Investigations in Geophysics* No. 10.

Appendix

The following are raw data for well logs and figures that were used in some of the analysis and discussions included as supporting documentation.

1- Log inventory for 5 wells used in my survey.

Log Type	Keith#1	Keith#2 (Digitized)	Squier 1-18 _Producing well	Squier 'A' 1-18	Wierman 1-19_ Producing well
Density	RHOB_CRHOBSON, RHOC,		RHOB, RHOC,	RHOB, RHOC,	RHOB, RHOC
FD					
FI					
Brittleness					
Gamma Ray	GR_CDILSON	GR	GR	GR	GR
Sonic	DT,	DT	DT	DT	
Shear Sonic					
Resistivity	RLL3 (OHM-M), RILD, RILM,		RLL3 (OHM-M), RILD, RILM,	RLL3 (OHM-M), RILD, RILM,	RILD, RILM, RLL3
Conductivity	CILD				
Saturation					
Porosity	DPOR, SPOR		DPOR, SPOR, CNPOR	CNOPR, DPOR,	DPOR, SPOR, CNPOR
Permeability			Perm		
Caliper from Density Tool	DCAL, MCAL,		DCAL, MECAL	DCAL,	DCAL, MELCAL
Neutron	CNLC, CNLS				
Spontaneous Potential	SP, SPC		SP	SP	
Delta Time	DT,		DT	DT	DT
Mico Log					MEL15, MEL20
Neutron Porosity			Neut_por	Neut_por	Neut_por
Rxo / Rt	RxoRt				RxoRt
Sonic Porosity	SPOR			SPOR	SPOR
DIL Spontaneous Potential					SP
P wave Velocity			Vp		Vp
Shallow Water Saturation			Sh_Sx0		

2- Well information and seismic perimeter coordinates:

```

wells      X              Y              KB      TD
Keith_1    1628475.943    726761.145    2455    4520
Keith_2    1627806.495    726887.051    2456    4510
Snodgrass_1 1627253.592    731258.282    2442    4466
Squier_1_18 1630602.596    727305.409    2446    4578
Squier_A_1_18 1630747.299    730526.645    2455    4520
w_s_Unit_1_17 1632194.337    729607.384    2441    4550
wierman_B_1_17 1632297.720    727409.281    2449    4530

```

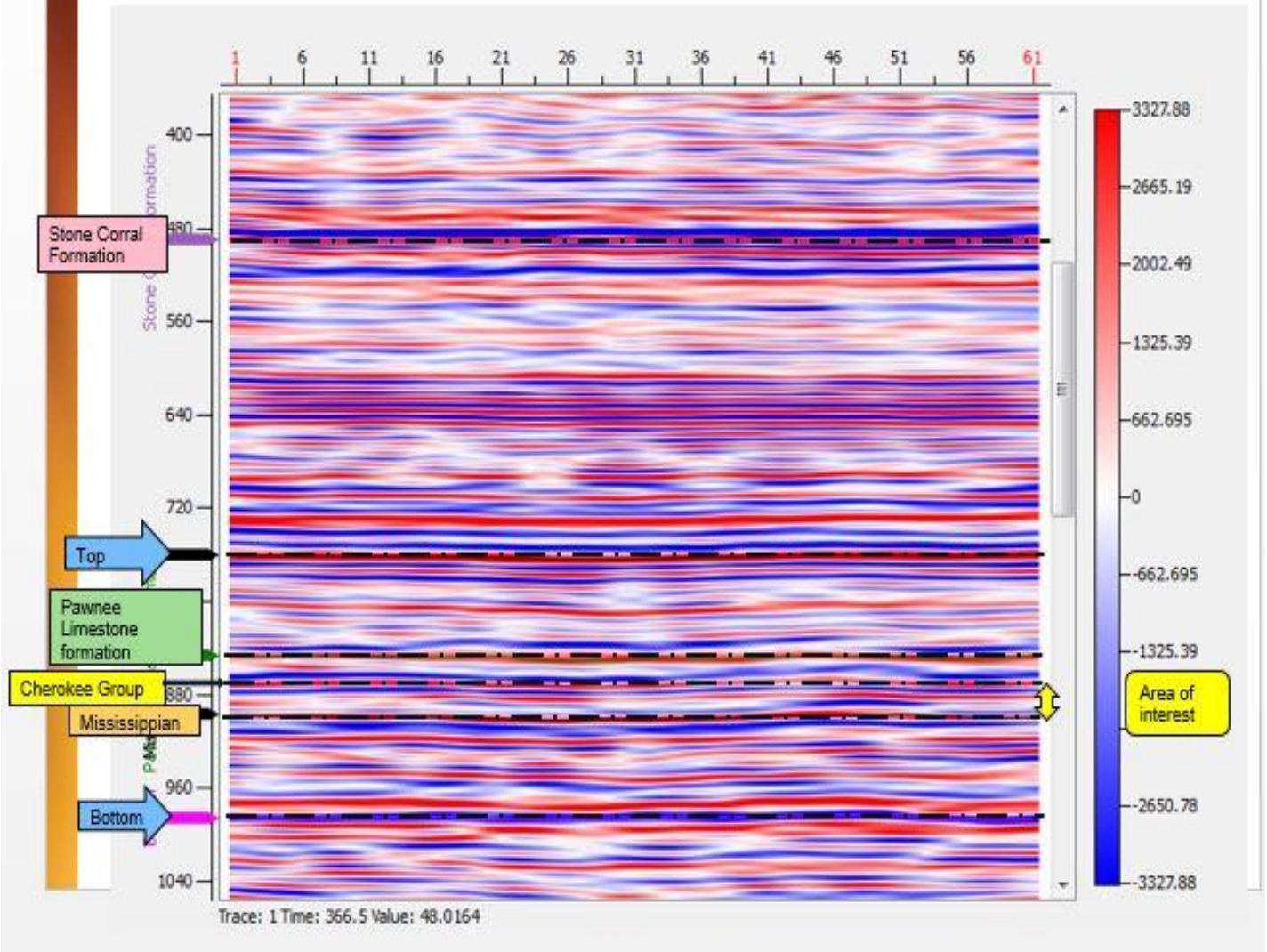
```

Seismic volume perimeter coordinates
X              Y
1626652,02     721250,009
1631599,02     721090,009
1631959,02     732222,009

```

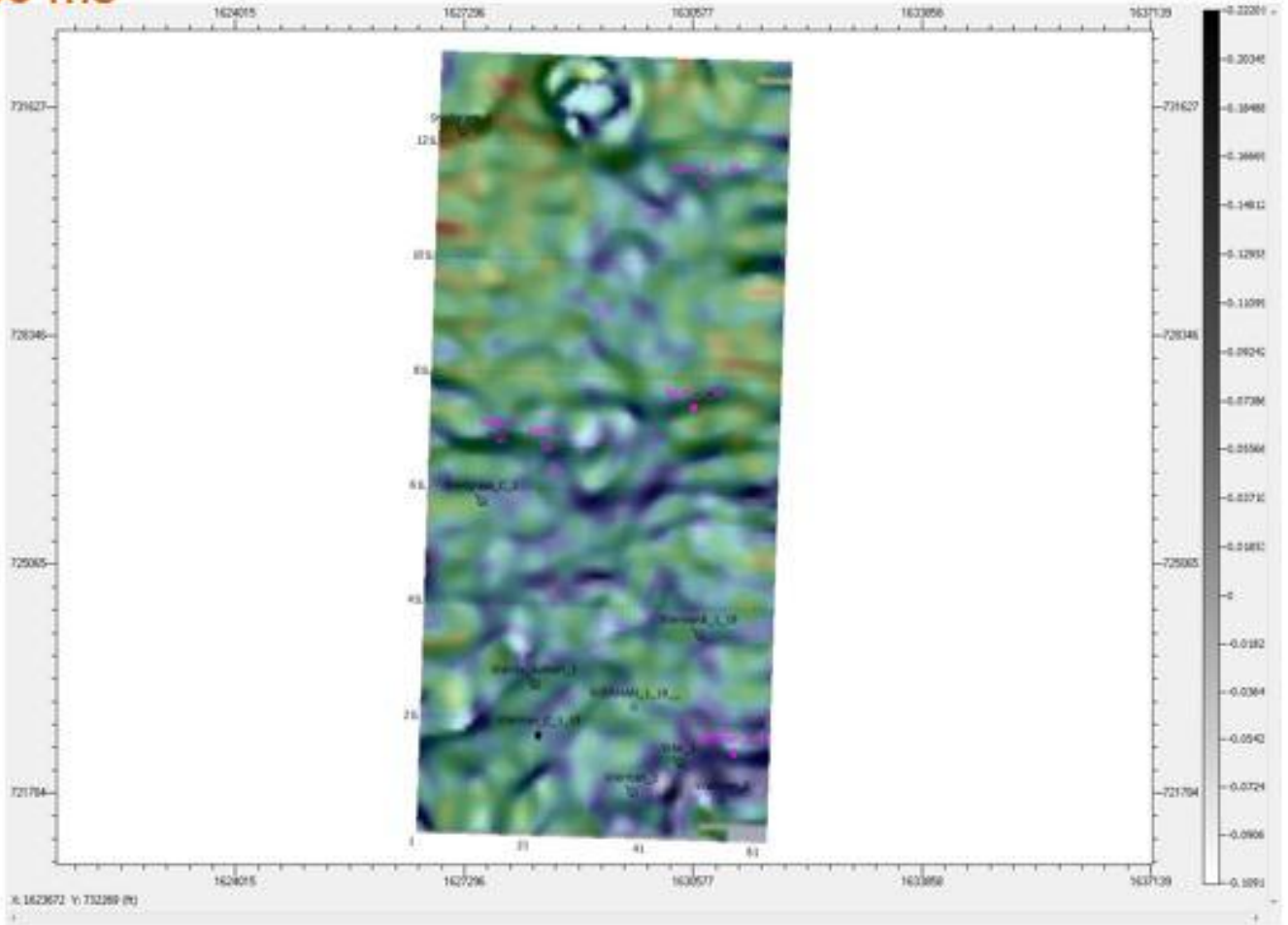

- 3- Cherokee group is located in the time range between 870 and 900 msec, which is our area of interest, top and bottom horizons are needed for running acoustic impedance inversions.

Horizon picking by SMT, AOI 903ms

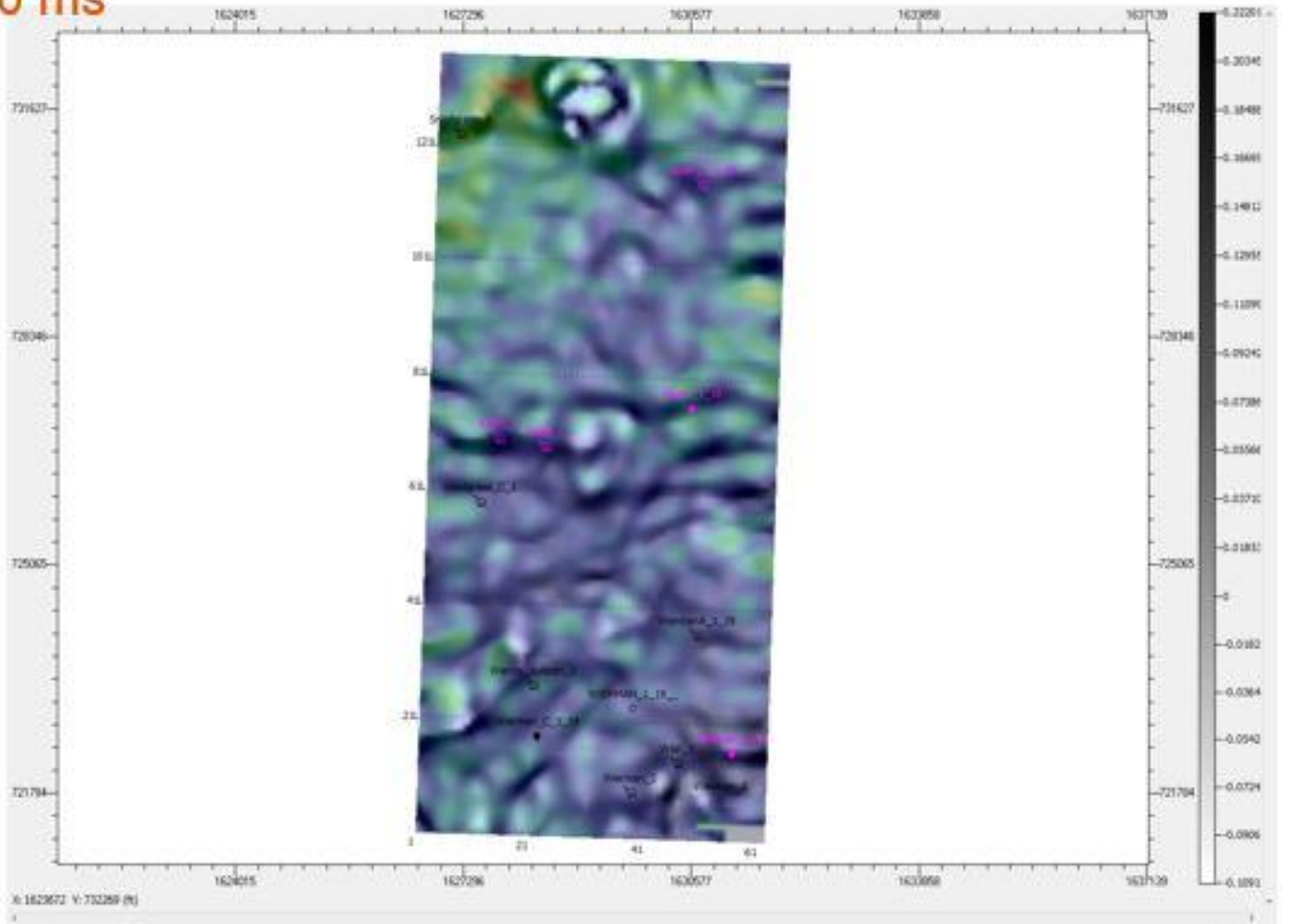


4- Overlay of seismic attributes around area of interest

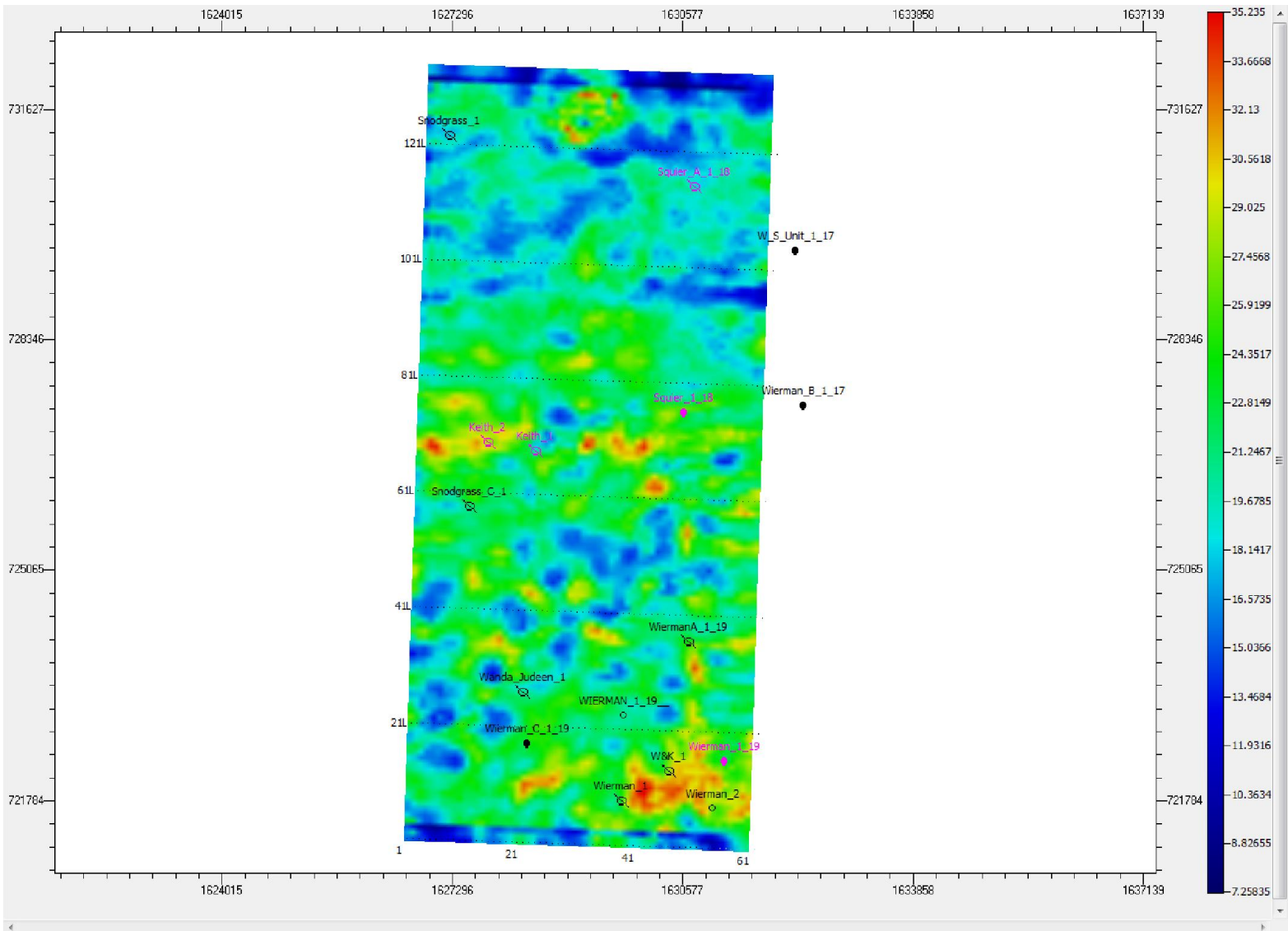
Max Amp Above Avg Mean Overlay on Most Positive Curvature at 880 ms



Total Energy Mean Overlay on Most Positive Curvature at 880 ms



5- Porosity Avg. Top Map derived from sequential geological modelling using neural network



6- Gamma Ray Average Top Map derived from sequential geological modelling using neural network

